# SEFOP2018 Field Guide

***Geophysics, Geochemistry, and Biogeochemistry of the Southern Piedmont Critical Zone***

*Assembled by:*
*The Calzones*
*of the Calhoun CZO*
*http://criticalzone.org/calhoun/*

*Welcome to the*
*Calhoun CZO Time Machine!*

DEM, digital elevation map, of 70,000ha Enoree District of Sumter National Forest, SC. The Calhoun Critical Zone Observatory is in the red box.

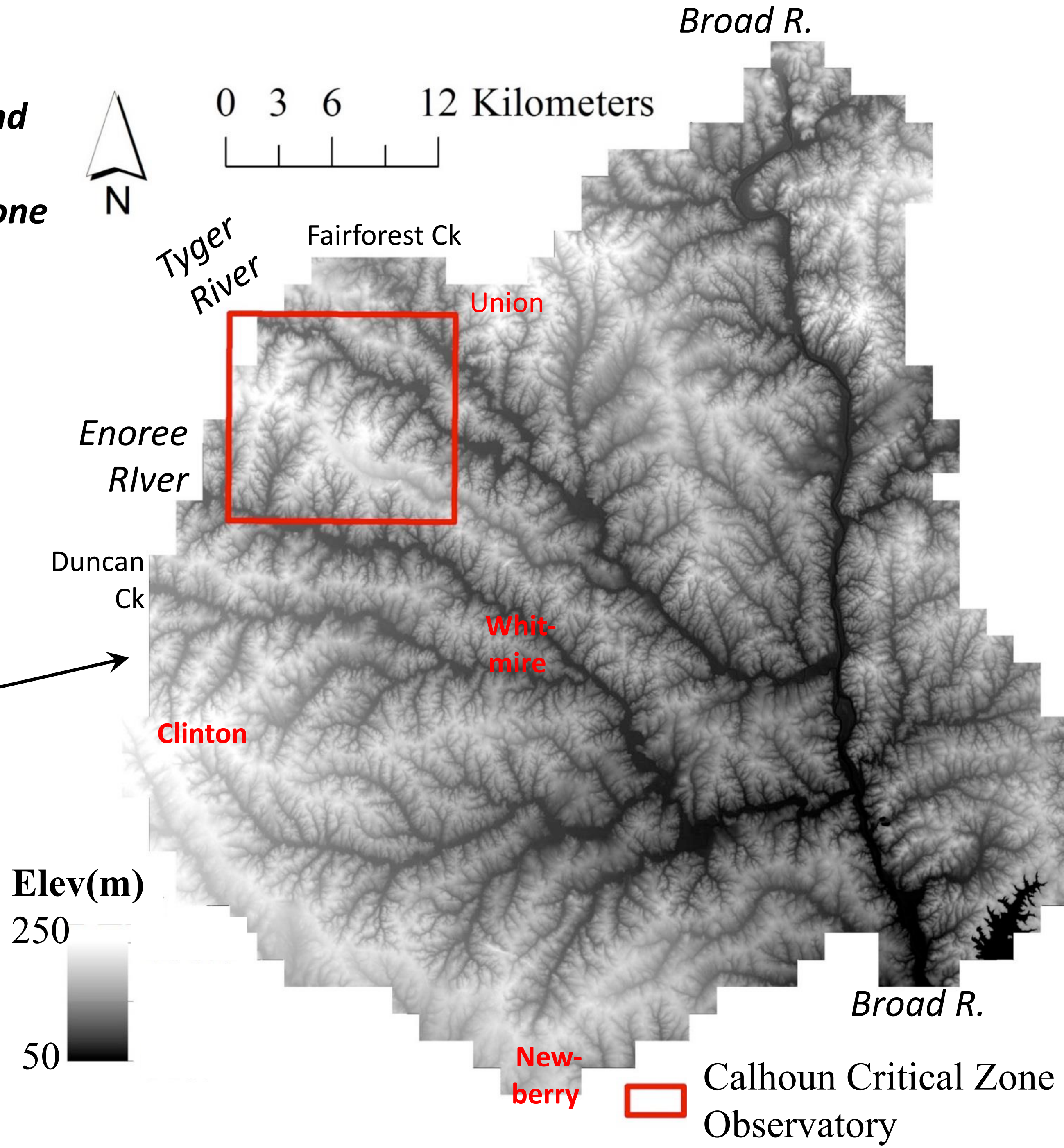

**SEFOP Stops (pages)**

***Saturday***

1 Mary Lou Quarry (p3-9)

† Padgett's Cr Baptist Church (p10-11)

3 70-m deep well (p12-30),
"Tyger Stripe" Cataula soil (p31-32)
60-year Calhoun LTSE (p-33-34)

4 Rose Hill (p35-36)

5 Sardis Rd Profile, Environmental History, & Interfluve orders (p37-39)

6 Hwy 49 Weathering Profiles (p40)

7 Sedalia CG (p41)

***Sunday***

8 Relic & historic landforms (p42-44)

9 Holcombe's Branch Watershed and Legacy Sediments (p45-51)

4 Rose Hill – Novel Field Ed Disc

*Abstracts* (p52-55)

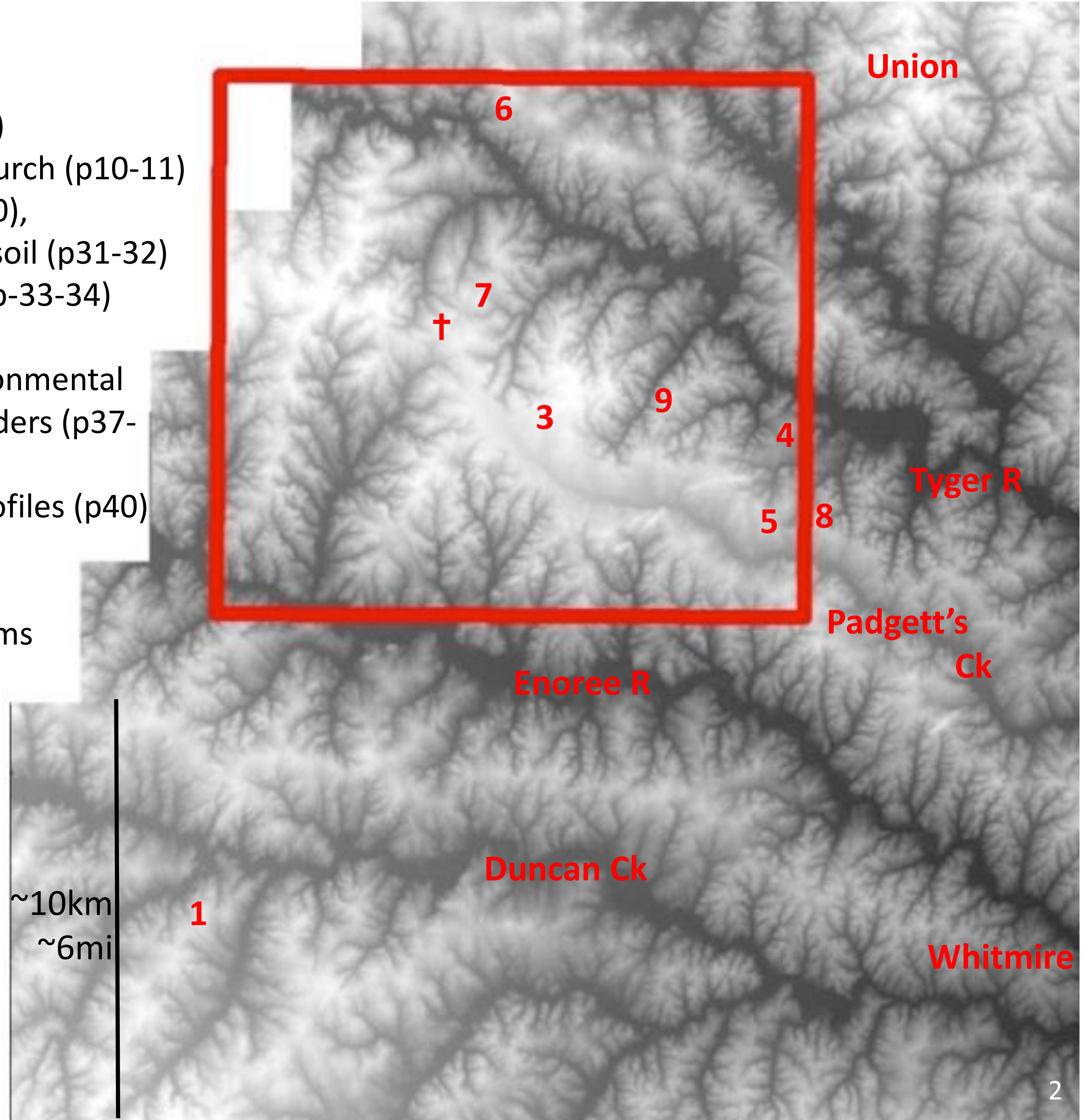

# Geology of the Mary Lou Quarry*

Paul A. Schroeder[1,2]
Tyler Cannida[1]
Alp Unal[2,1]
Jay Austin[3,1]

[1] University of Georgia, Department of Geology
[2] Istanbul Technical University, Geological Engineering
[3]Duke University, Nicholas School of the Environment

South East - Friends of the Pleistocene Field Trip
February 23-25, 2018

*Special thanks to Doug Larson and Hanson Aggregates, Greer, SC

Neoproterozoics have been mapped by Wright and Connie (2001) where they generally found either biotite-quartz-feldspar gneiss in the region of the Whitmire Complex or metadiorite in the Wildcat Complex (comprised of plutons and sub-volcanics)

Horton, J. Wright, and Dicken, Connie L., 2001, Preliminary Geologic Map of the Appalachian Piedmont and Blue Ridge, South Carolina Segment: U.S. Geological Survey, Open-File Report 01-298

The Belowground Critical Zone

Hwy 49 Roadcut, Sat pm

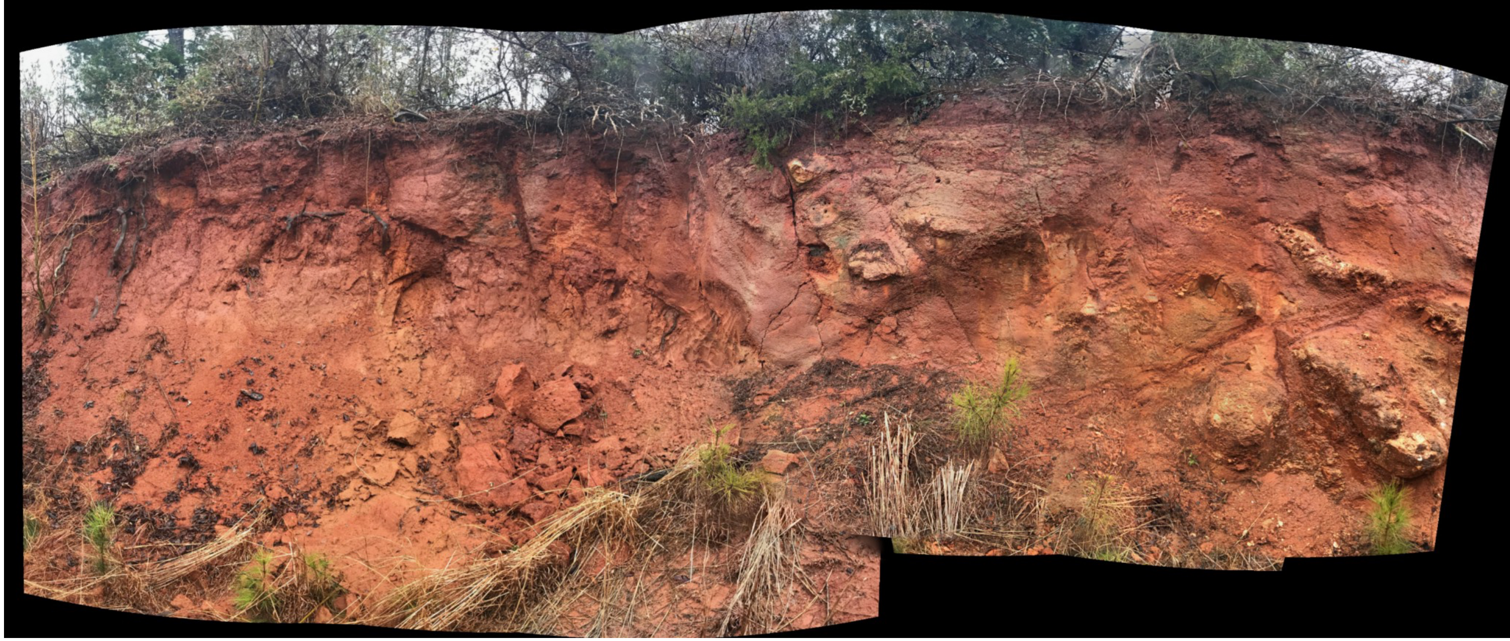

**Mary Lou Quarry, protolith to the Calhoun critical zone**

The preconditioning of bedrock for Earth's critical zone

Anderson 2015

GEOPHYSICS

# Pinched topography initiates the critical zone

## Geophysical imaging provides a clearer picture of how rock turns into soil

*By* **Robert S. Anderson**

In Earth sciences, the critical zone represents the intersection of the biosphere with the atmosphere, hydrosphere, and lithosphere (*1*, *2*). The myriad interactions and feedbacks among these systems assure us of a world with considerable complexity, in which the critical zone varies in thickness, mineralogy, permeability (*3*), and structure of ecosystems (*4*). It is no wonder, then, that we lack a general theory of how the critical zone works. On page xxxx of this issue, St. Clair *et al.* (*5*) argue that we must take the broadest possible view of, and acknowledge a role for, large-scale tectonic stresses in guiding the pattern of cracking of rock in the subsurface.

Consider a hillslope bounded by stream channels (see the figure). Rock is released as transportable particles into the soil on its surface, which then carries the particles through physical and biological transport processes to streams. Water, by contrast, is poured onto the landscape from above, either as rain or as snowmelt, with chemistry that is effectively distilled through evaporation from its source. The water travels downward through the soil, and through rock fractures that ultimately deliver it to the stream. As the water travels, interaction with the minerals of the soil and rock, catalyzed by biological interactions, both changes the strength, porosity, and permeability of the rock, and charges the water with ions that constitute the nutrient supply for plants. The generation of porosity transforms the rock into a substrate capable of sustaining an ecosystem, which in turn, through the action of roots, aids in the breakdown of rock (*2*, *3*). These two trajectories, of rock particles and of water molecules, tangle in the critical zone, where their manifold interactions are indeed critical to life—hence the "critical zone."

The most difficult of these processes to document are those that herald the arrival of rock into the surface environment and initiate its transformation from unweathered fresh rock. Any debate about the relative importance of processes tied to the surface, and those initiated at much greater depths (*6*), in promoting the transformation of fresh rock must ultimately be informed by field data.

Seismic refraction and electrical resistivity methods, often used in deep crustal studies, are seeing greater use in shallow settings (*7*, *8*). St. Clair *et al.* undertook a campaign-style geophysical characterization of the subsurface across ridge-channel pairs in multiple landscapes. They leveraged the geologic and climatic diversity of accessible, well-studied sites within the U.S. Critical Zone Observatory network. Using sites in the humid eastern United States and in the Rockies of the arid western United States, the team found surprisingly different patterns of seismic velocities across the ridge-slope-channel transects. In some sites, low seismic velocities, interpreted as high density of cracks in the subsurface, were confined to a thin surface-parallel layer. In others, the zone of low-velocity, cracked rock extends more deeply beneath the ridges than below the stream channels, generating a "bowtie" image. These very different patterns of deep critical zone structure are not easily explained with climate. The authors used a numerical model of the state of stress in an elastic rock mass into which a landscape has been carved (*9*) to calculate the pattern of expected cracking of the rock. The topographic stresses arise from both the topography itself, and the far-field horizontal stresses imposed by the tectonic setting (arrows in figure) constrained by an existing world map of stresses. As the far-field stresses are increased, the pattern of expected cracking morphs from the surface-parallel to bowtie patterns, capturing both end-members of the observed seismic images. This is indeed an encouraging result.

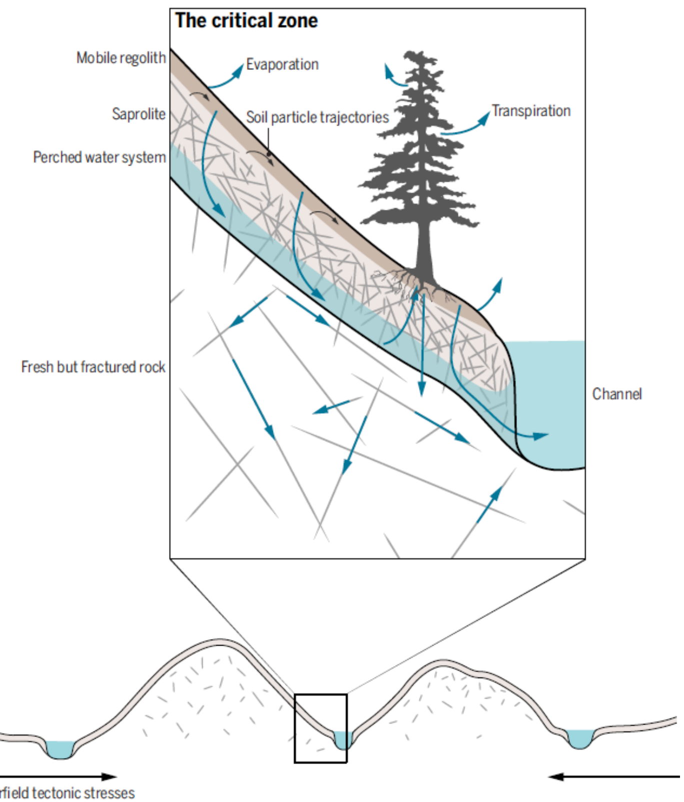


**The critical zone.** Transformation of fresh rock into soil involves cracking of the rock, and chemical attack of its minerals. Coevolution of the permeability of the rock mass, the pattern of water flow (blue arrows), and the ecosystem constitute a complex system that varies in time and location as a result of rock type and climate. St. Clair *et al.* argue that the pattern of cracking of the rock as it nears the surface also depends on topographic stresses, reflecting the interplay between the topography itself and the far-field stresses that pinch the topography (arrows).

Are we to believe their results? In many mountain ranges, the rock arriving in the near-surface zone is already riddled with flaws that have accumulated as it moved through the tectonic stress fields of present and past orogenies (*10*). To what degree does the presence of such preexisting flaws violate the assumption that the rock behaves as a uniform elastic medium? How well does the present state of stress reflect the long-term history of stress to which a rock has been subjected? One can also imagine situations in which other processes that generate near-surface cracks [for example, frost-cracking (*11*)], or that chemically weather the rock as it nears the surface (*12*), are instead the rate-limiting steps in damaging the rock.

Whatever the answers, the results reported by St. Clair *et al.* will challenge the broader community to entertain a role for the state of stress imposed by the topography itself and its tectonic setting. They have also demonstrated the utility of classical geophysical methods and of a network of sites to test their ideas. ■


**REFERENCES**

1. S. P. Anderson, F. von Blanckenburg, A. F. White, *Elements* **3**, 315 (2007).
2. D. deB. Richter, S. A. Billings, *New Phytol.* **206**, 900 (2015).
3. R. C. Graham, A. M. Rossi, K. R. Hubbert, *GSA Today* **20**, 4 (2010).
4. D. T. Milodowski, S. M. Mudd, E. T. A. Mitchard, *Ecology* **96**, 31 (2015).
5. J. T. St. Clair *et al.*, *Science* **350**, XXX (2015).
6. D. M. Rempe, W. E. Dietrich, *Proc. Natl. Acad. Sci. U.S.A.* **111**, 6576 (2014).
7. A. D. Parsekian, K. Singha, B. J. Minsley, W. S. Holbrook, L. Slater, *Rev. Geophys.* **53**, 1 (2015).
8. K. M. Befus, A. F. Sheehan, M. Leopold, S. P. Anderson, R. S. Anderson, *Vadose Zone J.* **10**, 1342, (2011).
9. M. Slim, J. Taylor Perron, S. J. Martel, K. Singha, *Earth Surf. Process. Landf.* **40**, 512 (2015).
10. P. Molnar, R. S. Anderson, S. P. Anderson, *J. Geophys. Res.* **112**, F03014, (2007).
11. R. S. Anderson, S. P. Anderson, G. E. Tucker, *Earth Surf. Process. Landf.* **38**, 299 (2013).
12. M. I. Lebedeva, S. L. Brantley, *Earth Surf. Process. Landf.* **38**, 1793 (2013).


10.1126/science.aad2266

*Institute for Arctic and Alpine Research, University of Colorado, Boulder, CO 80303-0450, USA. E-mail: robert.s.anderson@colorado.edu*

# Geologic Map

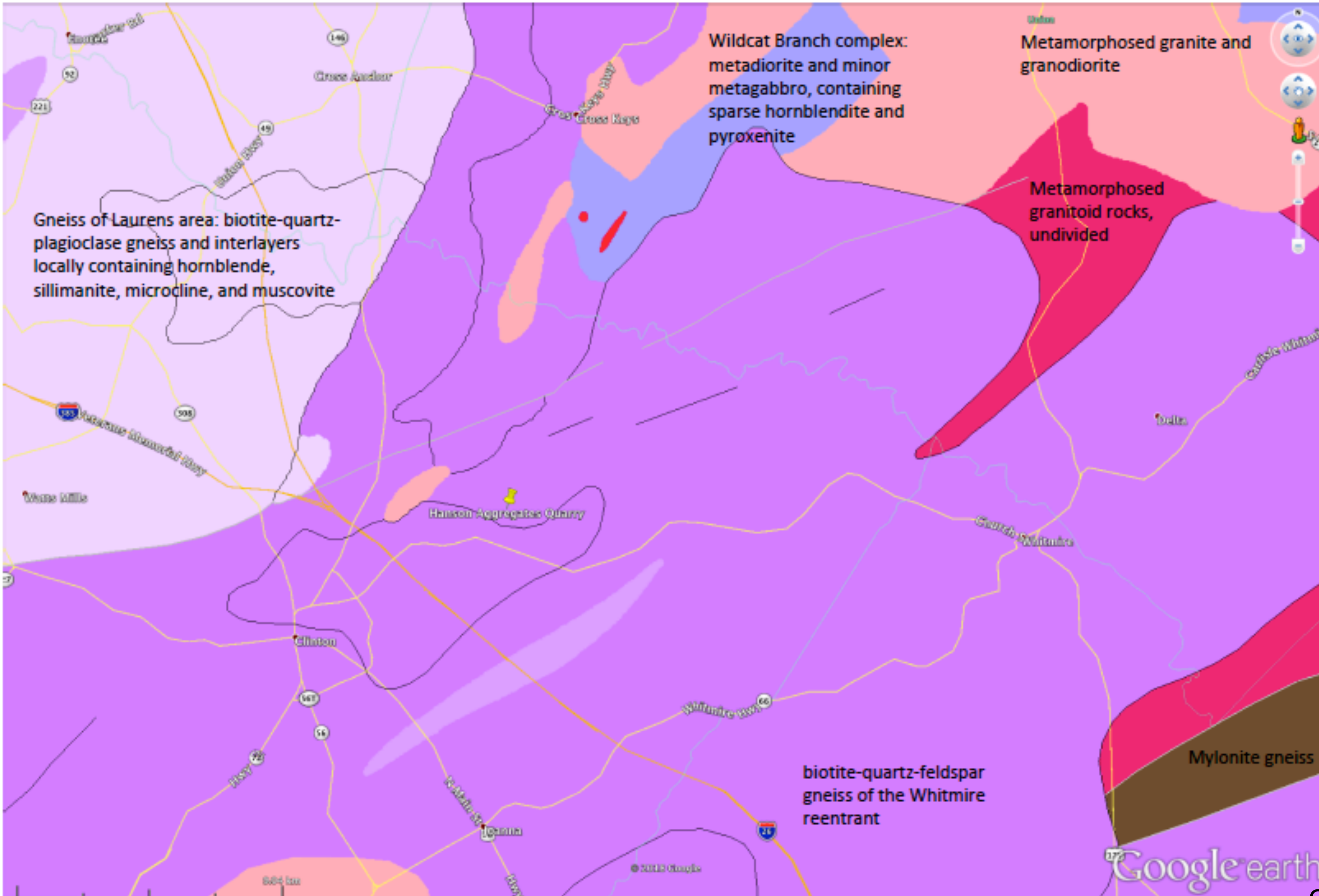

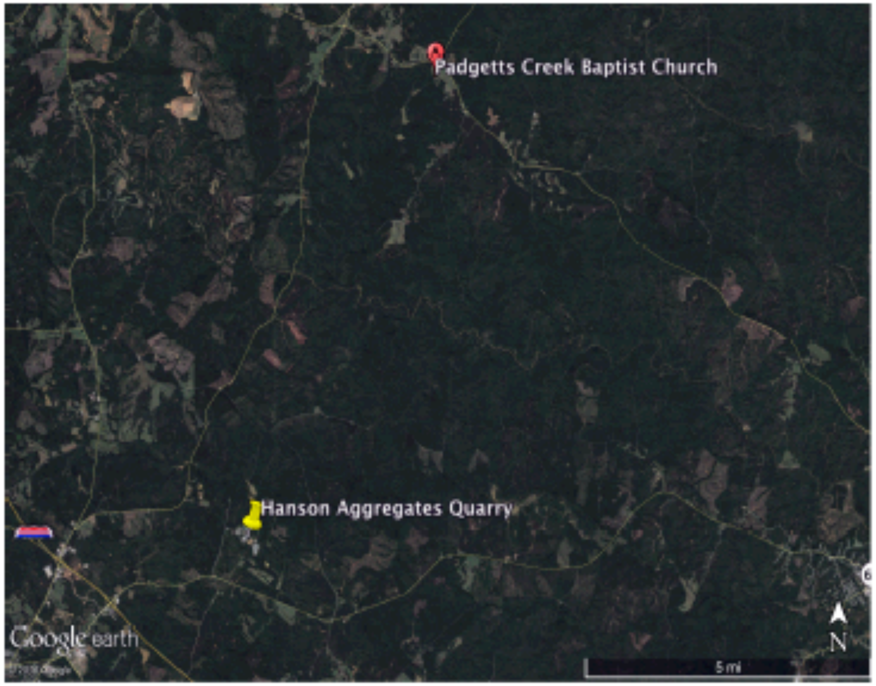
Padgetts Creek Baptist Church
Hanson Aggregates Quarry
Google earth
5 mi
N

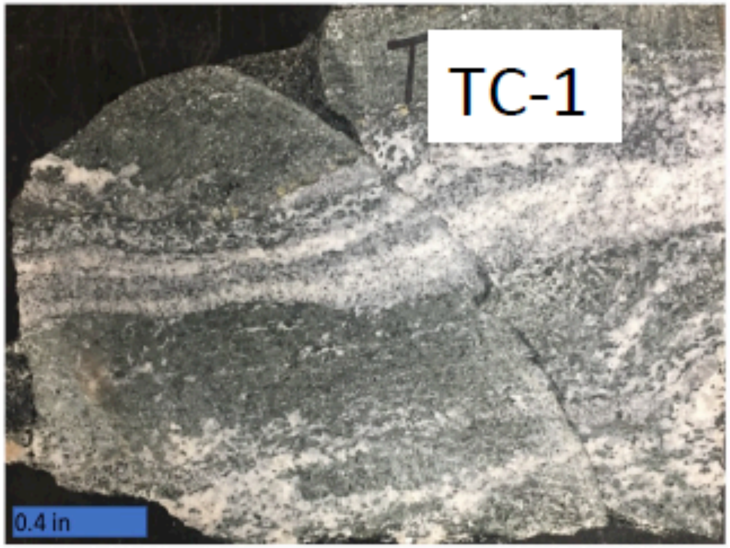


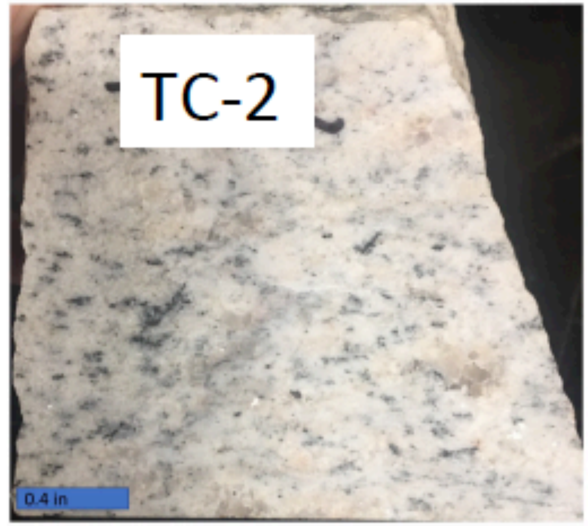



Tremolite
Biotite

Quartz
Plagioclase

Chlorite
Biotite

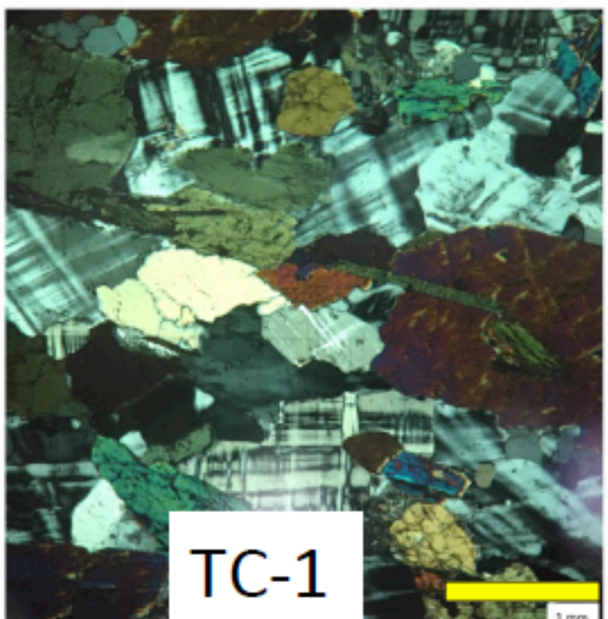


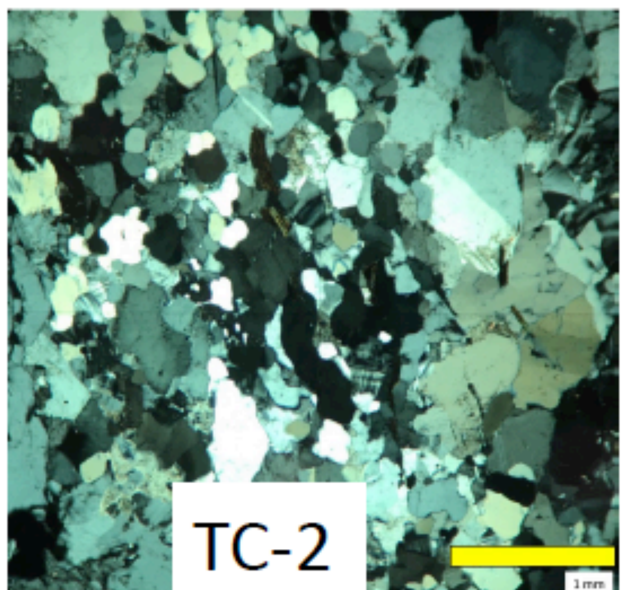


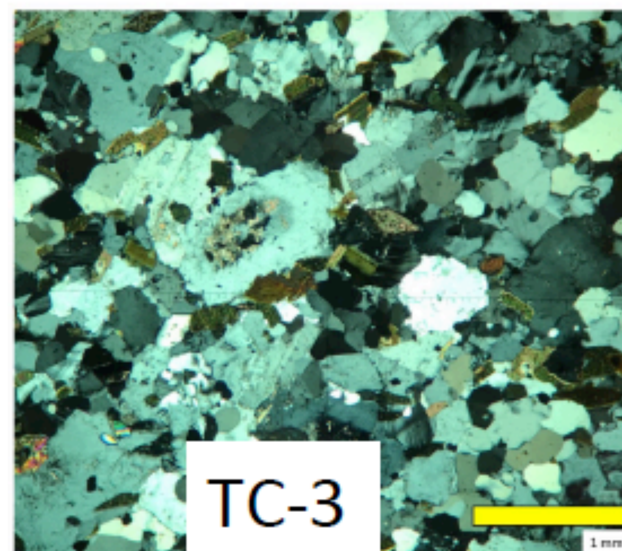

Mary Lou Rock Samples

# X-ray Powder diffraction

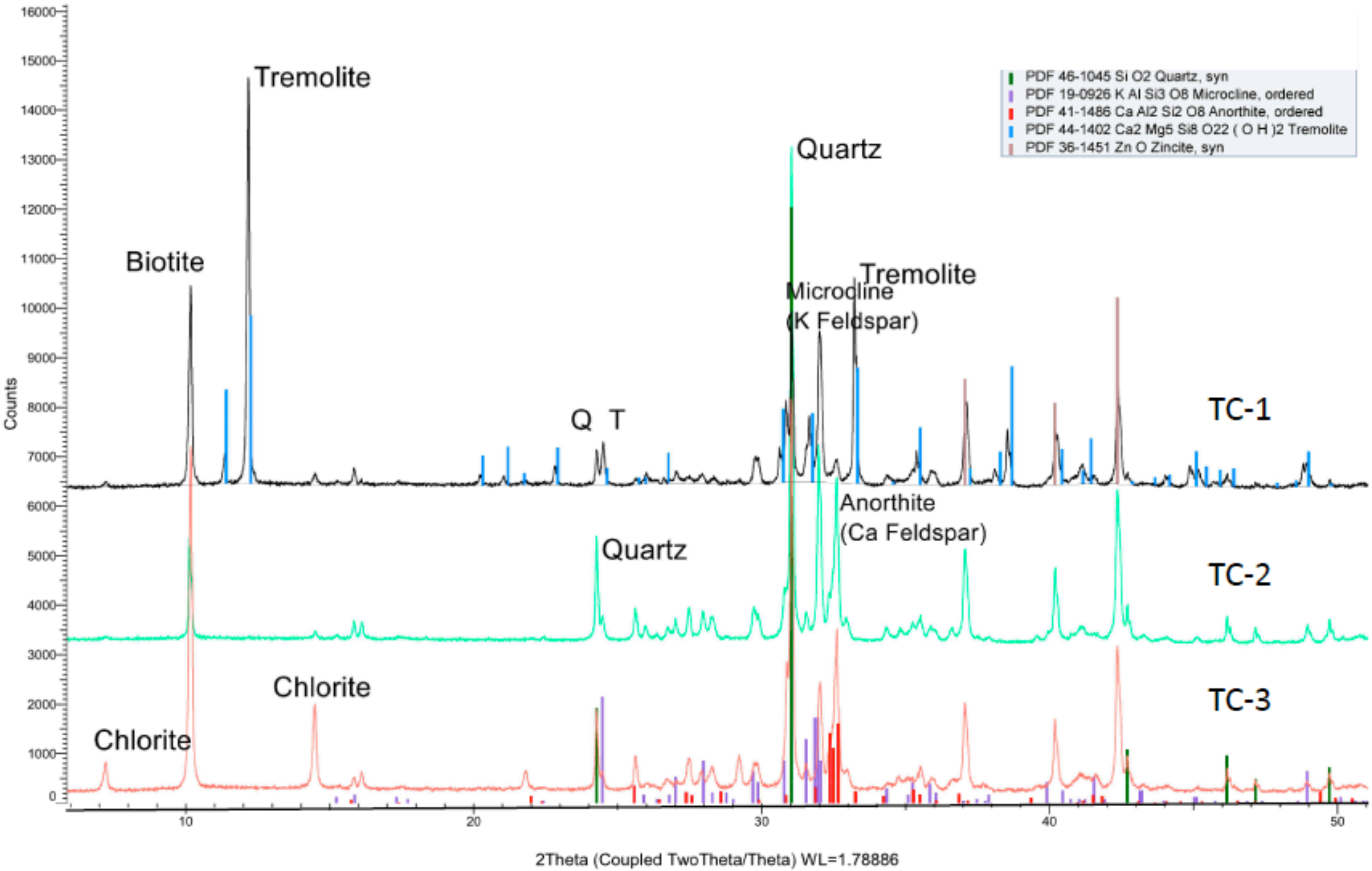

Welcome to Padgett's Creek Baptist Church †

and to the *understudied* ***but remarkably exciting***, *rolling Piedmont!*

Start with a topo map to illustrate how far we have come!!

Compare with next image from LiDAR data of same landscape

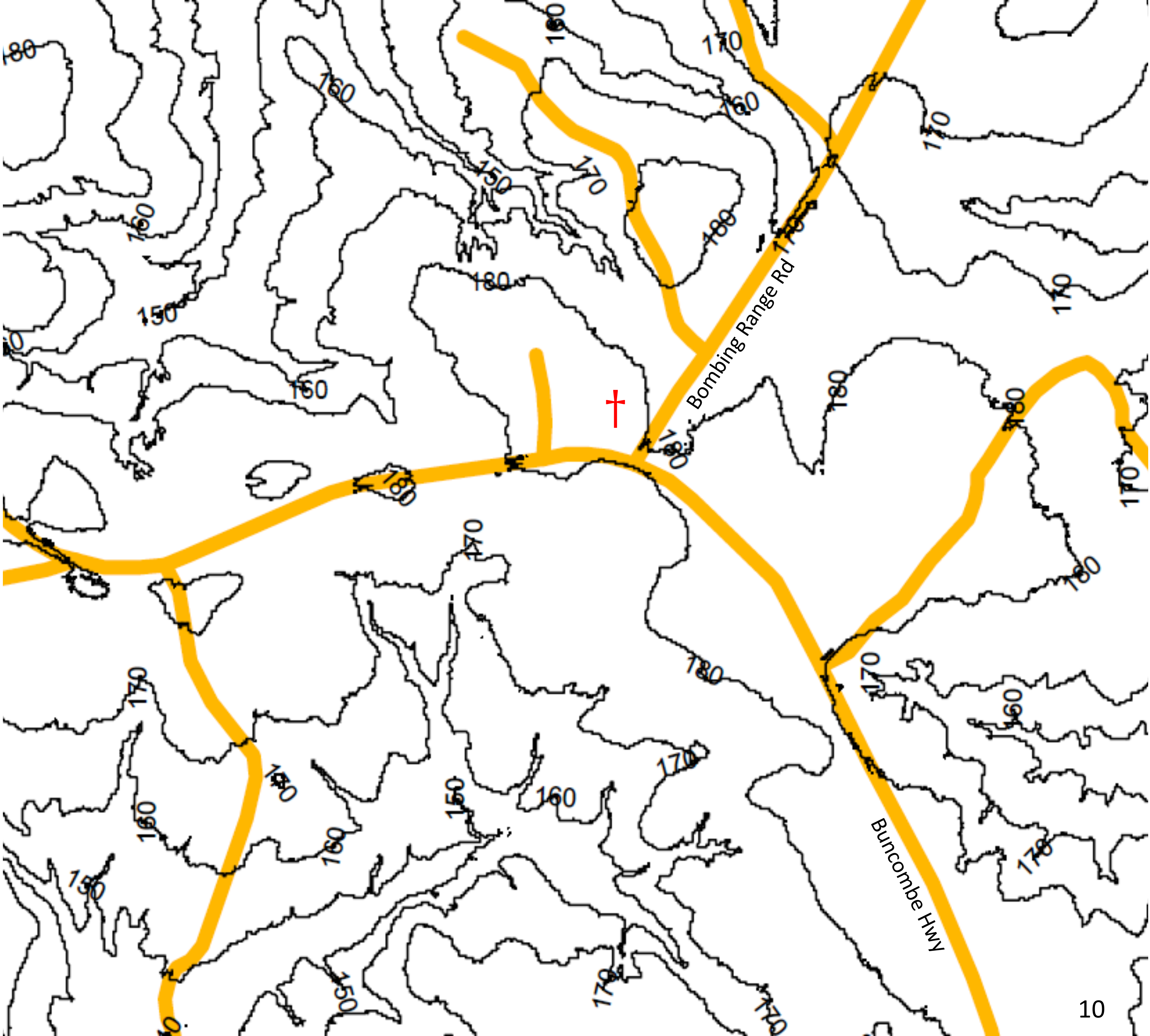

Welcome to Padgett's Creek Baptist Church †

and to the *understudied but remarkably exciting, rolling Piedmont*

The vista from church is of broad, low-curvature landforms, common to much of the Southern Piedmont

Ancient landforms, roughly in steady state, with v slow weathering & erosion.

Textbook vision:
Soil and regolith that is 10s meters in depth, covering weathering crystalline bedrock.

High resolution $100\ km^2$ LiDAR on opentopography.org w/ >50 ground returns per sq meter!

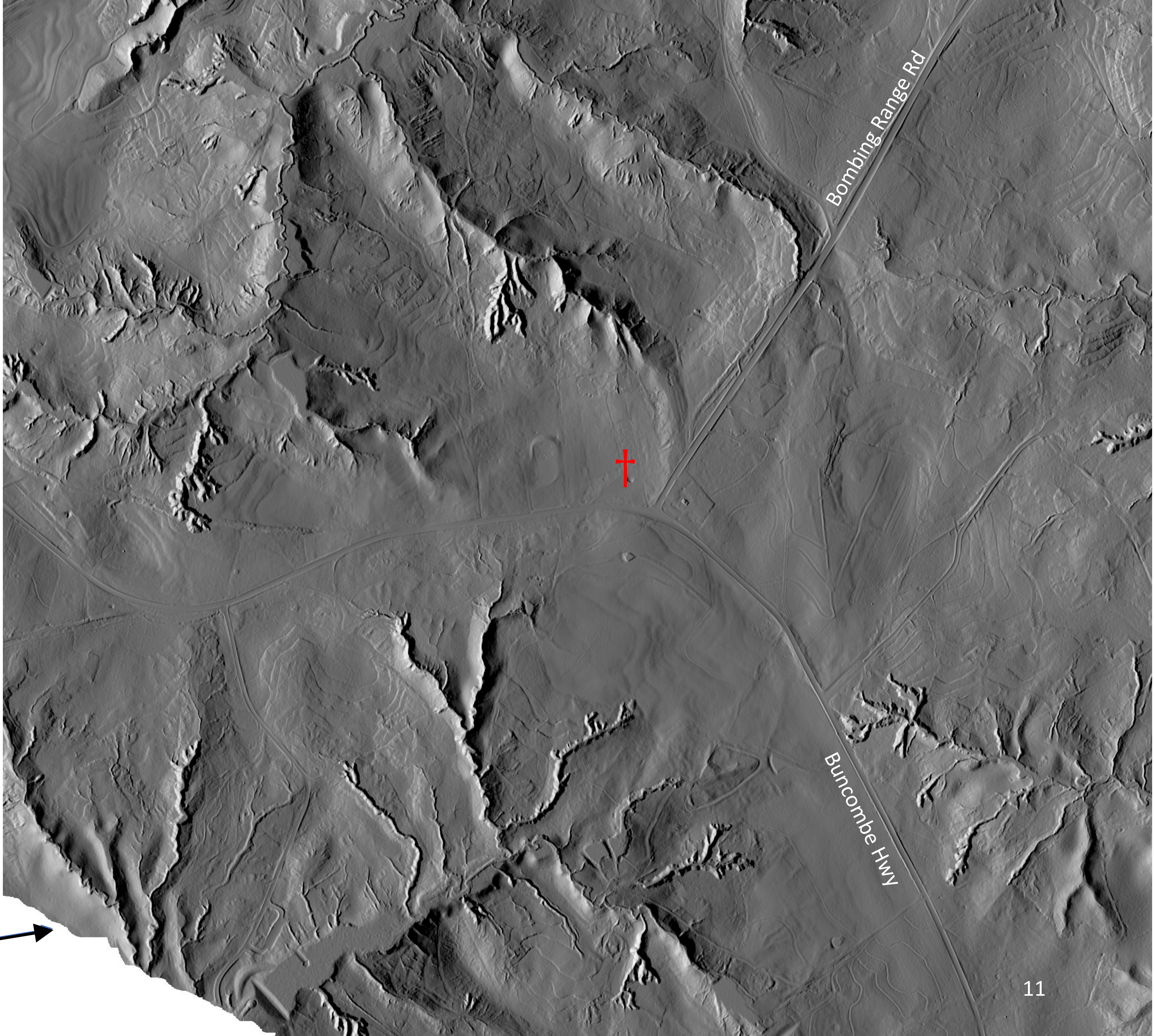

2013 NAIP aerial


**Research Area 1**

1. 70-m deep well, with 38-m regolith
2. Cataula soil profile
2. 60-year LTSE

3. LT Cultivated Field (Dove Field)
4. Reference Hardwood

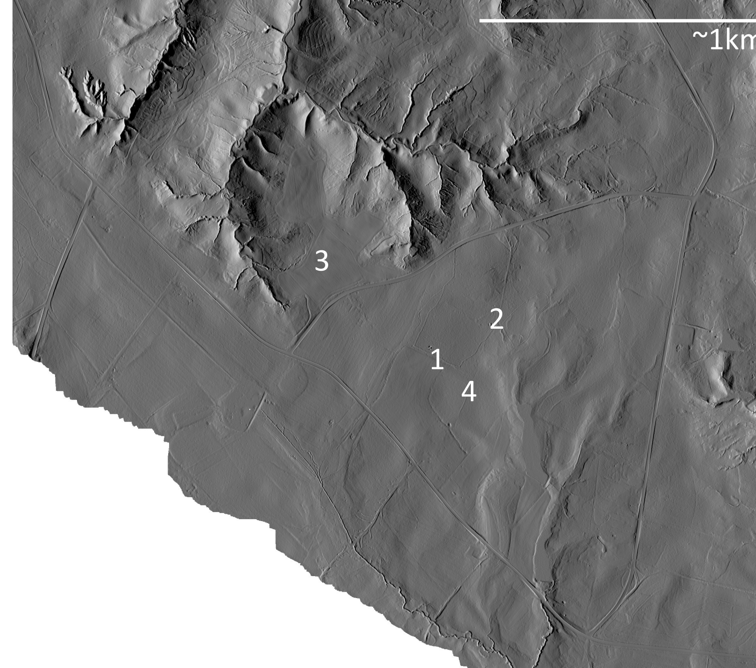


Feb 2016 High resolution LiDAR

1933 USFS Purchase Photo

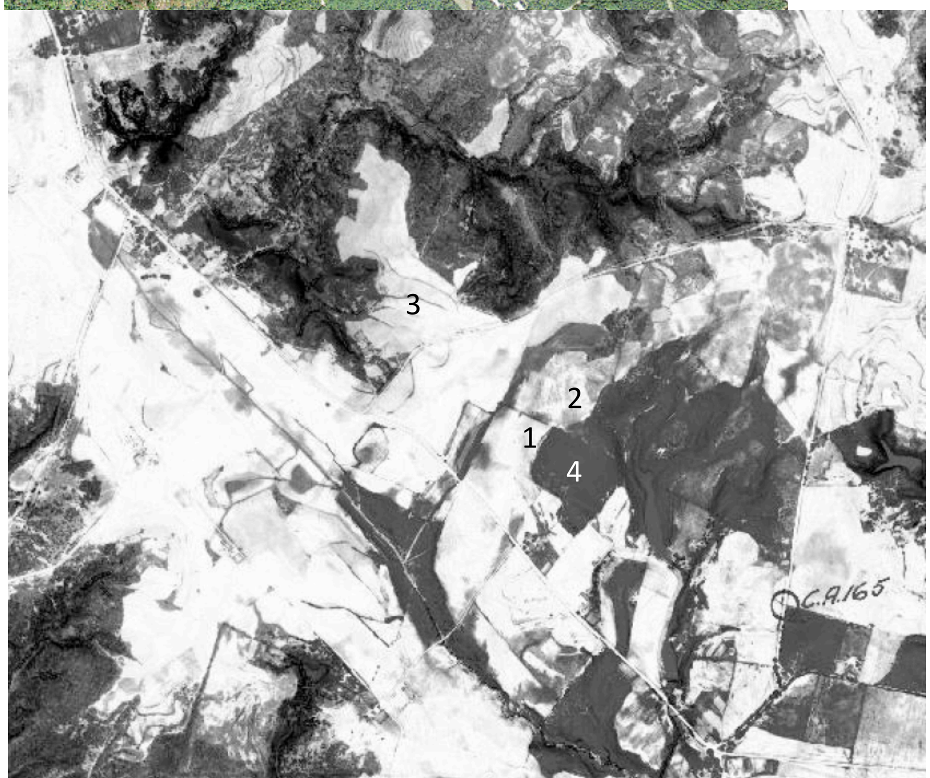


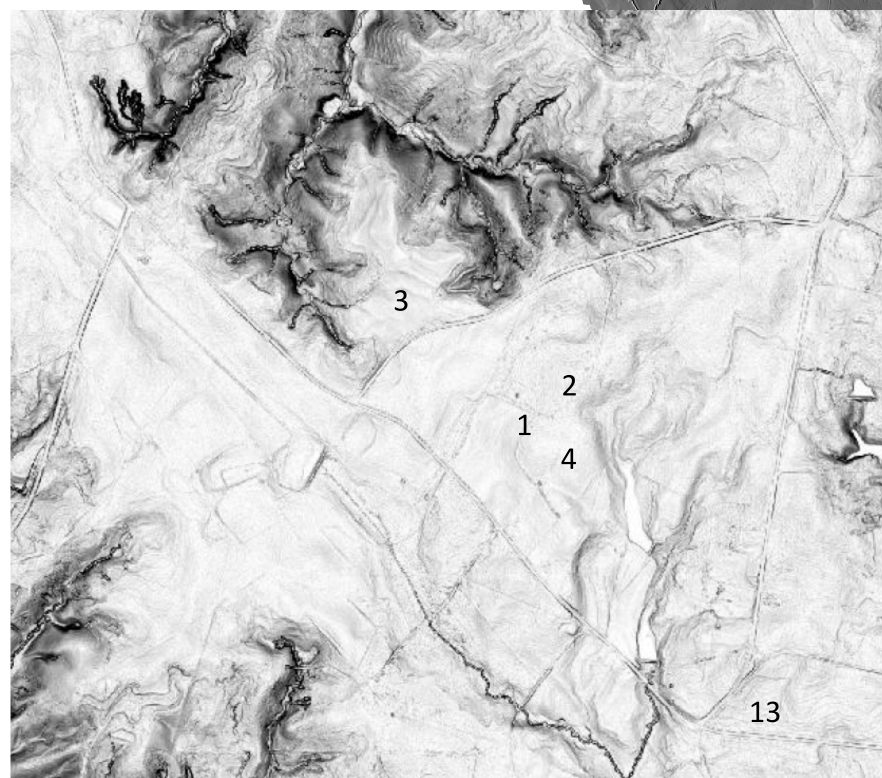


2008 Slope map from SC statewide LiDAR

# Soil as a Clay Factory -

- ~ 25% of soils globally have coarse-over-fine textures,  aka COF
- Nearly always attributed to e/illuviation, ie, lessivage
- Argillic (Bt) horizons
- Pedoturbation & lessivage

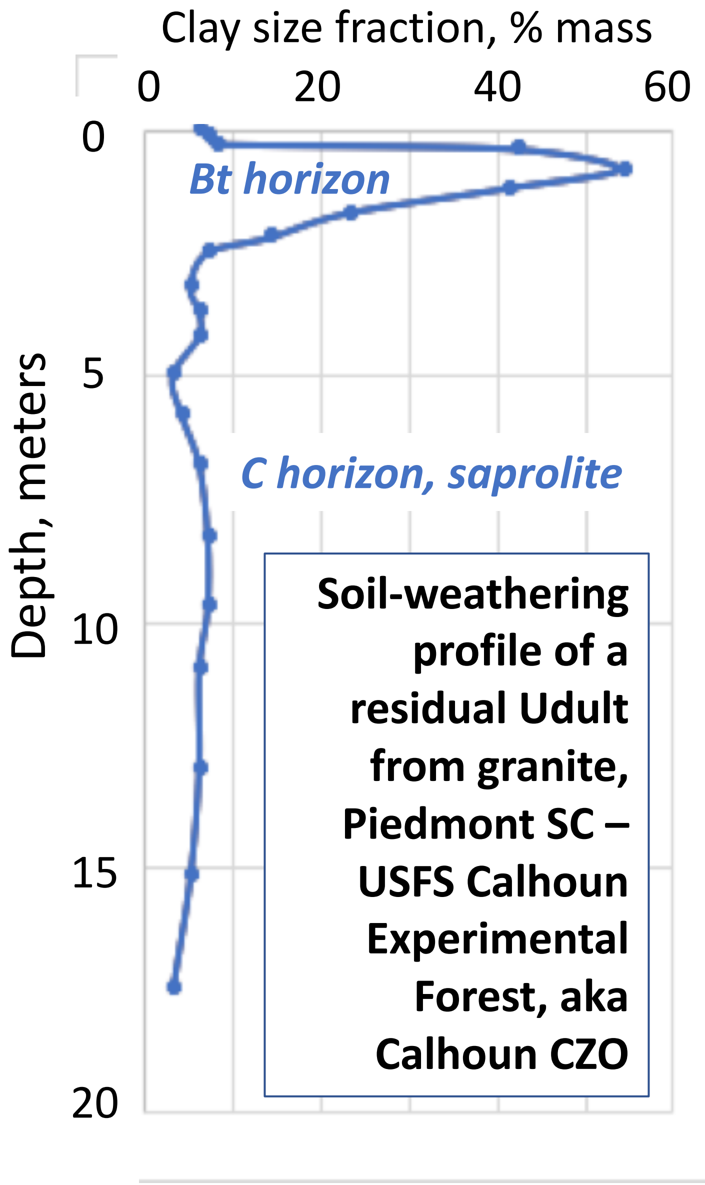

# Soil or Regolith Production –

from “an unrecognized pedologist”, Grove Karl Gilbert, one of Dutton’s ensemble along with John Wesley Powell

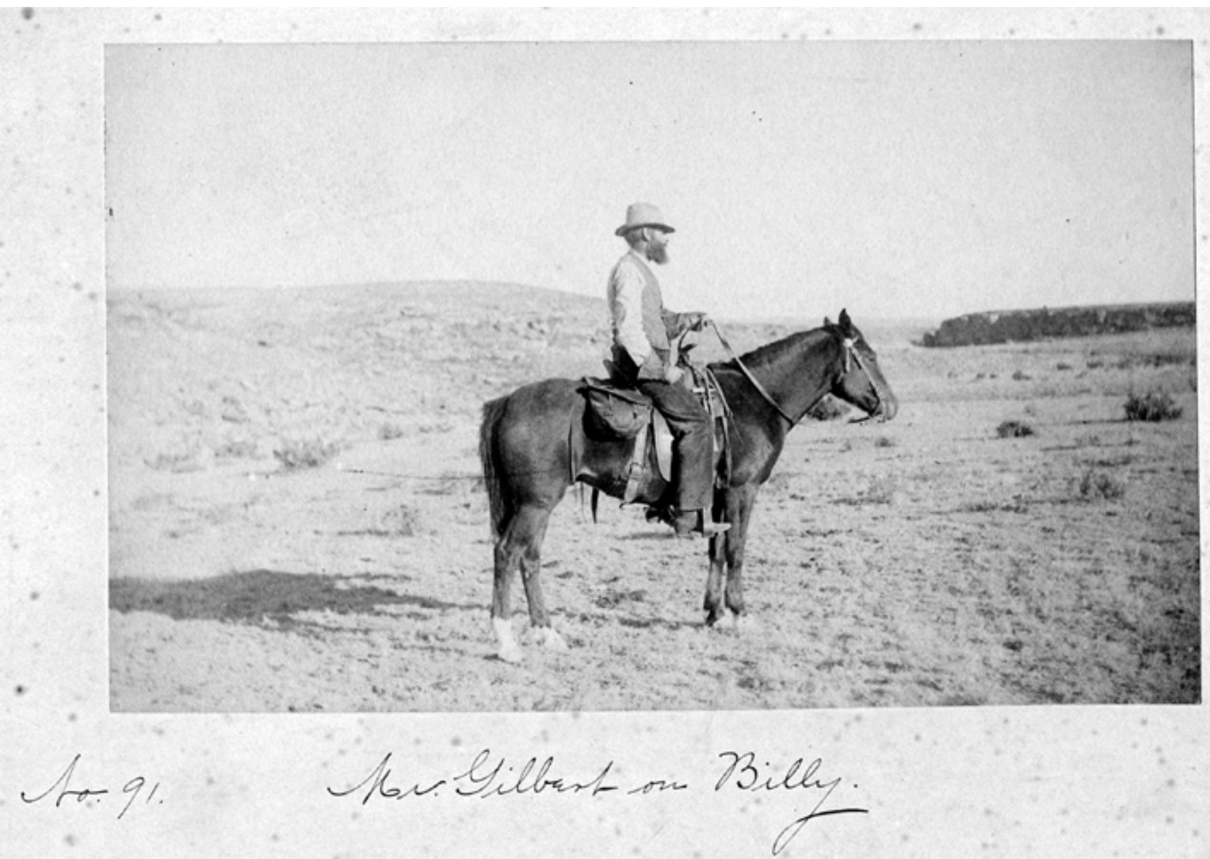


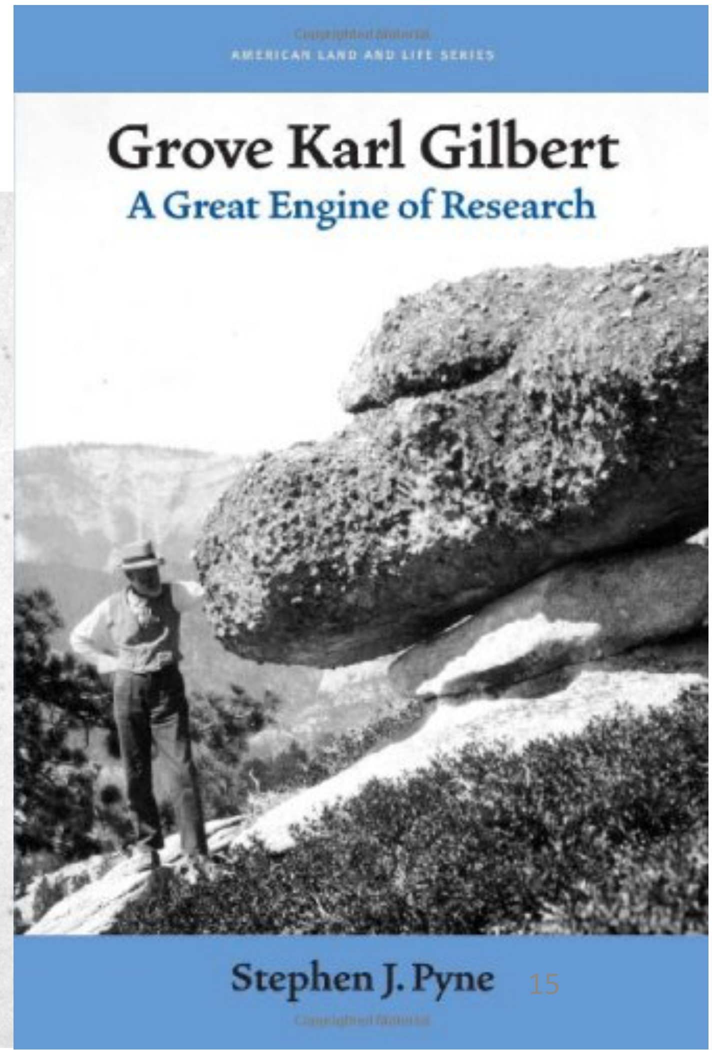

In 1877, G.K. Gilbert, in the *Geology of the Henry Mountains*, stated with wonder,

"Over nearly the whole of the earth's surface, there is a soil, and wherever this exists we know that conditions are more favorable to weathering than to transportation."

***Weathering-*** the liberation of particles & solutes from parent rock

***Transportation-*** the erosional & soluble loss of the products of weathering

Gilbert‘s soil, later to be called “regolith“ by Merrill (1898) a fundamental attribute of Earth

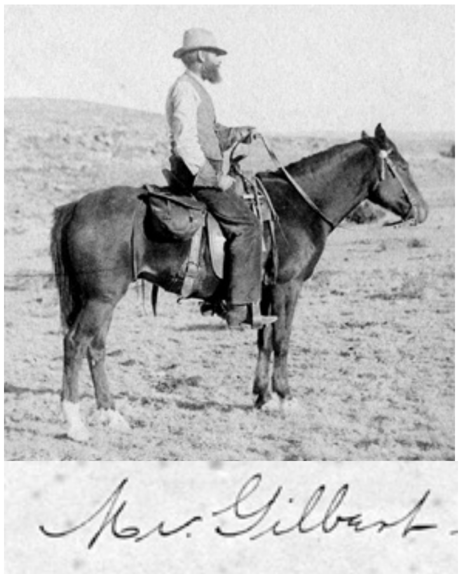


Remarkably, Gilbert‘s work went uncirculated until re-discovery by geomorphologists & landscape evolution modelers

# Gilbert's ideas on soil have formally been introduced to the soil sciences, "a fly yet to be taken"

Available online at www.sciencedirect.com

ScienceDirect

ELSEVIER

Geoderma 139 (2007) 73 – 78

GEODERMA

www.elsevier.com/locate/geoderma

## The soil production function: A brief history and its rediscovery

Geoff S. Humphreys *, Marshall T. Wilkinson [1]

*Department of Physical Geography, Macquarie University, NSW, 2109, Australia*

Received 4 January 2006; received in revised form 16 December 2006; accepted 8 January 2007
Available online 15 February 2007

Humphreys & Wilkinson 2007 *Geoderma*

Gilbert's simple & elegant expression of soil or regolith production

across most of Earth's surfaces, climates, lithologies, biomes, anthromes, there is a soil or a regolith,
i.e., over time,
W > T

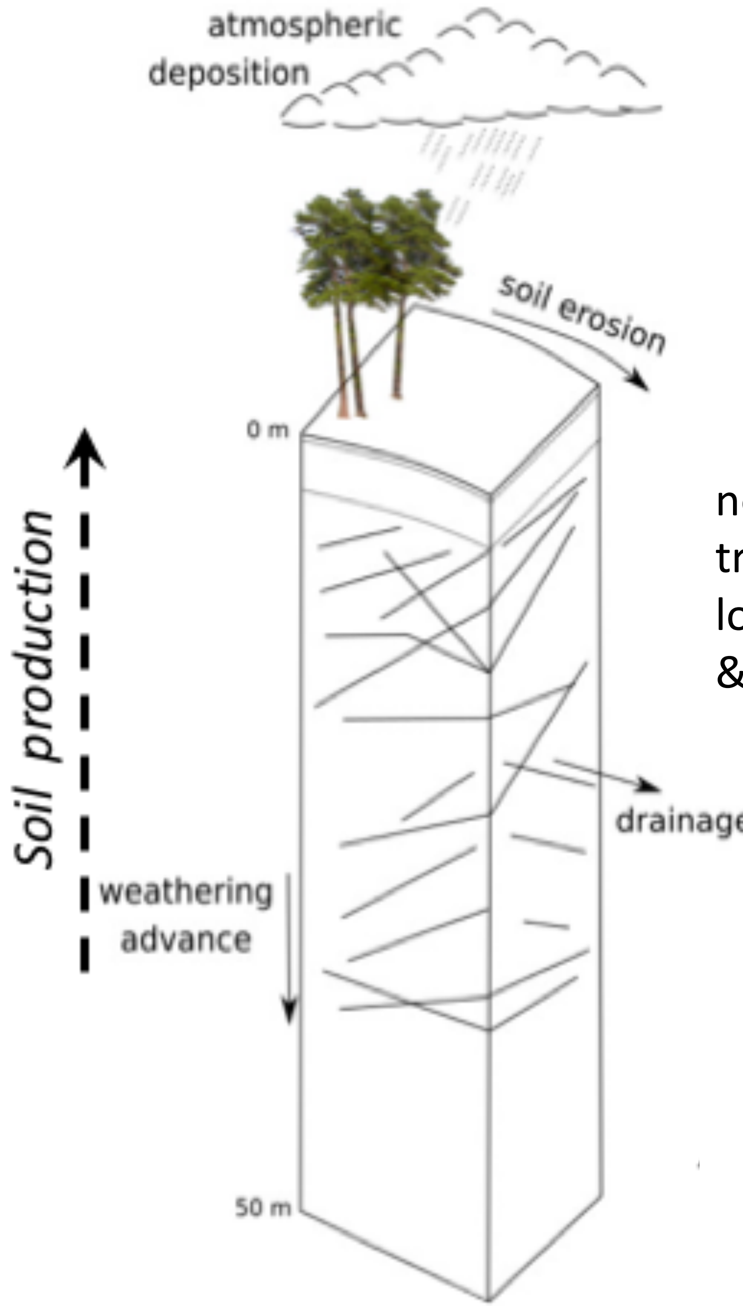


net transportation losses, erosion & drainage (T)

# To study the full weathering profile, Bacon led a bore hole drilling project, down 38-m thru soil, saprolite, & weathered & fractured granite, & ~30-m into the protolith itself.

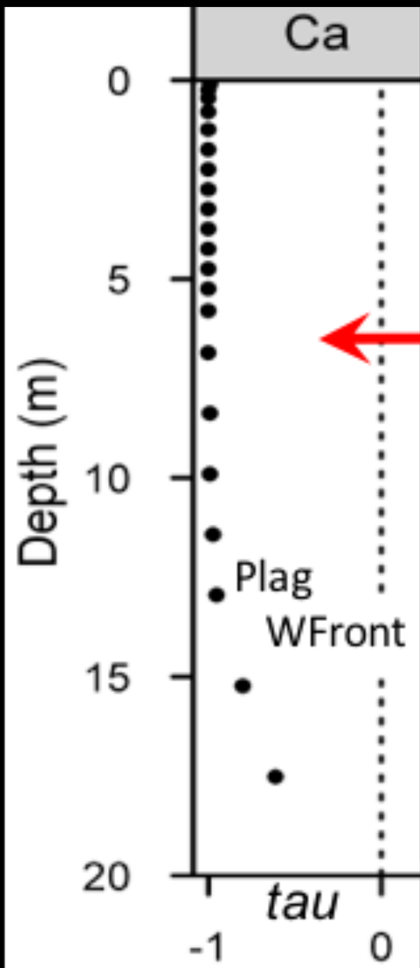


Element mass balances

Seismic velocities across the landscape, Holbrook et al. in review

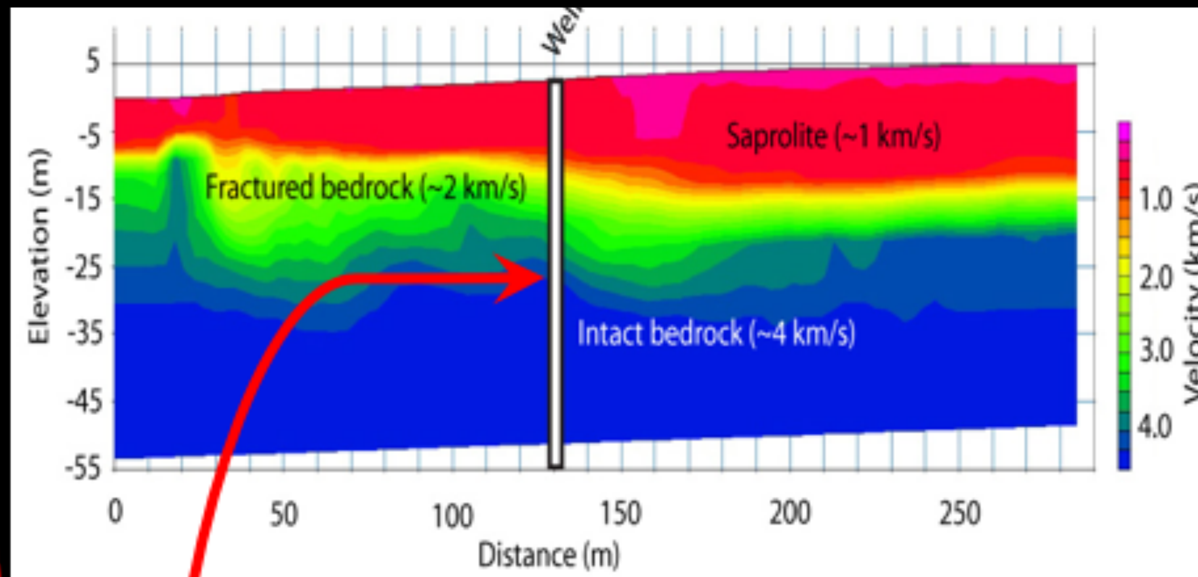


- $^{10}Be$ residence time >2 million y!
- Weathering fronts 12-40-m!
- pH ~4 to 12-m!
- Bacon et al. 2012 *GEOLOGY*

# The soil-weathering profile, regolith, as a physical structure

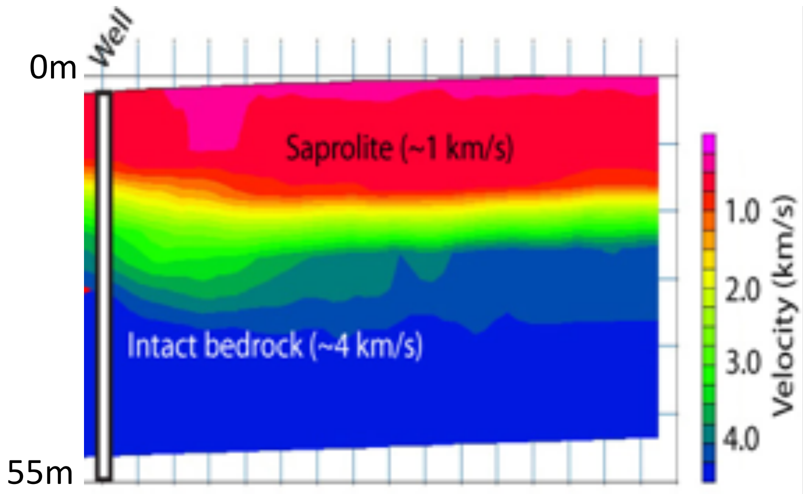


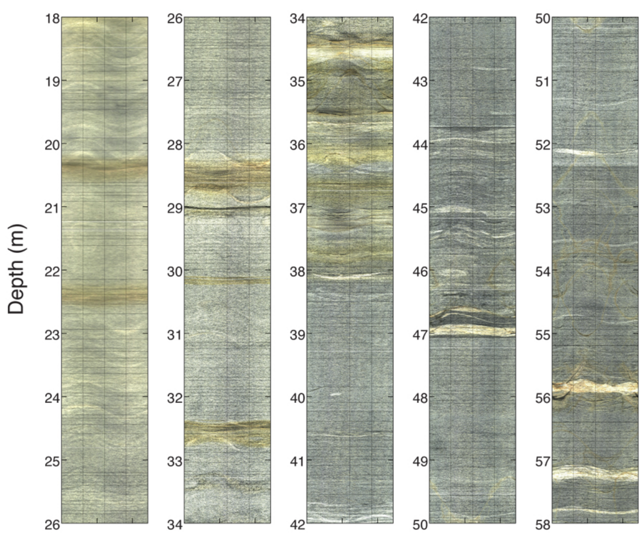


360° optical image of borehole wall

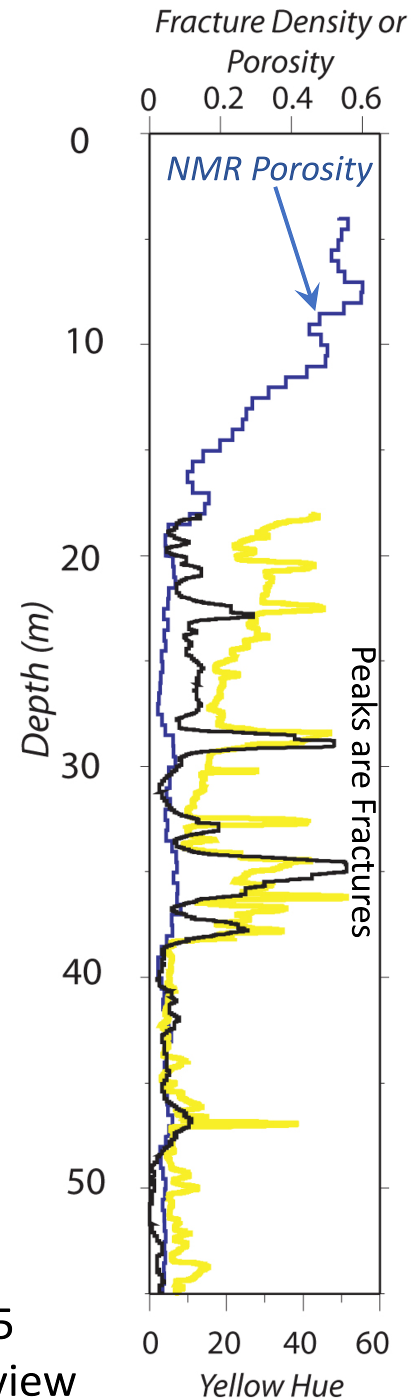


Downhole science

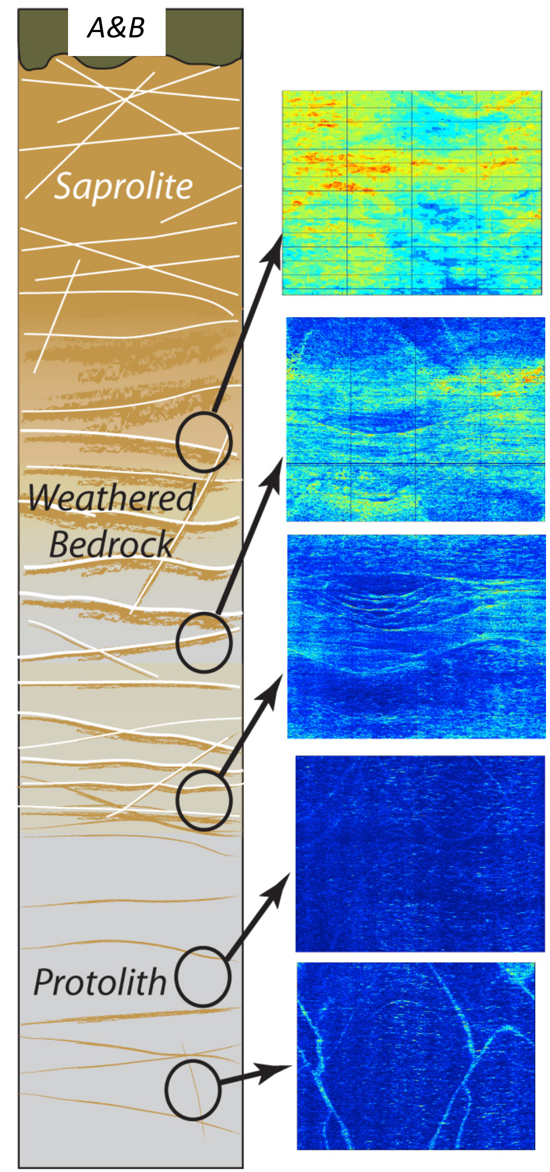


St. Clair et al., 2015
Holbrook, et al., in review

# Two processes that drive regolith formation

1. Regional/local-topographic stresses fracture & *precondition* bedrock for the critical zone (bottom up)

Seismic velocities (km/s) estimated by WyCEHG

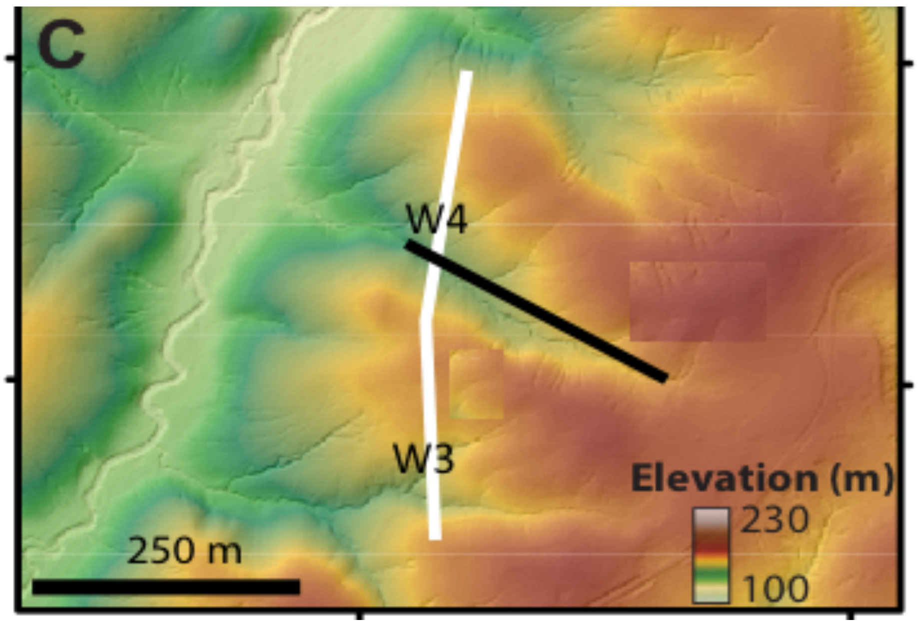


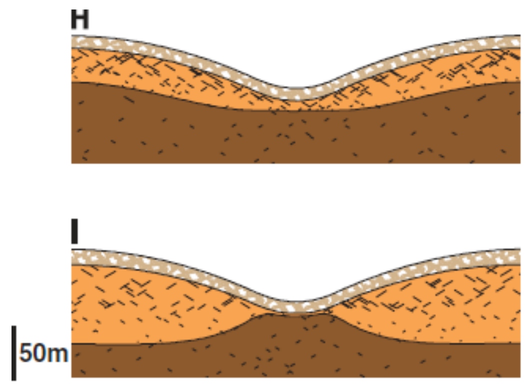


Textbooks

Stress modelling, Seulgi Moon – St. Clair et al. 2016

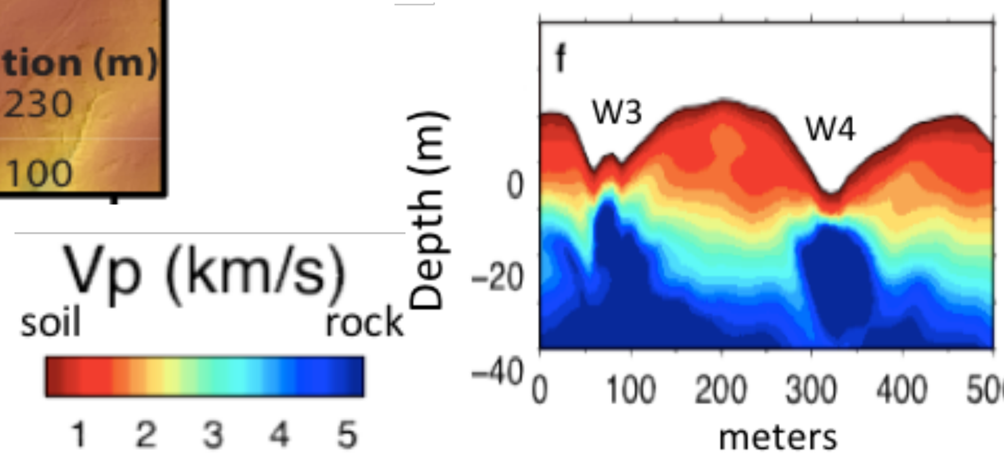


Calhoun's observed seismic velocity "bowtie" in St.Clair et al. 2016, SCIENCE 350

**Processes that drive weathering & regolith formation**

C cycle
Duke FACE
Forest

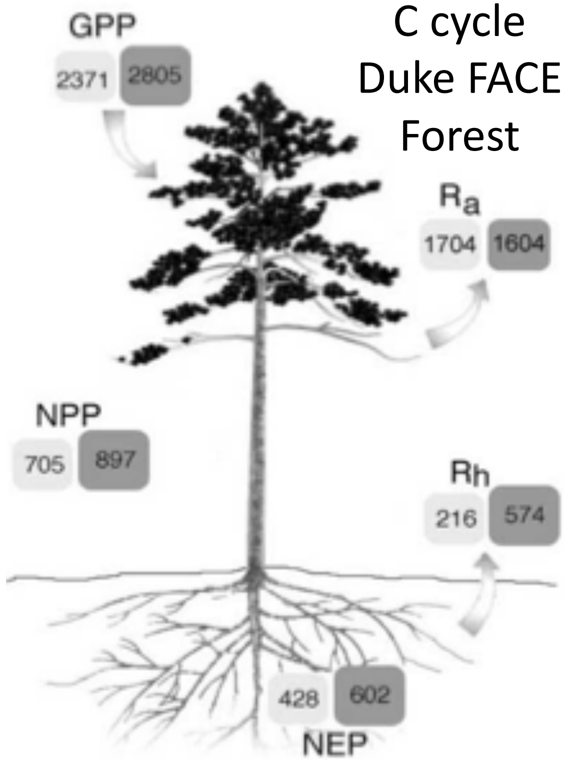


Finzi et al. 2005, gC/m$^2$ y

## <u>2. Carbonic acid dissolution -</u>

Soil/CZ metabolism, ie, soil respiration, affects a potent bgc weathering attack on weatherable minerals

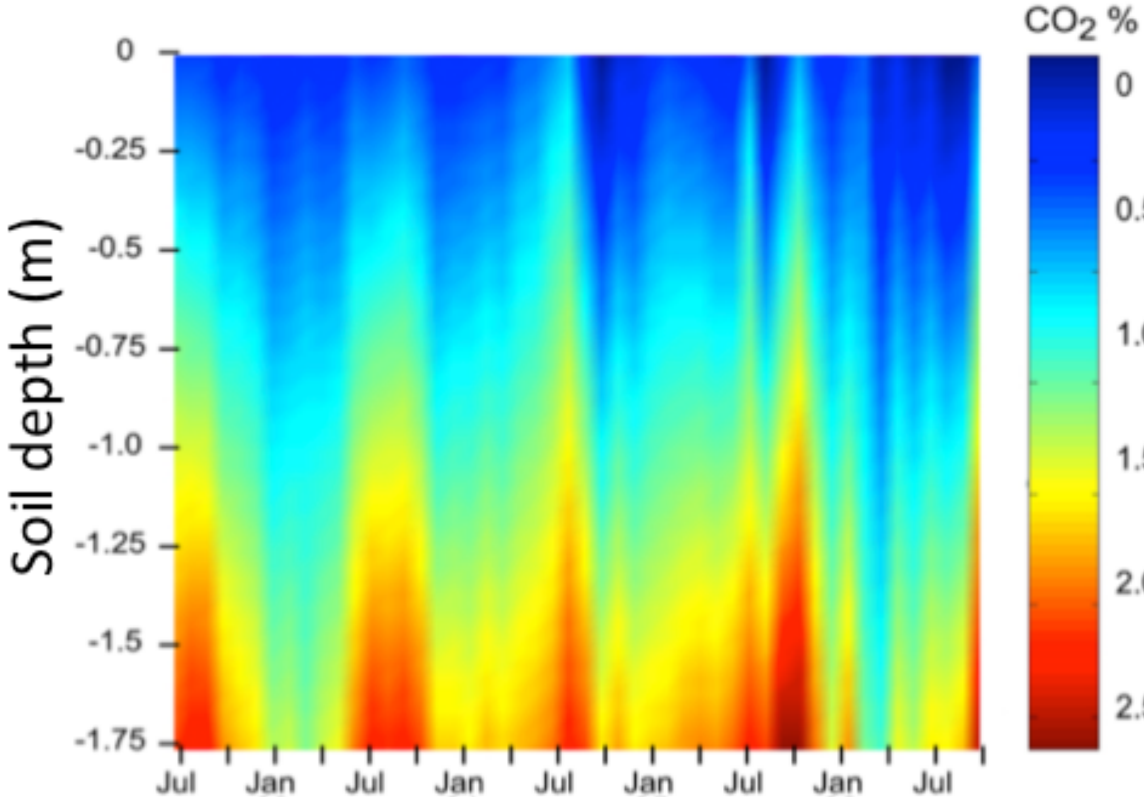


Four years of Dan Markewitz $CO_2$ data from Calhoun mid-1990s

**<u>Hypo</u>**: a small fraction of $CO_2$ & $H_2CO_3$* from soil respiration drives deep biogeo*chemical* weathering

Oh & Richter 2005

# Zach Brecheisen's soil $CO_2$ & $O_2$ research

$$CO_2 + H_2O \underset{\textit{respiration}}{\overset{\textit{photosynthesis}}{\rightleftharpoons}} CH_2O + O_2$$

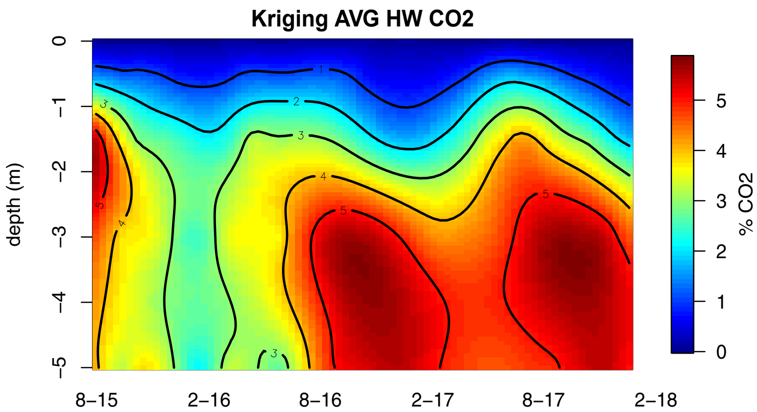


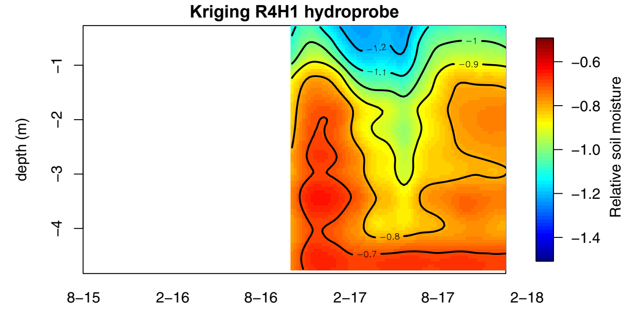


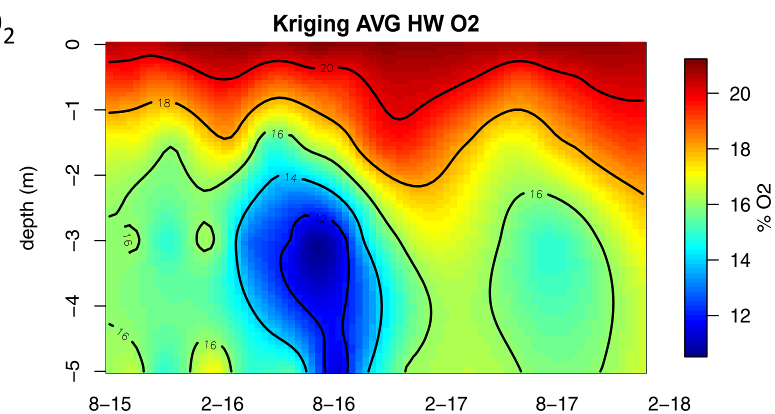


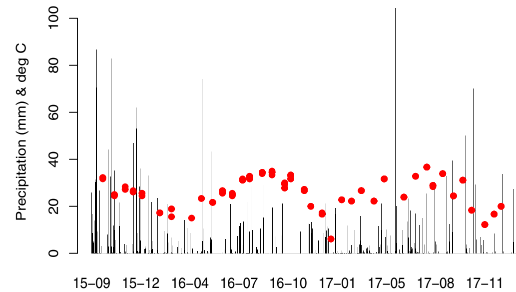


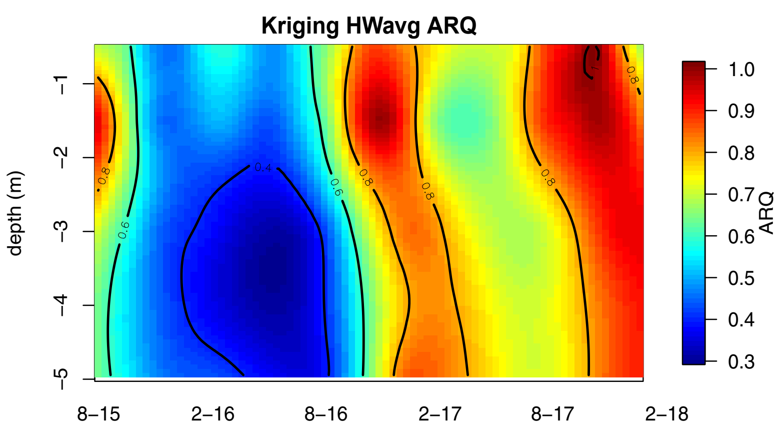


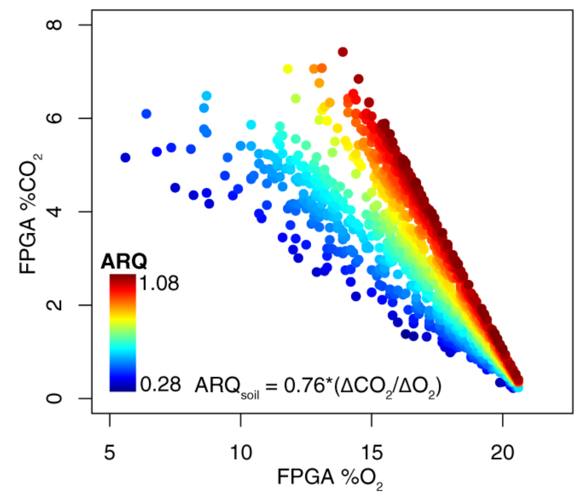

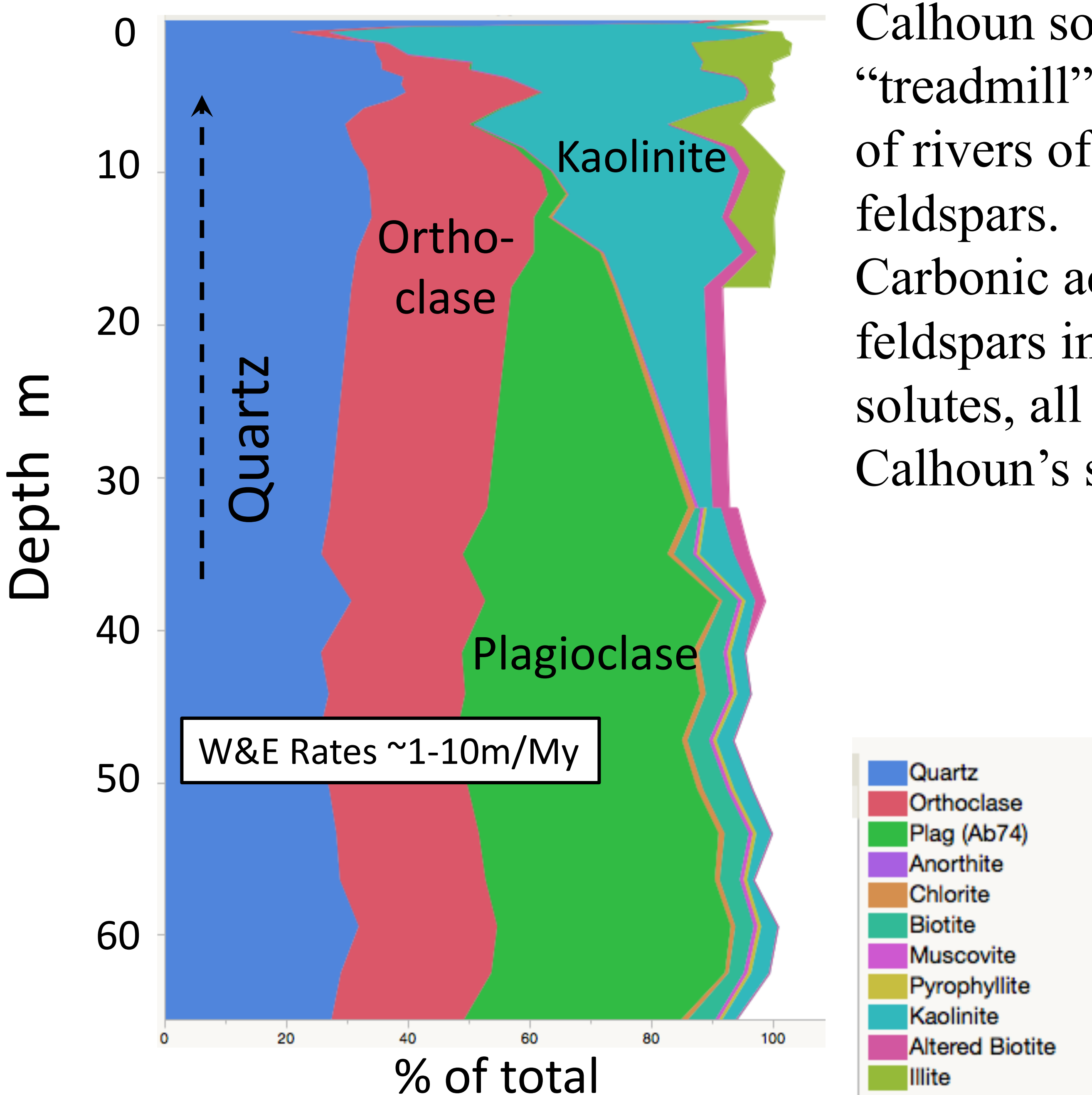


Calhoun soil production "treadmill" composed of rivers of weathering feldspars.
Carbonic acid dissolves feldspars into kaolinites & solutes, all within 'the Calhoun's soil clay factory"

Total elementals
Bacon et al. 2012

Geochem model
V. Marcon, &
S. Brantley, PSA

# Remarkable are depth distributions of particle sizes

- ~ 25% of soils globally have coarse-over-fine textures, aka COF
- Nearly always attributed to e/illuviation or lessivage
- Argillic (Bt) horizons indicate that lessivage keeps pace with bioturbation

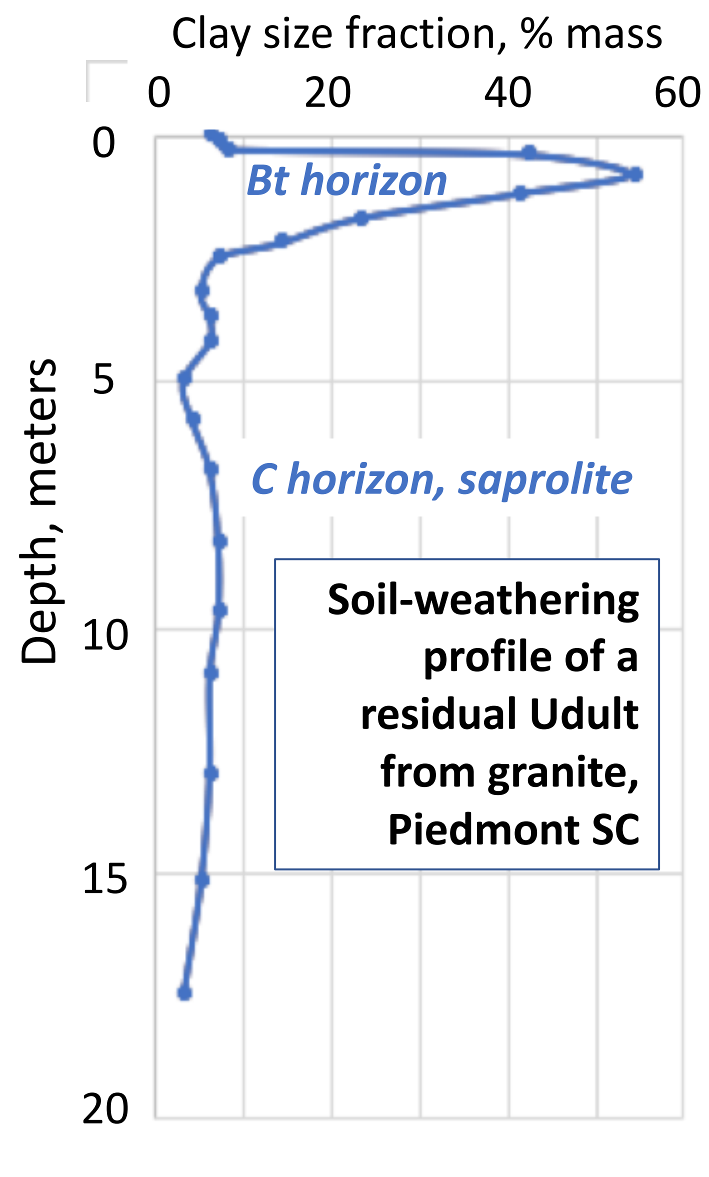

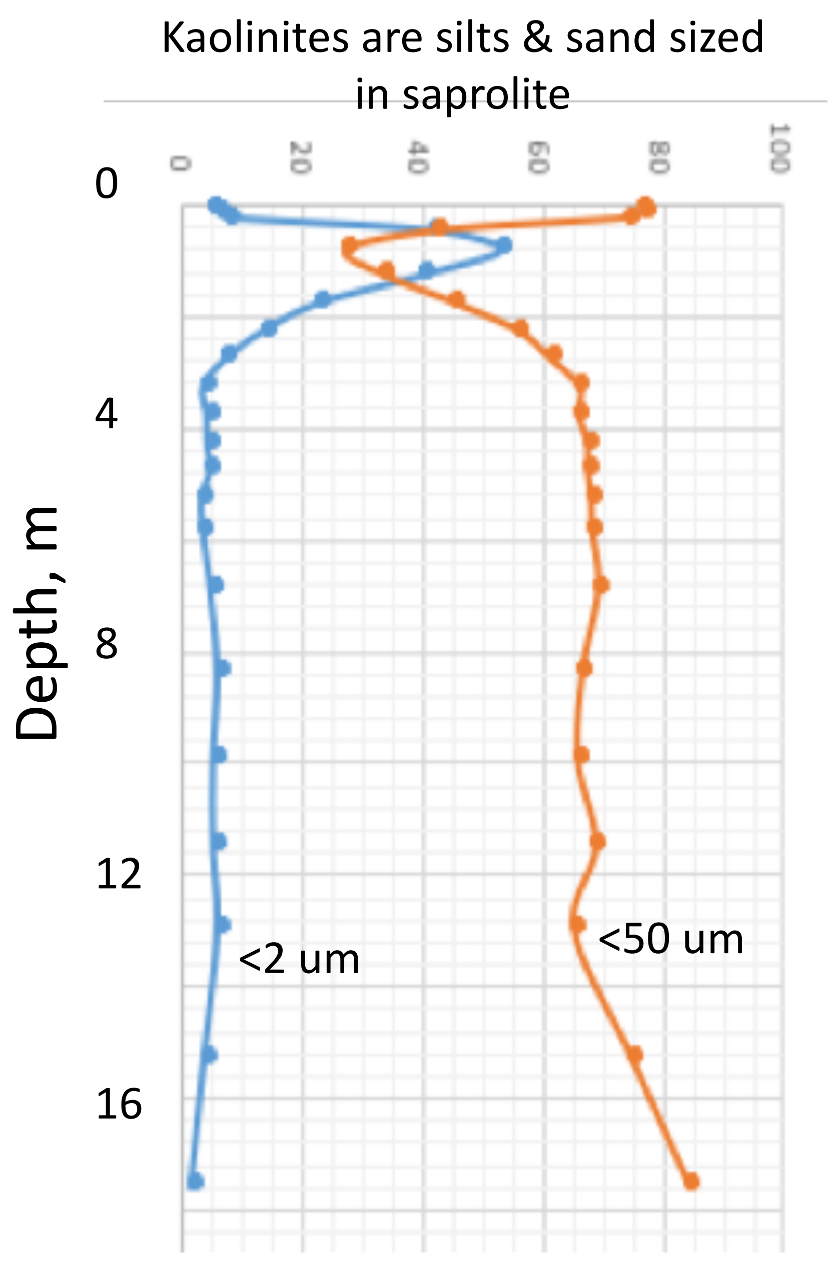
Kaolinites are silts & sand sized in saprolite
0
20
40
60
80
100
0
4
8
12
16
Depth, m
<2 um
<50 um

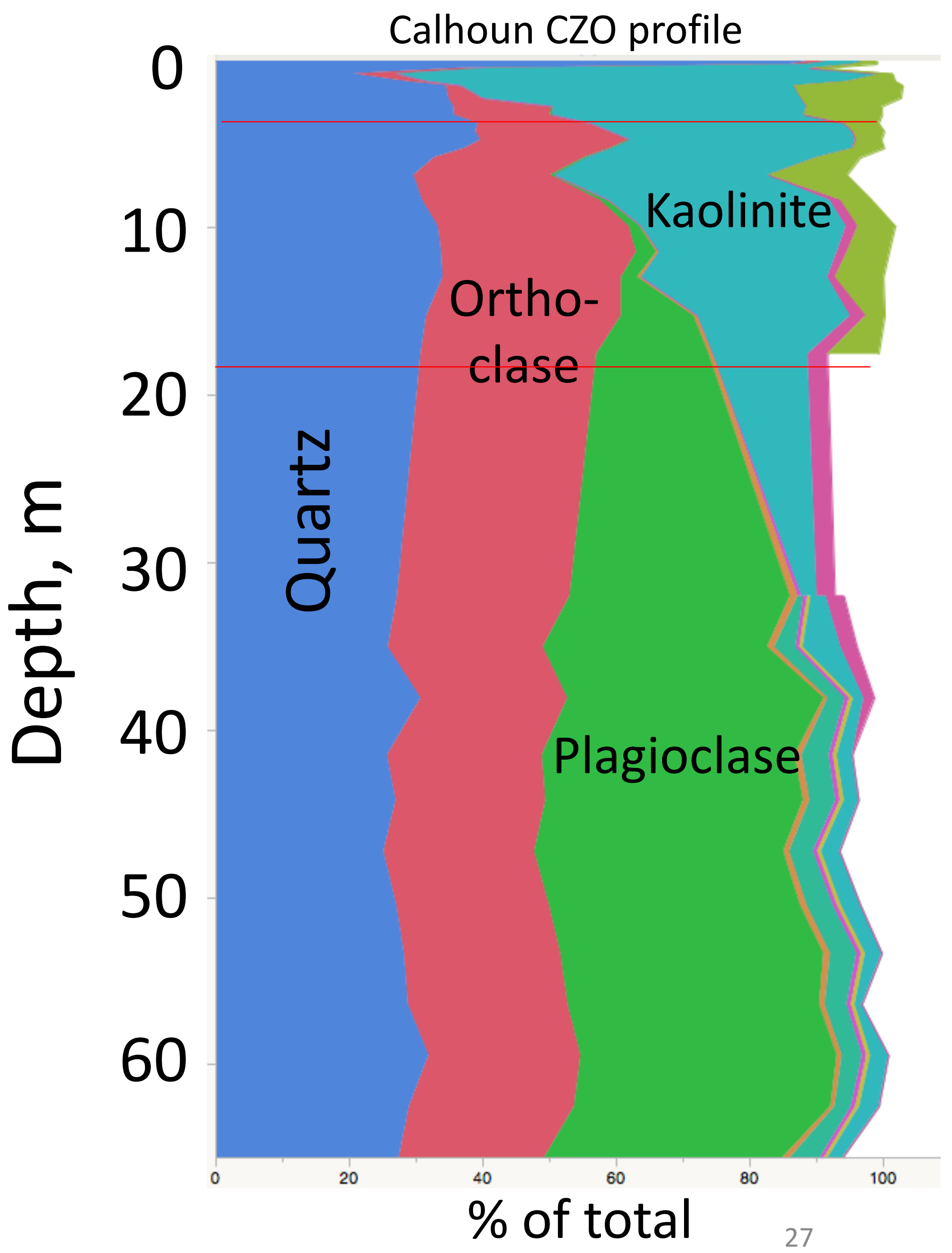
Calhoun CZO profile
0
10
20
30
40
50
60
Depth, m
Quartz
Ortho-clase
Kaolinite
Plagioclase
0
20
40
60
80
100
% of total

Hypothesis: Argillic clay depends as much on the soil production system, what it is fed from below, as it does on lessivage or e/illuviation

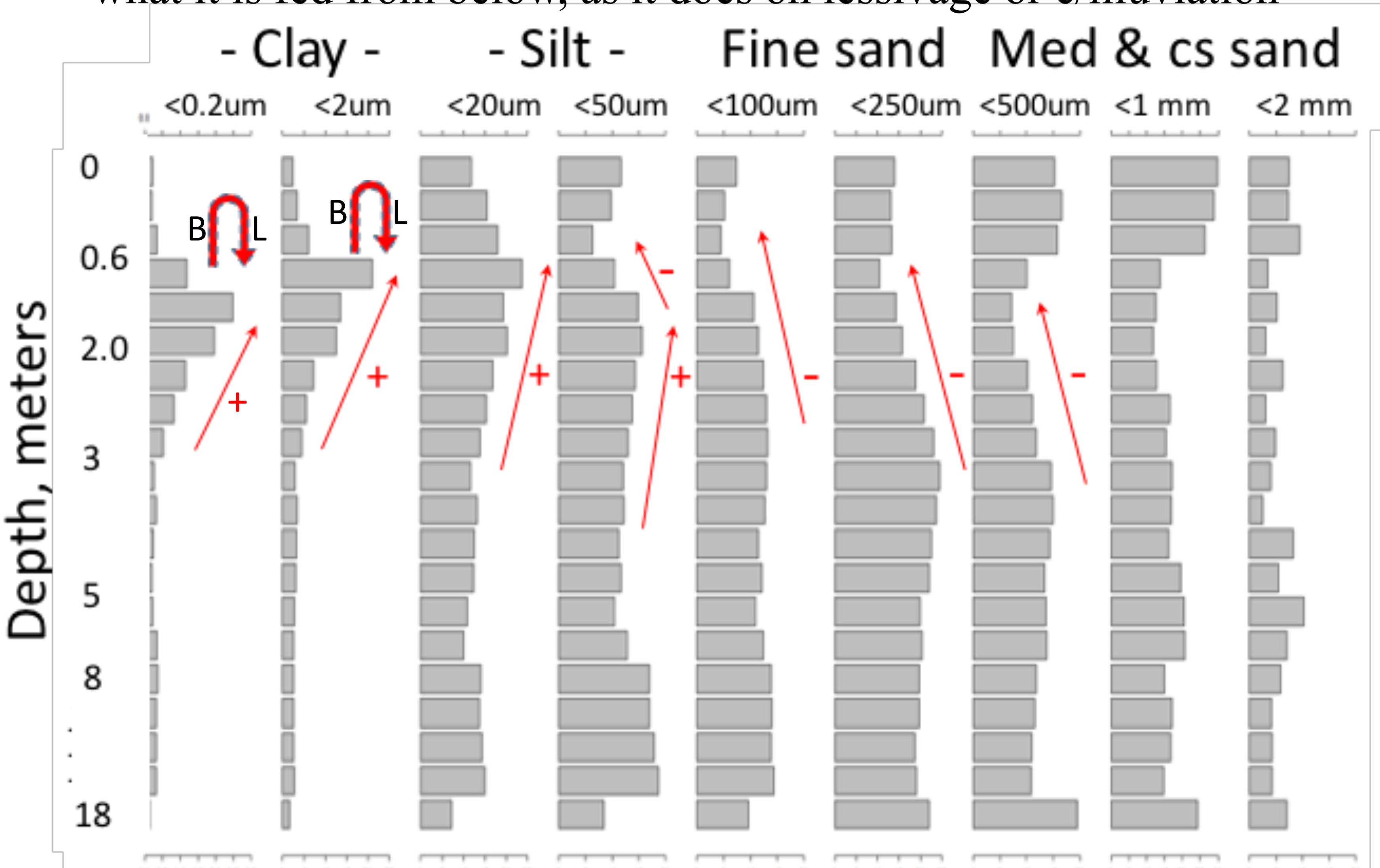


*Betw 3 & 1 m: Fine silt +15, Clay +25%*
*Sands – 40%*

PSA by Pachon & Bacon, UF

Jay Austin-Paul Schroeder's QXRD data appears to confirm the losses of sand-sized kaolinites & orthoclase were associated with gains in these minerals in smaller size classes:
Hypo: comminution is an underexplored soil process
by which small size fractions accumulate in soil

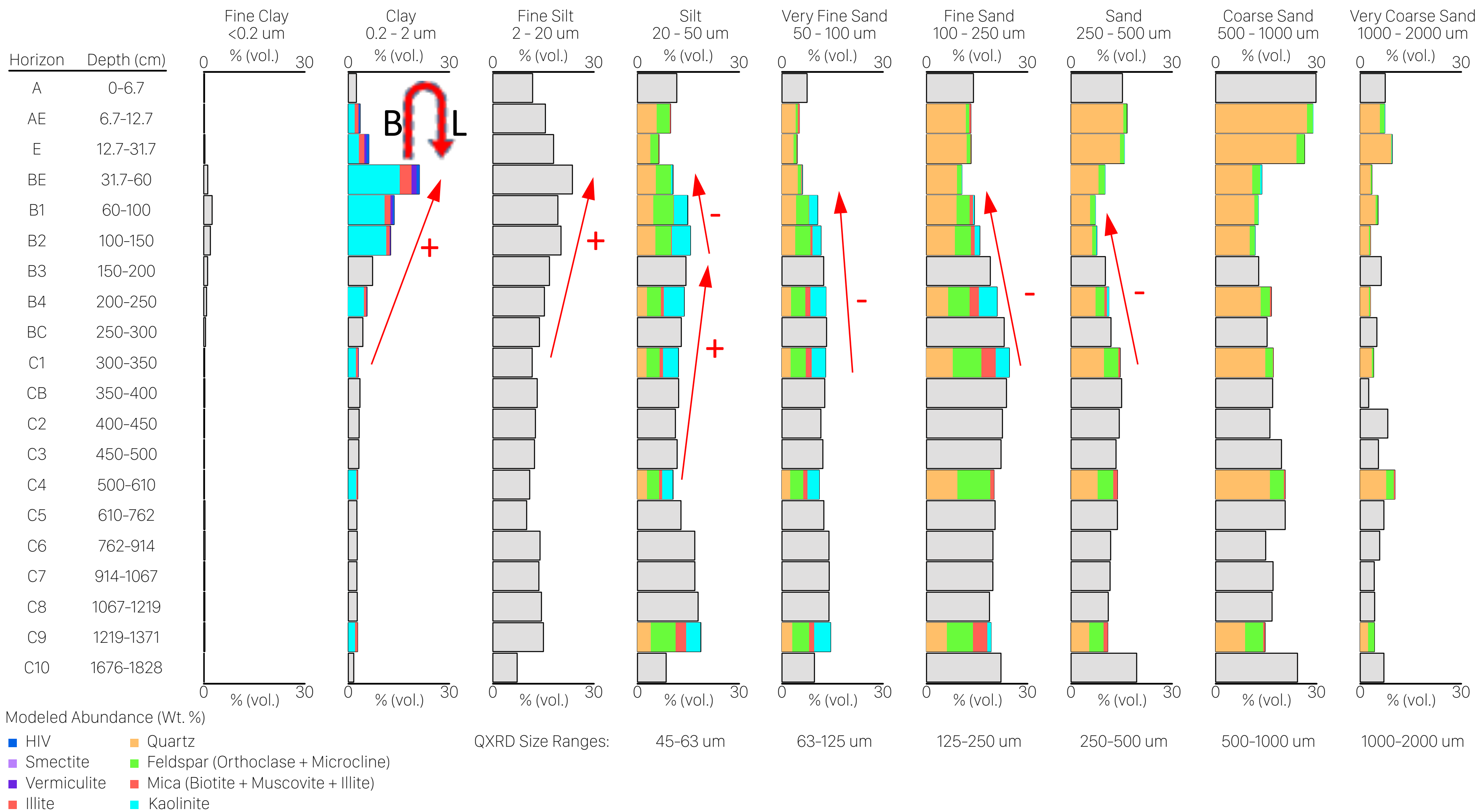

# Hypo: argillic clay depends as much on the soil production system, ie, what is fed from below, as it does on lessivage

Diabase, Enon series

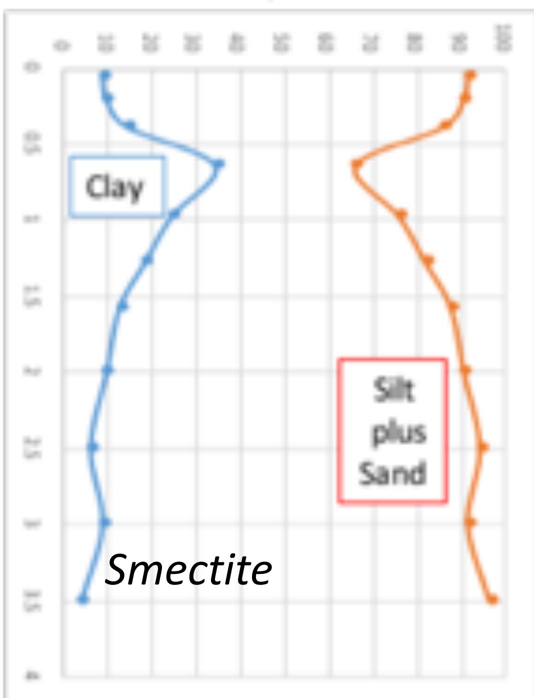


Phyllite, Tarrus series

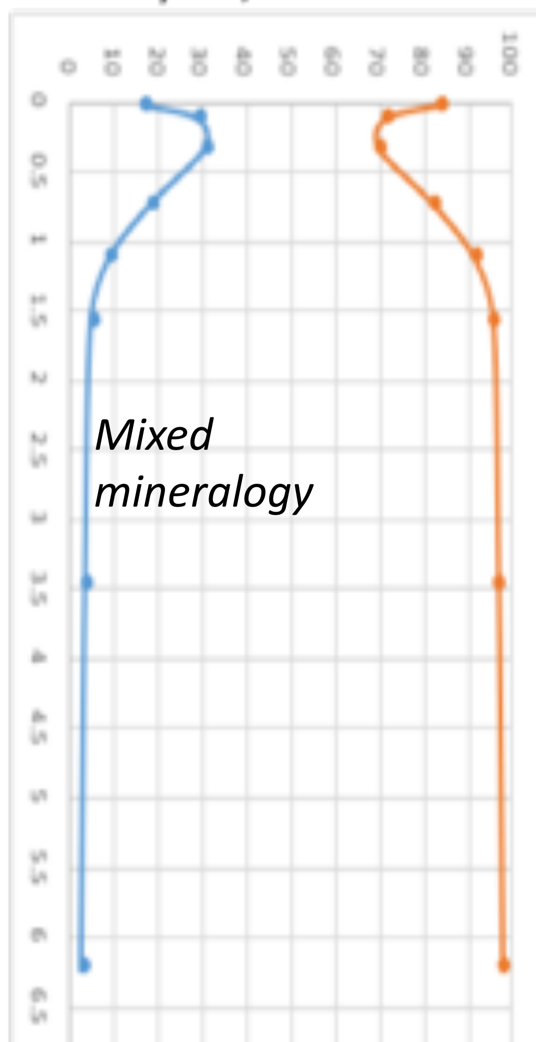


Granitic gneiss, Cecil series

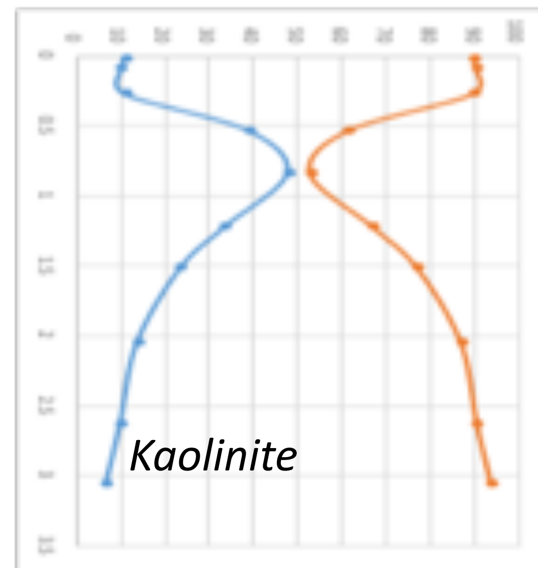


% clay and % silt + sand (x-axis) vs depth in meters in soils derived from three lithologies on Piedmont interfluves (Oh & Richter 2005, *Geoderma*)

*The figures illustrate vertical-contrast-texture (VTC) soils & coarse-fine-coarse textures of the soil production system*

# The Ultisol soil, Cataula series

TABLE 1. PHYSICAL AND CHEMICAL PROPERTIES OF THE SOUTHERN PIEDMONT ULTISOL

| Hor | Depth (m) | ρ* (g/cm$^3$) | Clay (%) | Sand (%) | pH | C (%) | ECEC† (cmol/kg) | EBS§ (%) | totZr (mg/g) | totCa (mg/g) | totAl (mg/g) | totFe (mg/g) | hheFe (mg/g) | tot$^{9}$Be (ug/g) | hhe$^{9}$Be (ug/g) | $^{10}$Be ($10^8$atm/g) | Strain** |
|---|---|---|---|---|---|---|---|---|---|---|---|---|---|---|---|---|---|
| A | 0.00–0.07 | 1.10 | 5.0 | 76.4 | 3.70 | 2.33 | 1.9 | 21.9 | 0.73 | 0.24 | 16.9 | 7.52 | 2.18 | 0.23 | 0.11 | 2.37 | –0.5 |
| AE | 0.07–0.13 | 1.42 | 6.1 | 76.8 | 4.05 | 1.33 | 1.3 | 19.2 | 0.77 | 0.27 | 19.3 | 6.96 | 2.51 | 0.27 | 0.10 | | –0.6 |
| E | 0.13–0.32 | 1.40 | 7.7 | 74.0 | 4.13 | 0.54 | 0.9 | 19.6 | 0.71 | 0.20 | 23.0 | 7.73 | 3.17 | 0.34 | 0.13 | 3.22 | –0.6 |
| Bt | 0.32–0.6 | 1.63 | 41.9 | 42.0 | 4.03 | 0.24 | 3.5 | 23.8 | 0.43 | 0.07 | 108.0 | 26.37 | 18.83 | 0.77 | 0.22 | 6.90 | –0.4 |
| Bt | 0.6–1.0 | 1.44 | 52.9 | 27.2 | 4.06 | 0.13 | 4.6 | 16.1 | 0.28 | 0.04 | 161.7 | 34.75 | 22.99 | 1.18 | 0.14 | 6.86 | 0.1 |
| Bt | 1.0–1.5 | 1.41 | 40.1 | 33.4 | 3.98 | 0.09 | 4.6 | 7.9 | 0.27 | 0.04 | 146.2 | 27.98 | 17.69 | 1.10 | 0.16 | 4.52 | 0.2 |
| BC | 1.5–2.0 | 1.41 | 22.9 | 45.2 | 3.99 | 0.04 | 3.8 | 5.4 | 0.35 | 0.04 | 132.5 | 23.47 | 12.69 | 1.19 | 0.22 | 2.94 | –0.1 |
| CB | 2.0–2.5 | 1.34 | 13.6 | 55.7 | 3.96 | 0.03 | 3.7 | 4.1 | 0.34 | 0.04 | 128.9 | 22.07 | 11.77 | 1.08 | 0.34 | 2.63 | 0.0 |
| CB | 2.5–3.0 | 1.32 | 7.3 | 61.1 | 3.92 | 0.02 | 2.9 | 4.3 | 0.34 | 0.04 | 114.0 | 19.24 | 8.90 | 1.03 | 0.37 | 2.27 | 0.0 |
| C | 3.0–3.5 | 1.27 | 3.6 | 65.9 | 3.89 | 0.01 | 2.8 | 4.9 | 0.36 | 0.06 | 113.0 | 20.10 | 9.61 | 1.18 | 0.50 | 2.08 | –0.1 |
| C | 3.5–4.0 | 1.29 | 4.1 | 65.6 | 3.88 | 0.02 | 3.1 | 6.6 | 0.32 | 0.06 | 105.4 | 19.18 | 8.81 | 1.05 | 0.46 | 2.18 | 0.1 |
| C | 4.0–4.5 | 1.26 | 4.2 | 67.2 | 3.88 | 0.01 | 4.0 | 6.5 | 0.33 | 0.06 | 104.5 | 18.56 | 9.07 | 1.03 | 0.41 | 2.60 | 0.1 |
| C | 4.5–5.0 | 1.29 | 4.6 | 67.3 | 3.94 | 0.02 | 2.7 | 7.0 | 0.34 | 0.07 | 100.0 | 18.40 | 8.32 | 1.00 | 0.40 | 2.06 | 0.0 |
| C | 5.0–5.5 | 1.26 | 3.3 | 67.8 | 3.94 | 0.01 | 2.7 | 7.4 | 0.36 | 0.07 | 105.8 | 18.52 | 8.05 | 1.05 | 0.43 | 2.13 | 0.0 |
| C | 5.5–6.1 | 1.27 | 3.5 | 68.0 | 3.95 | 0.02 | 2.5 | 9.8 | 0.37 | 0.08 | 106.3 | 20.20 | 9.53 | 1.07 | 0.54 | | –0.1 |
| C | 6.1–7.6 | 1.27 | 4.7 | 69.0 | 4.00 | - | 2.6 | 8.8 | 0.54 | 0.12 | 107.7 | 28.28 | 18.68 | 1.54 | 0.64 | 4.86 | –0.4 |
| C†† | 7.6–9.1 | 1.27 | 5.9 | 66.4 | 4.05 | - | 2.0 | 20.1 | 0.48 | 0.22 | 106.8 | 27.48 | 17.10 | 1.67 | 1.06 | | –0.3 |
| C | 9.1–10.7 | 1.27 | 5.2 | 65.6 | 4.17 | - | 2.1 | 49.9 | 0.42 | 0.32 | 105.8 | 26.68 | 16.10 | 1.80 | 1.09 | | –0.2 |
| C | 10.7–12.2 | 1.27 | 5.2 | 68.6 | 4.35 | - | 2.4 | 74.8 | 0.39 | 0.59 | 99.9 | 22.80 | 13.60 | 1.88 | 1.20 | 3.55 | –0.1 |
| C | 12.2–13.7 | 1.27 | 5.9 | 65.0 | 4.41 | - | 2.5 | 79.1 | 0.41 | 1.13 | 102.3 | 22.69 | 13.45 | 2.27 | 1.25 | | –0.2 |
| C§§ | 13.7–16.8 | 1.27 | 3.7 | 74.6 | 4.96 | - | 2.8 | 87.8 | 0.38 | 4.43 | 98.1 | 24.27 | 14.61 | 2.26 | 1.19 | 3.72## | –0.1 |
| C | 16.8–18.3 | 1.27 | 1.5 | 84.3 | 5.51 | - | 3.1 | 96.5 | 0.34 | 7.72 | 93.9 | 25.84 | 15.76 | 2.24 | 1.14 | | 0.0 |

*Notes*: Hor—soil horizon; tot—total; hhe—hydroxylamine hydrochloride extractable. Variability between the three continuous cores reported in Table DR1 (see footnote 1). Samples stored with the Calhoun Experimental Forest archives (Duke University, Durham, North Carolina). Hyphen (-) indicates that percent carbon was not measured below 6.1 m.

*ρ measured from 0.0–0.6 m with a bulk density corer (n = 3), ρ from 0.6–5.0 m data from Markewitz et al. (1998), and below 5.0 m ρ is assumed to be the mean from 3–5 m.

†Effective cation exchange capacity (ECEC) calculated as the sum of exchangeable base cations (Na, Mg, K, and Ca) and exchangeable acidity.

§Effective base saturation (EBS) calculated by dividing the sum of the exchangeable base cations (Na, Mg, K, and Ca) by effective cation exchange capacity.

**Referenced to Zr in the 16.8–18.3 m horizon.

††Due to incomplete fusion, total concentrations not estimated at this depth. Total Zr, Ca, Al, Fe, and $^{9}$Be reported are means of the overlying and underlying horizon.

§§No samples collected from 13.7–16.8 m. Reported values are the mean of the overlying and underlying horizon.

##$^{10}$Be not measured from 13.7–18.3 m (see text).

Cataula soil's C-Fe rhizogenic redox cycling: *Carbon oxidation under moist conditions with low O2, can readily reduce FeIII to FeII, increasing the solubility of Fe by >6 orders*

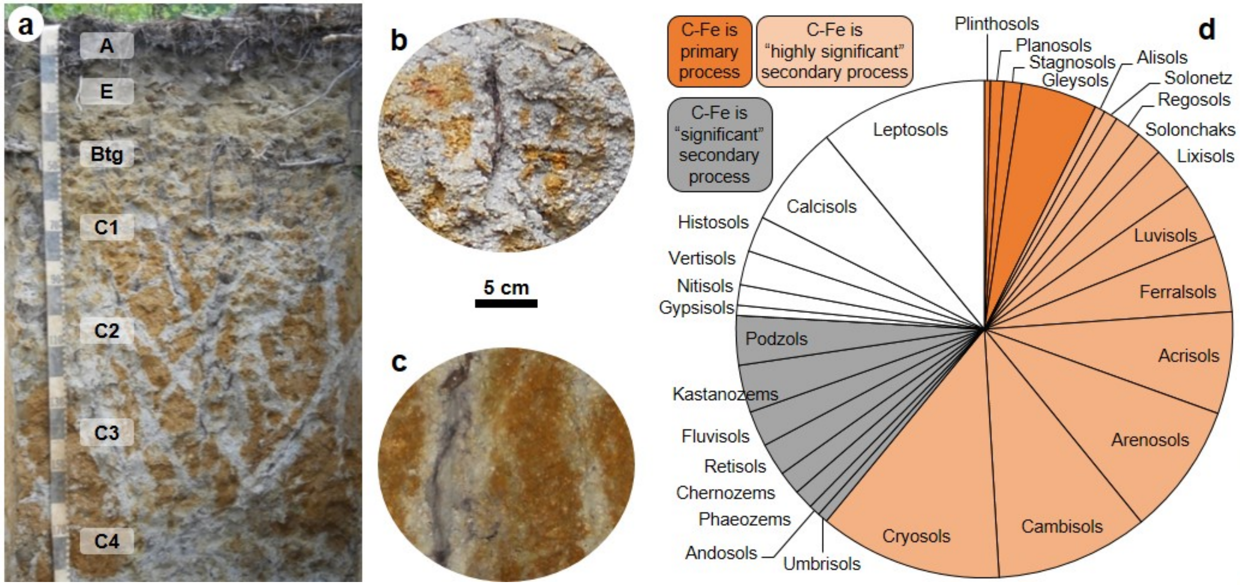


Why do we care?
Direct evidence of water table conditions

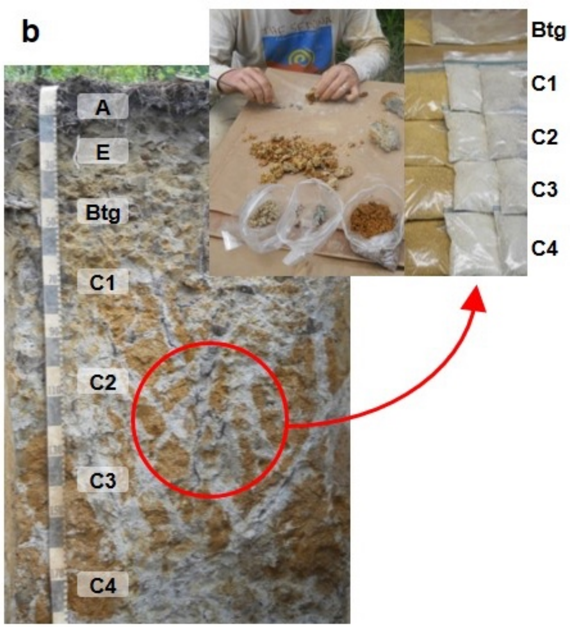


C-Fe cycling recorded in Fe-enriched & Fe-depleted microsites

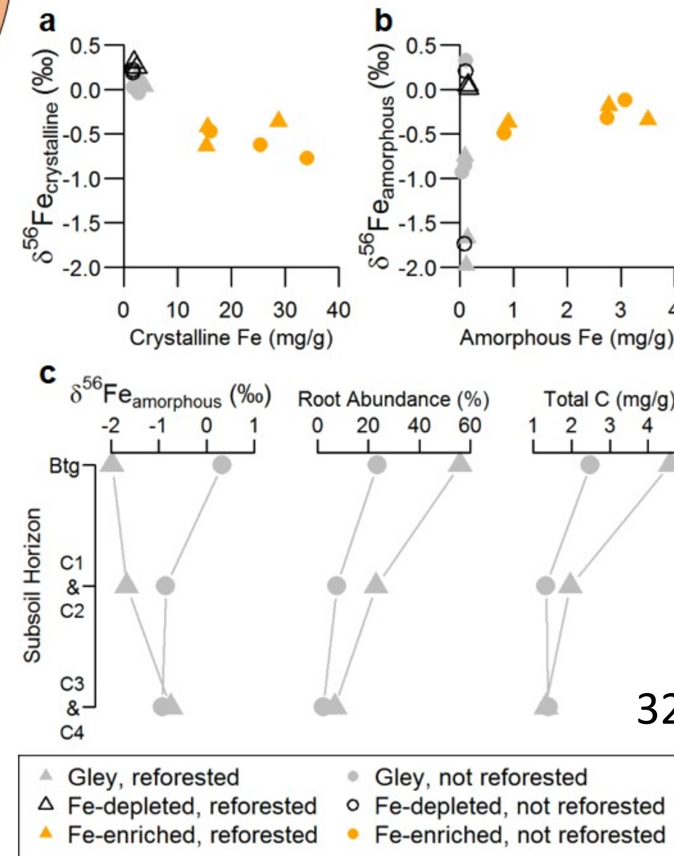

# Invaluable 60-yr field experiment with sample archive in which long cultivated, eroded cotton fields were planted with *Pinus taeda,* which have both demanded much from but also benefited the upper soil environment

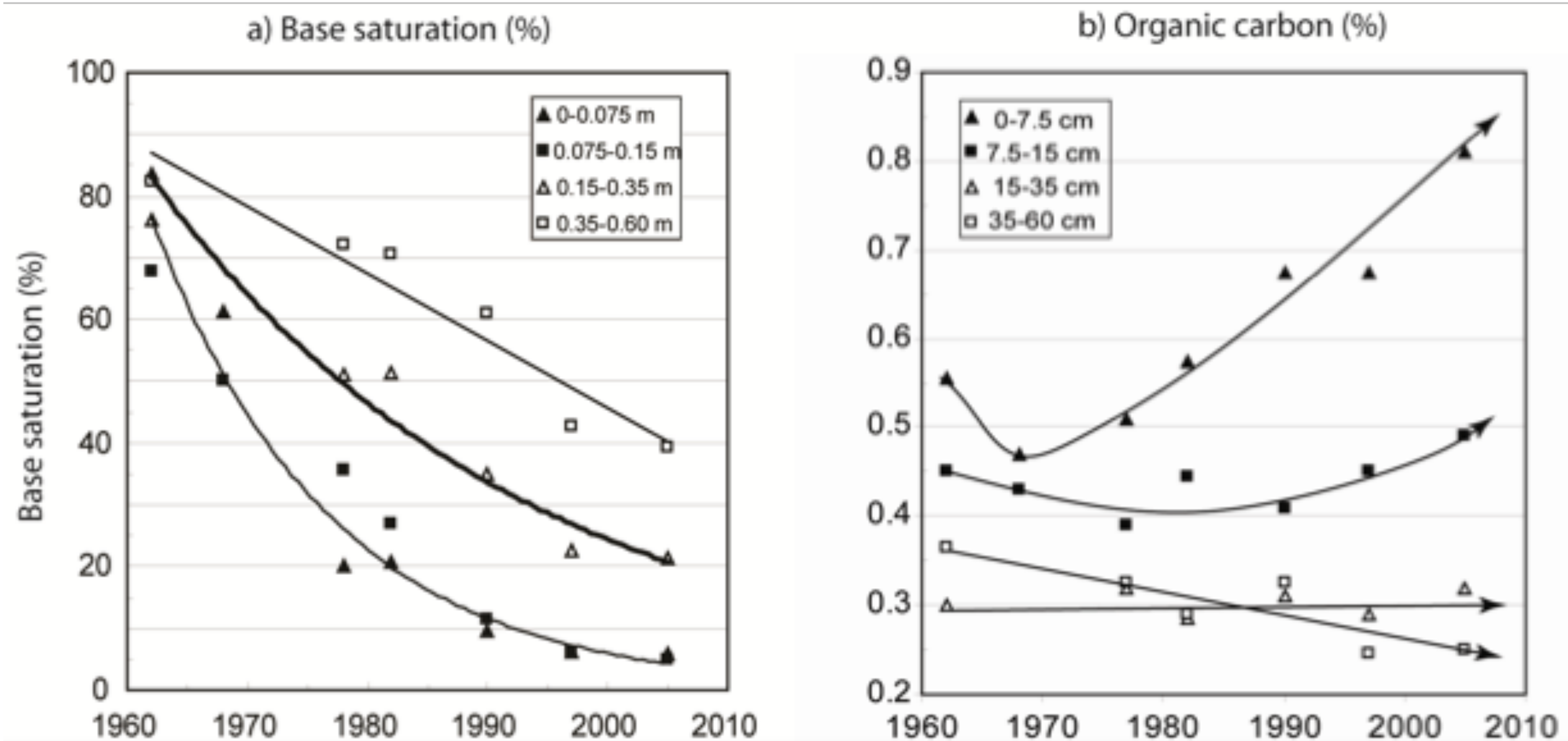

Very rapidly and deeply, forest C was incorporated into the soil's organic matter from the atmosphere's near doubling of $14C\text{-}CO_2$ during aboveground nuclear bomb testing

As the forest regrew on the previously limed soil, acidification was pronounced

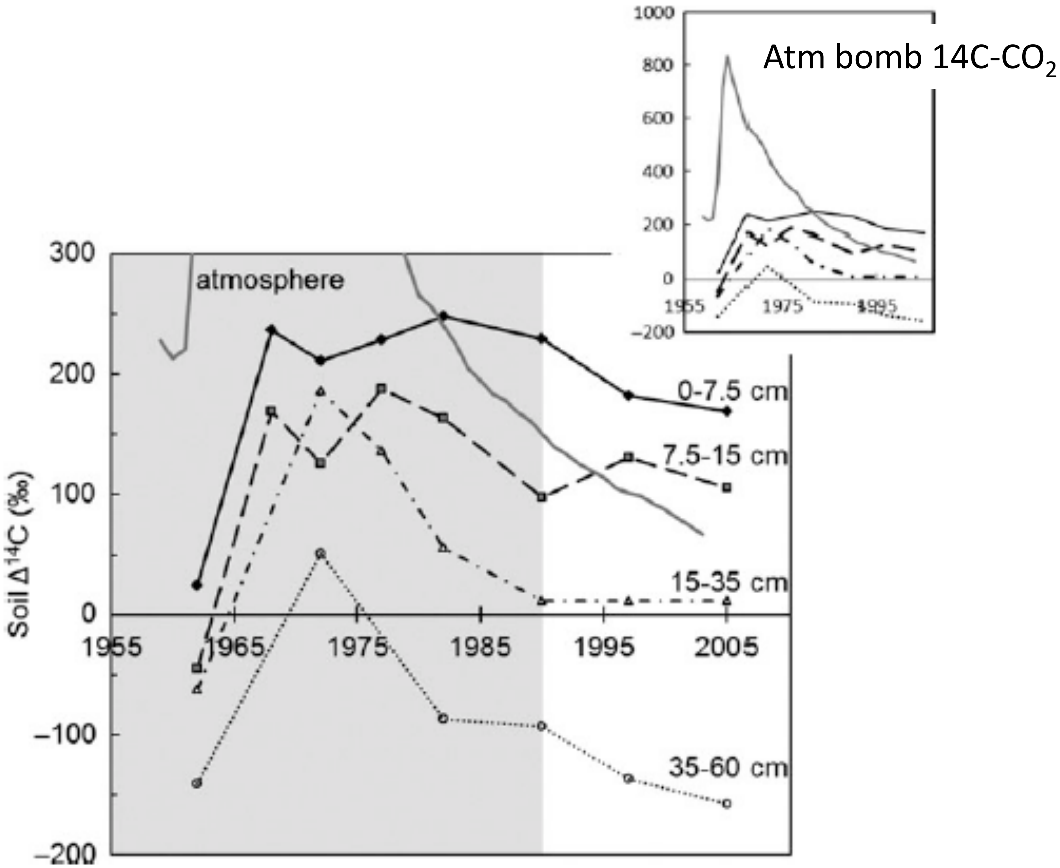


Mobley et al. 2015

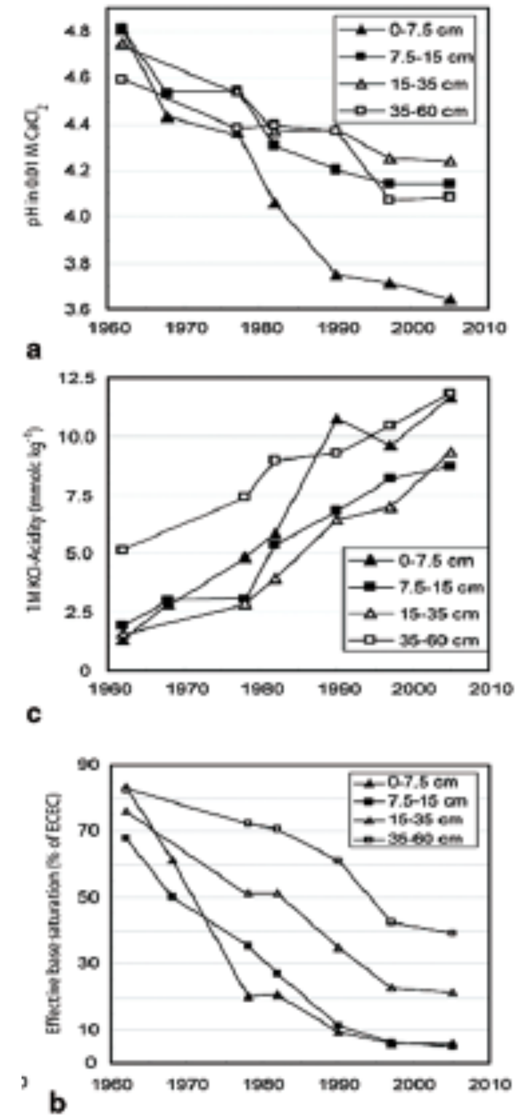


Richter et al. 2014

# Rose Hill State Park

## Gov. Gist Plantation with cotton era gullies approaching from 360$^{o}$

Planning proceeding with SC State Park, Sumter NF, & local churches for park re-Interpretation that involves environmental history of land & people

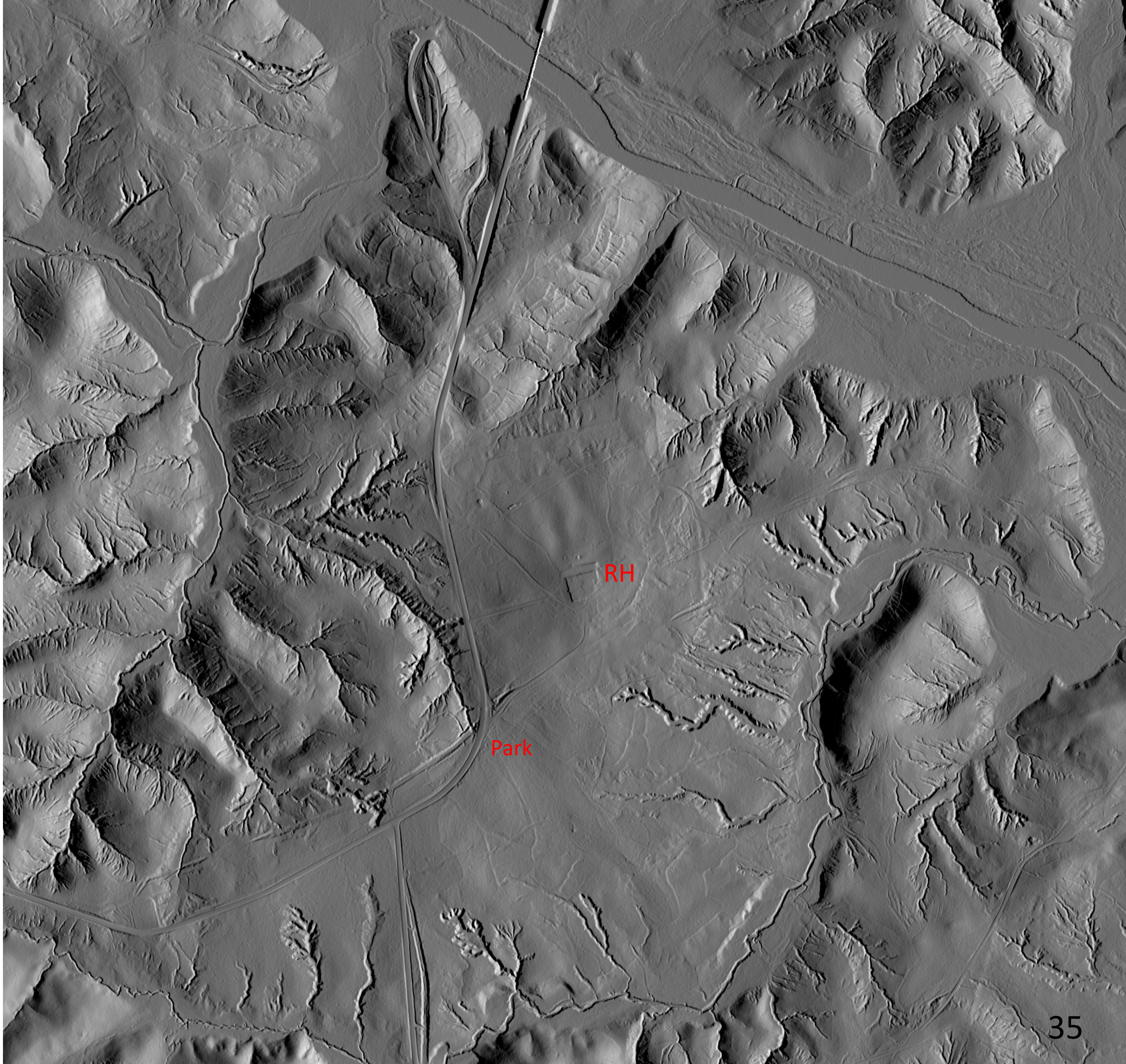

# USFS Purchase photos demonstrate farmers' frequent use of terraces in attempt to control soil erosion, many likely dating from 19th c.

1933 Purchase photos


2008 Slope map from SC statewide LiDAR

Sardis Road Site

Cecil Soil Profile with Richter and Environmental History with Mike Couglan

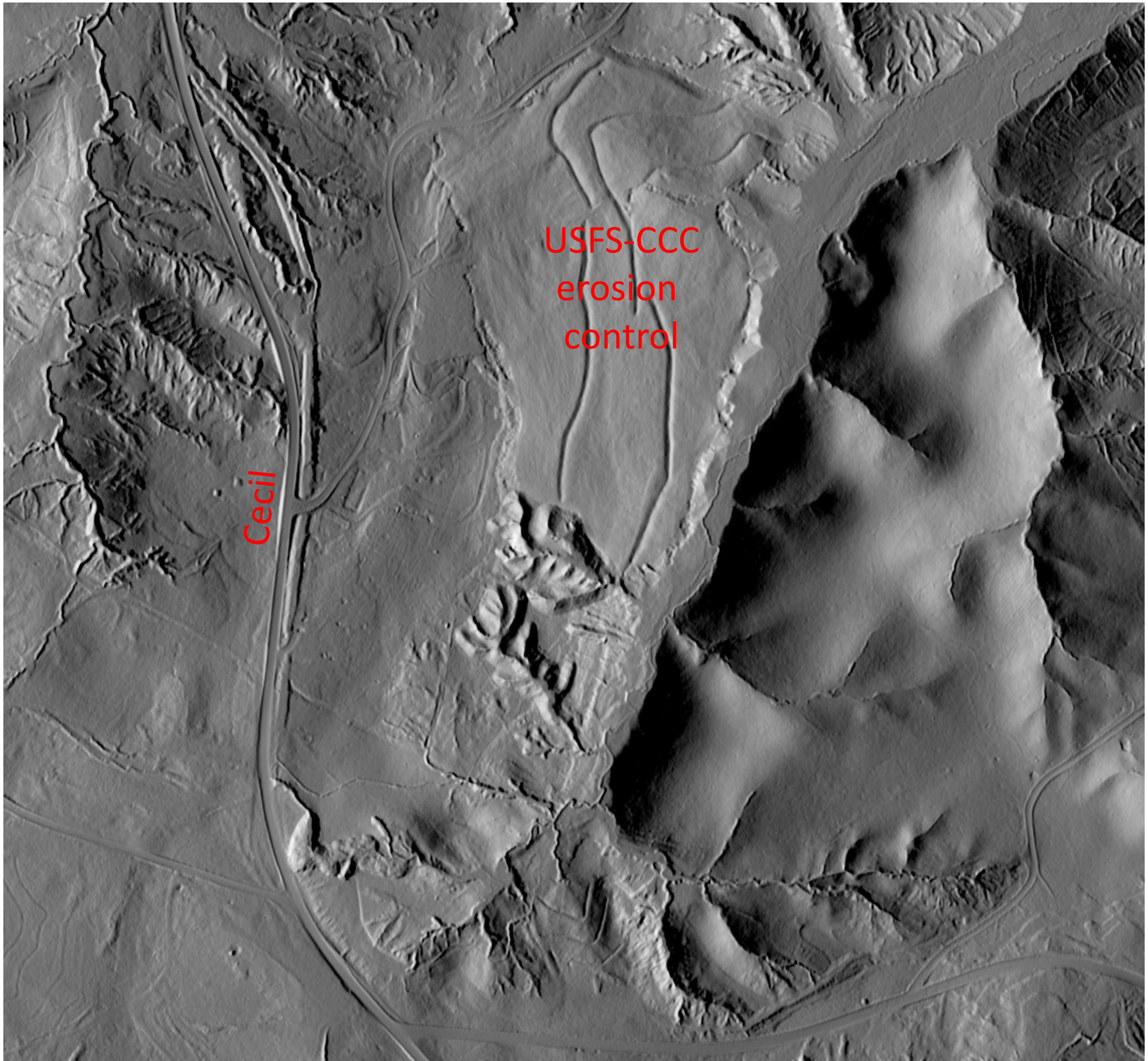

Zach Brecheisen's Hortonian ordering of upland interfluves

We've spent most of our time today on high-order interfluves, those that are broad & with low curvature.

Hwy 49 roadcut site is on a low order interfluve, with relatively higher geologic erosion.

Interfluve ordering

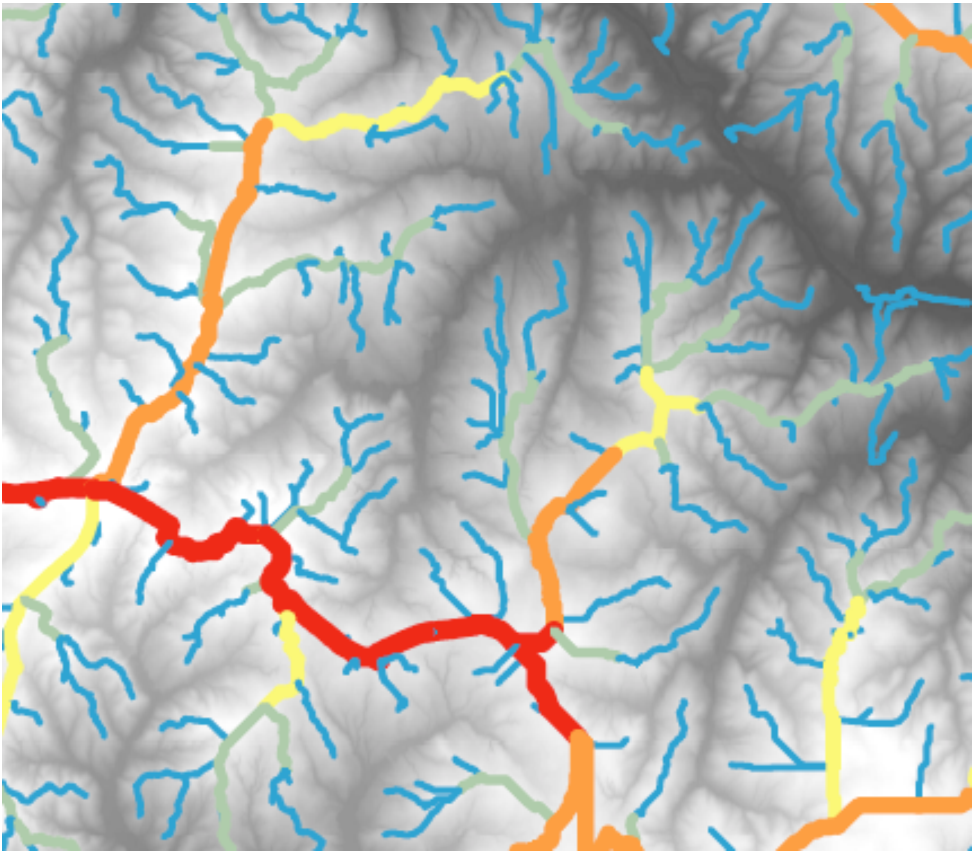

"Landshed" ordering

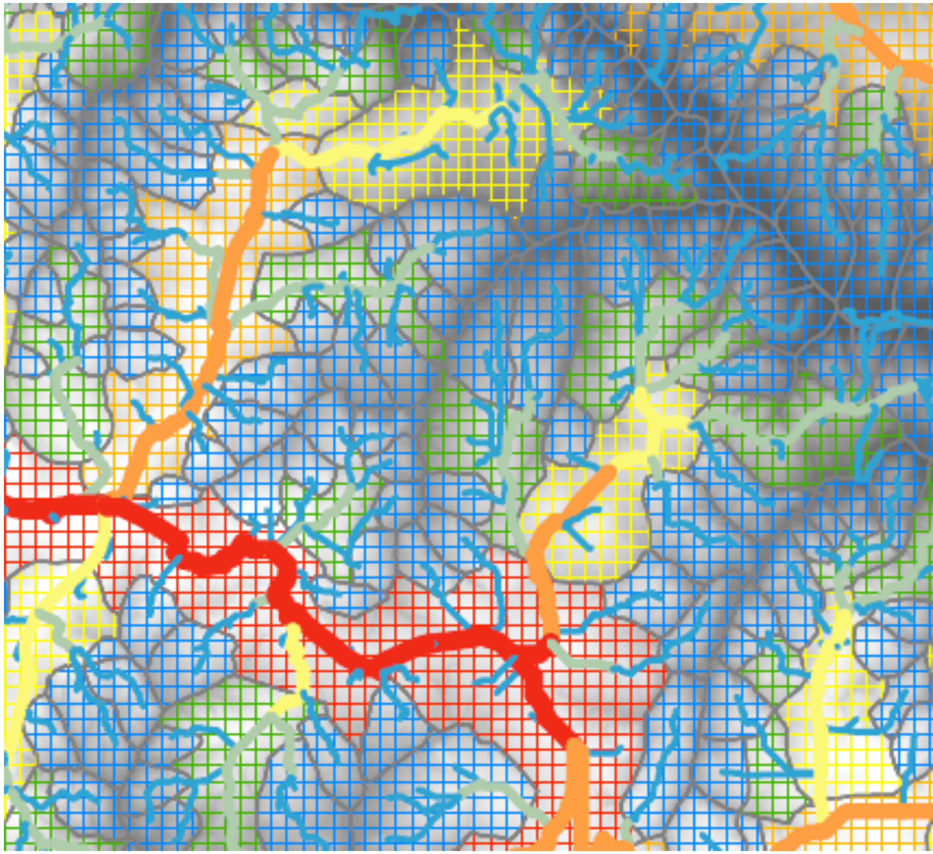

# Brecheisen-Hortonian Interfluve ordering

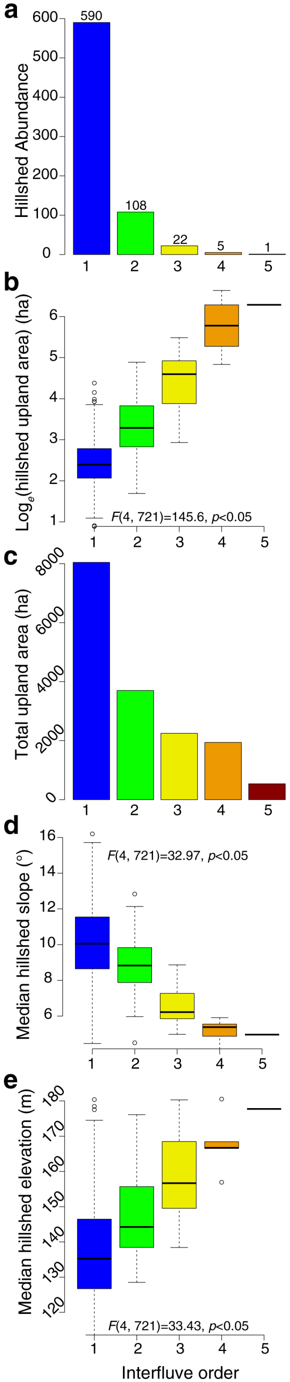


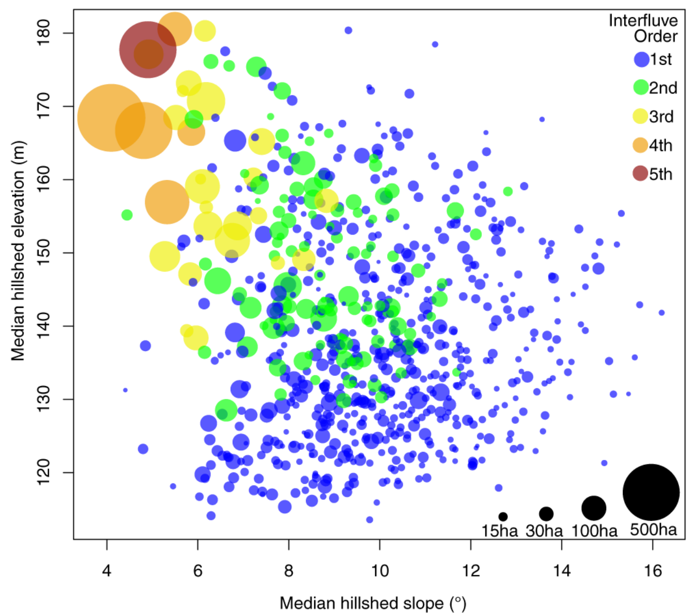


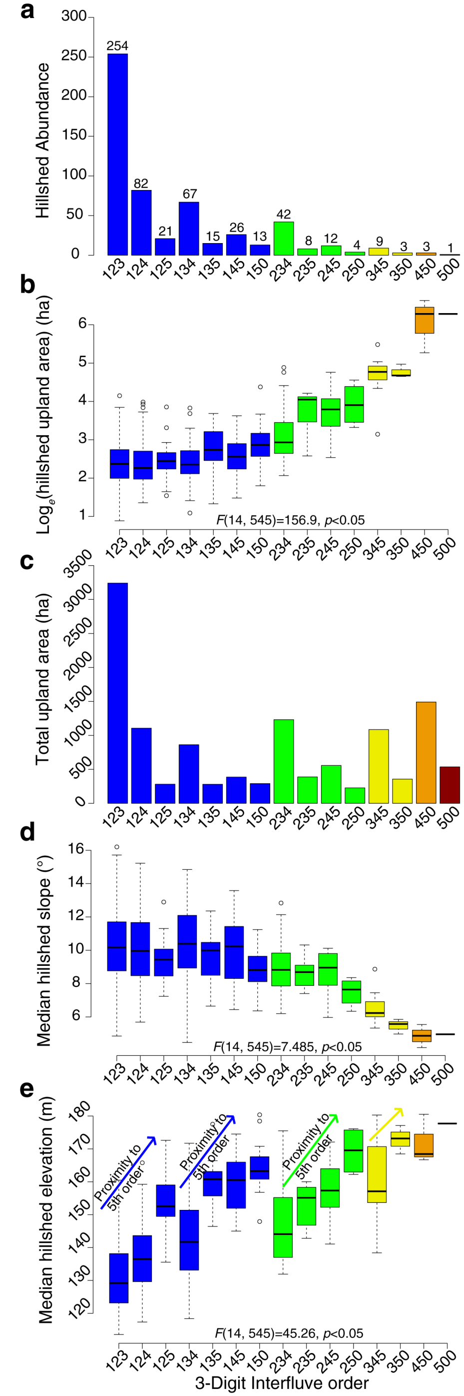


Literally an idea first discussed around a Calhoun campfire

The low-order interfluves of the Hwy 49 Roadcuts:

Tyger River

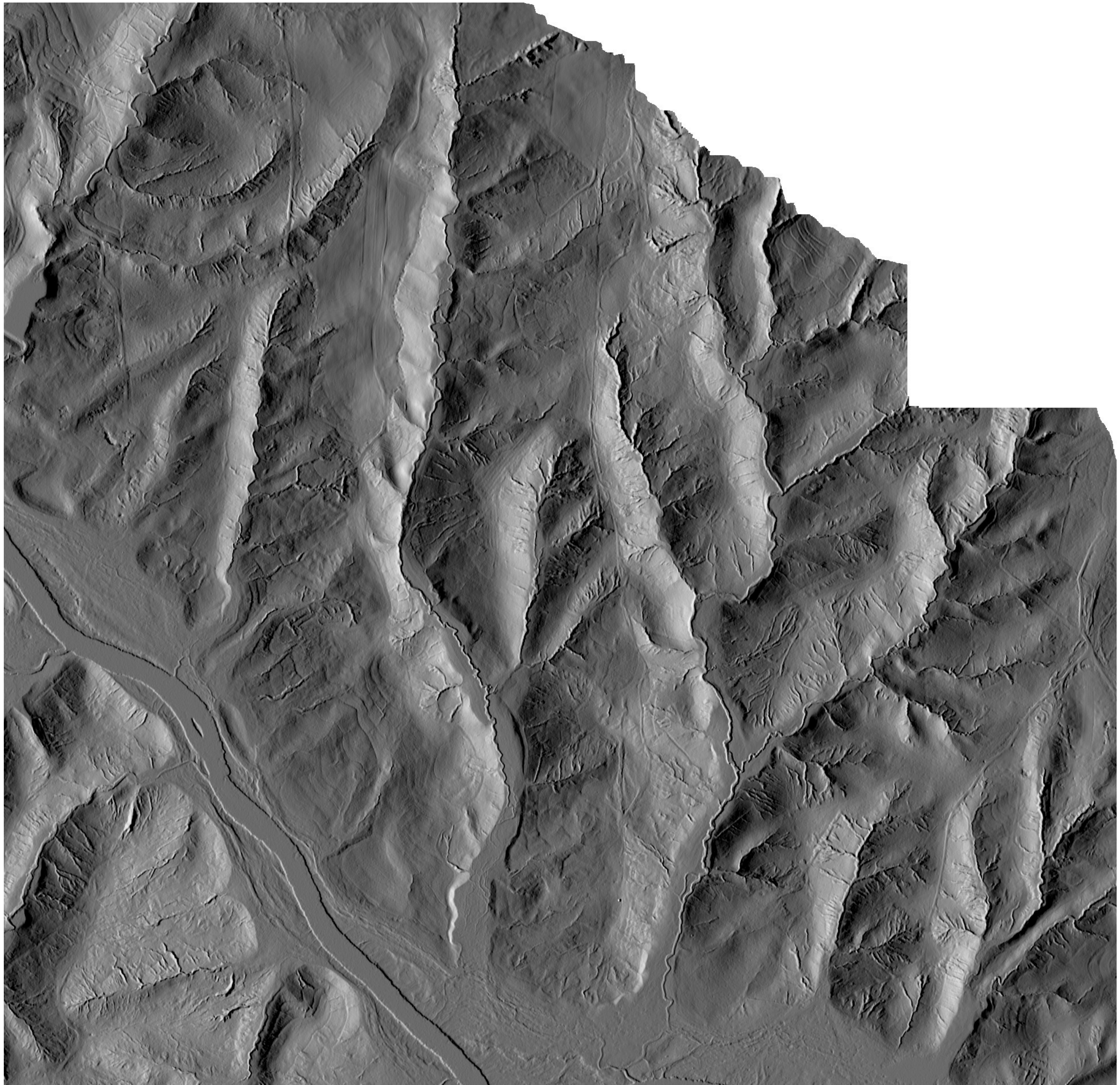

Sedalia Camp Ground, Bombing Range Rd

Surrounded by terraces

2016 Ground Returns from Calhoun High Res LiDAR
Opentopography.org

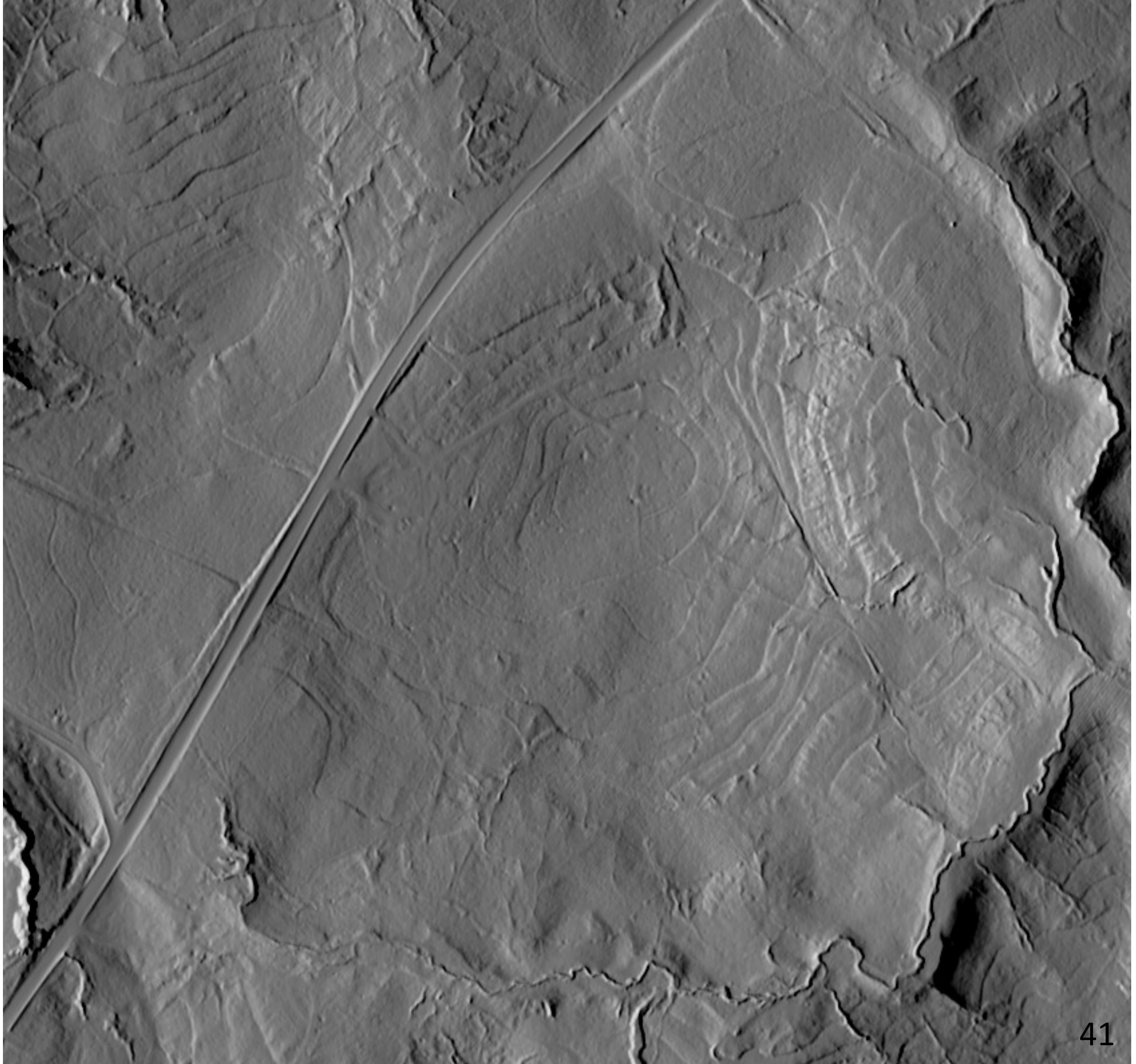

Diffusion-controlled, “relic Landforms” occupy <0.1% of the upland landscape

Various local-scale human disturbances dominate the Piedmont’s surface, including advectively formed gullies

Slope map:
Black steep
White level

Diffusion
and
advection
on landscapes

Brecheisen's
approach to
identifying
relic landforms

Brecheisen &
Richter,
submitted.

CCZO
Research Area 8
With Feb 2016
High Res LiDAR

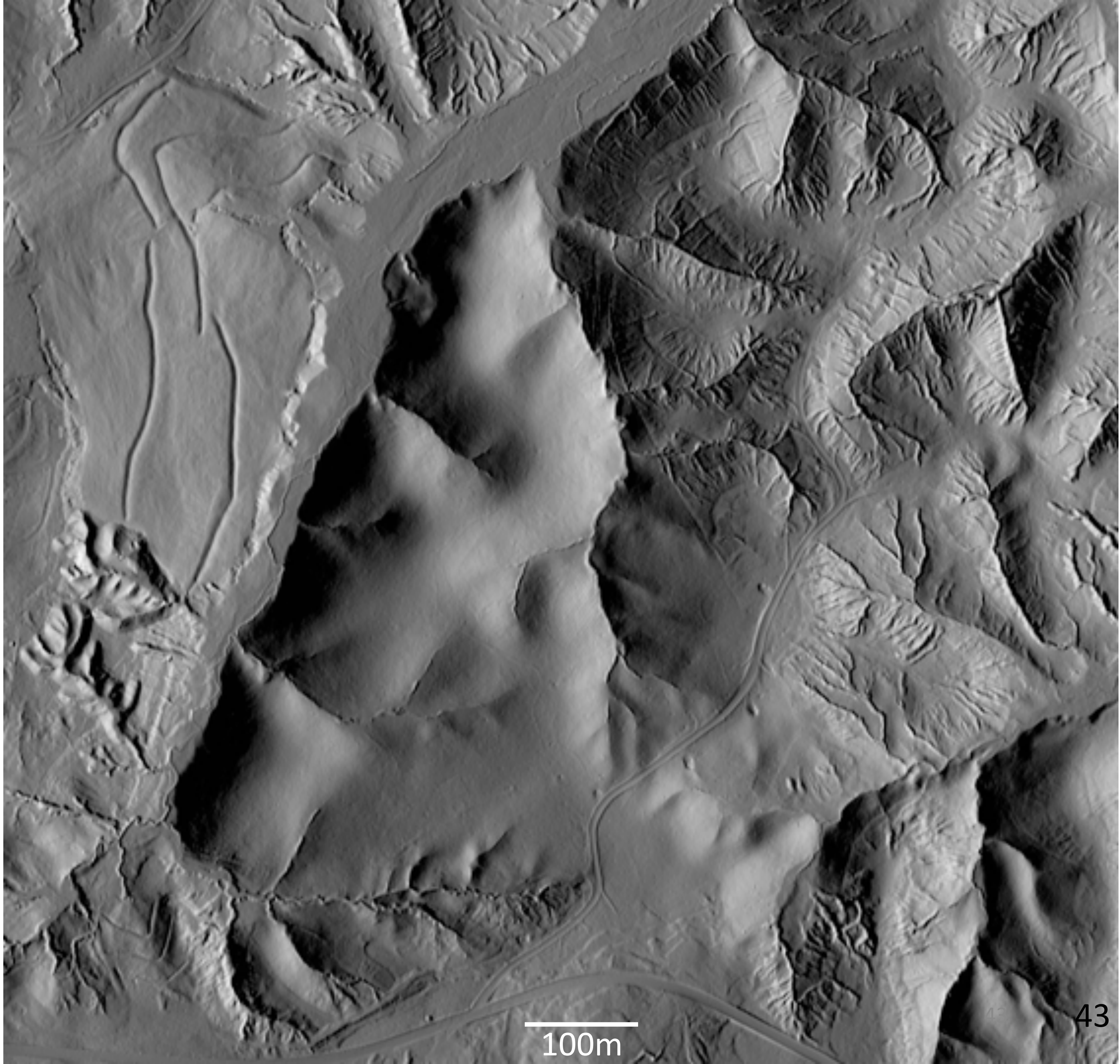

Combining:

- Local surface roughness from 2016 LiDAR
- 1933 canopy brightness
- Winter canopy redness 2015

Brecheisen identified about about a dozen relic-landform, “reference hardwood”, small watersheds across the Calhoun CZO, watersheds that occupy <0.1% of the CCZO.

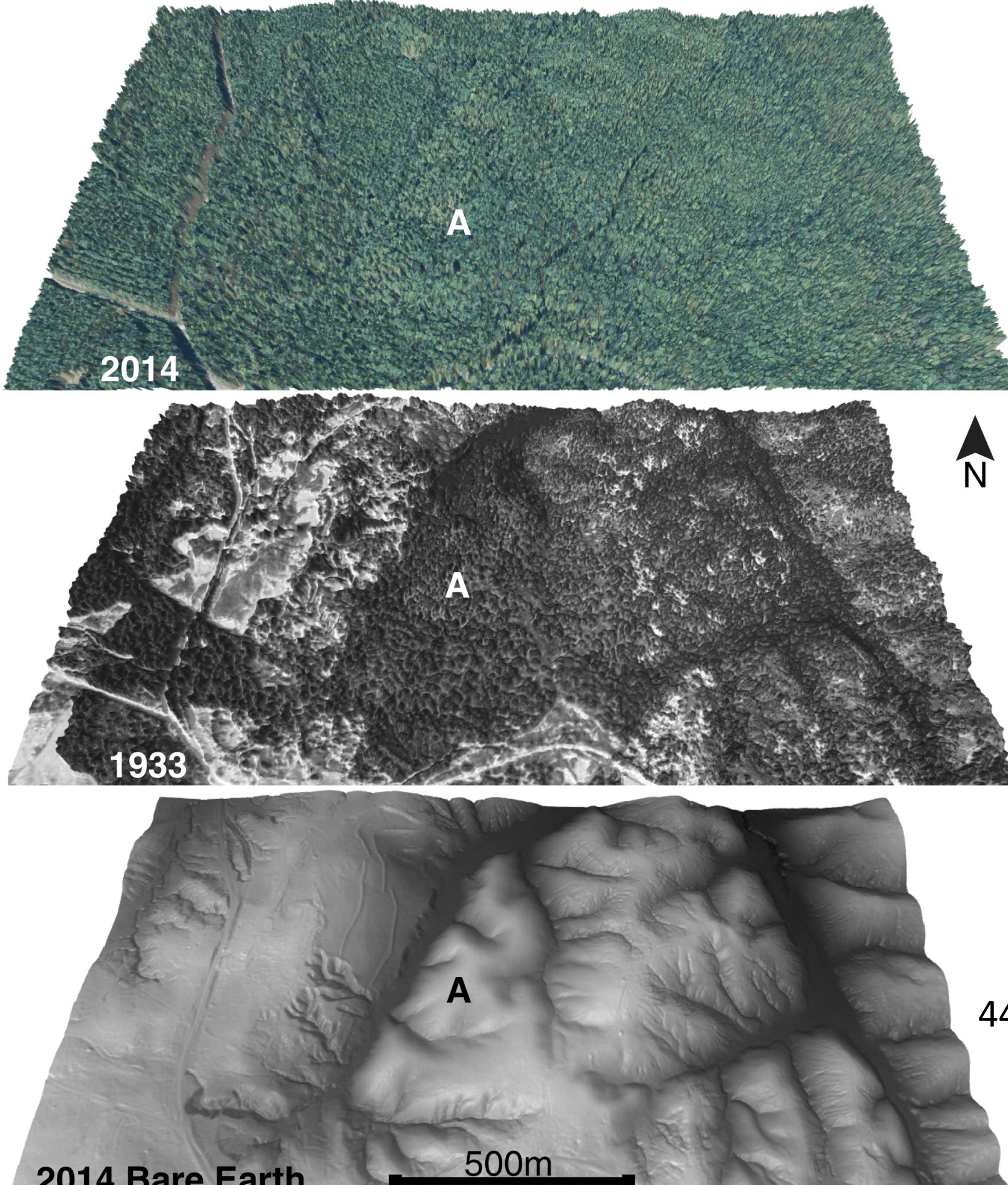


CCZO
Research Area 8

Holcombe's
Branch
Watershed
~600 ha

2016
High Res LiDAR
Opentopography.org

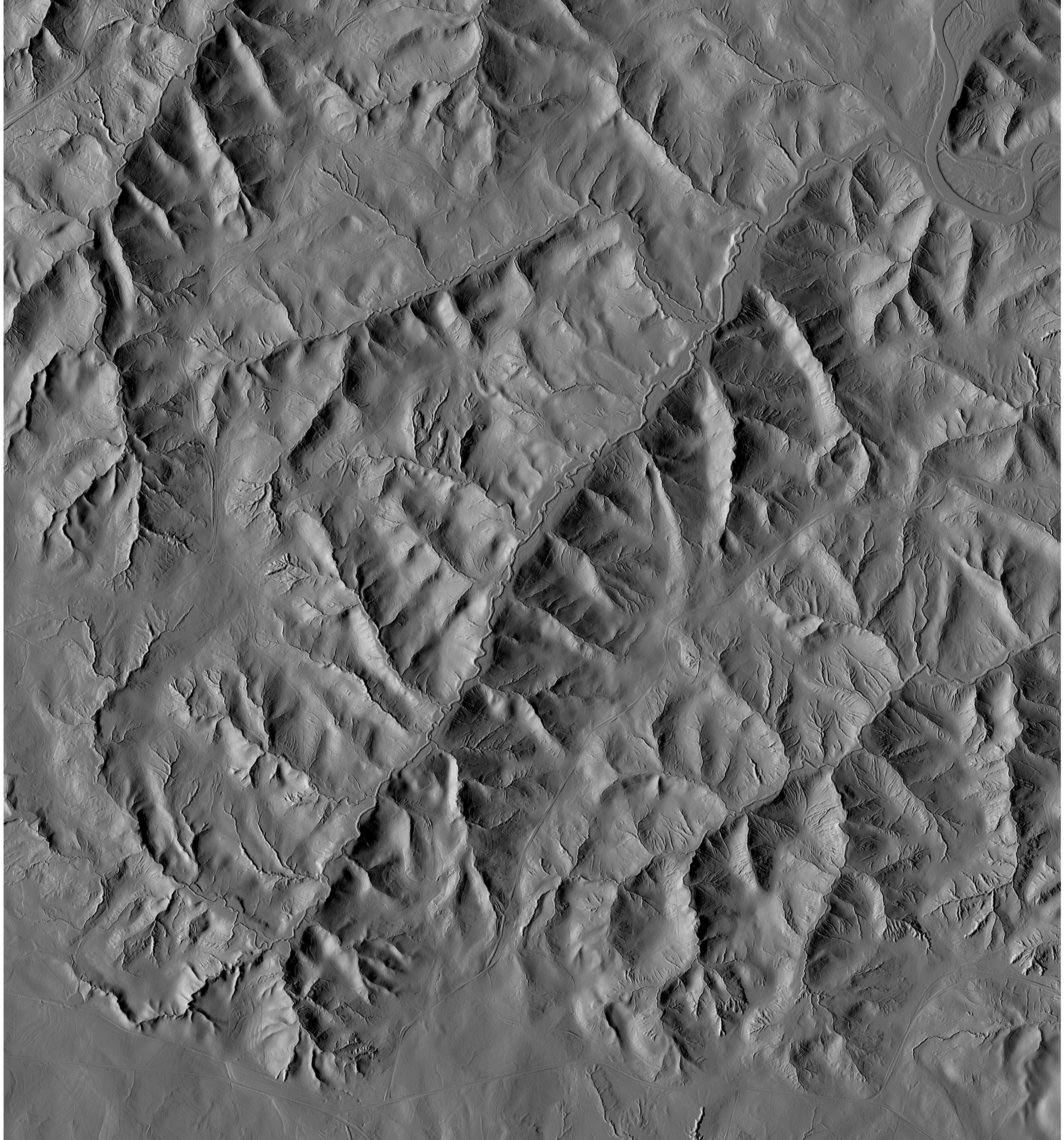

Tyger
River

Holcombe's
Branch
Watershed
~600 ha

Slope map from
2008 SC LiDAR

1933
Aerial photo of
Holcombe's Branch
Watershed

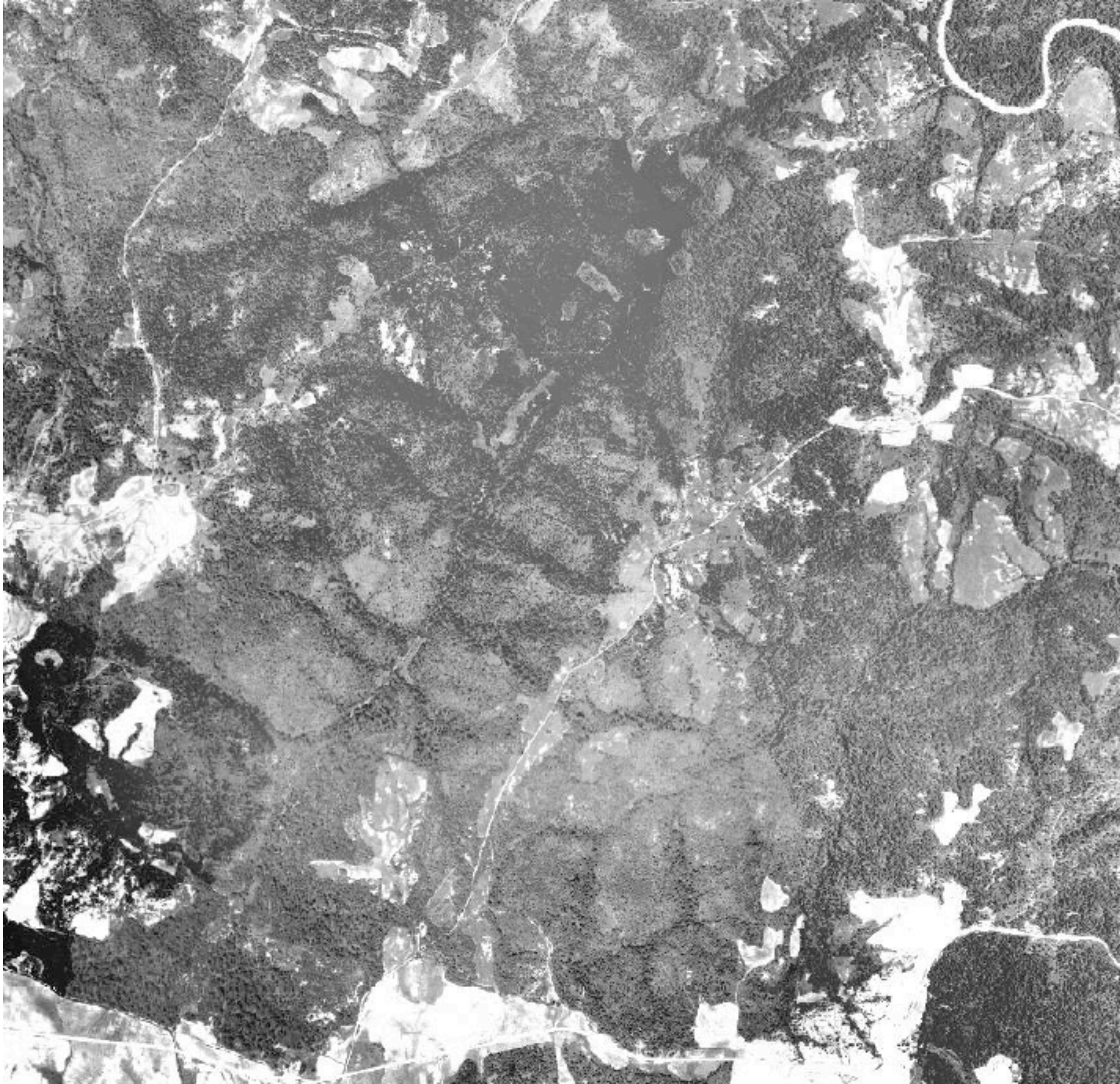

Calhoun Experimental Forest's Re- and Up-instrumented Experimental Watersheds
~1947-1962, 2014-present

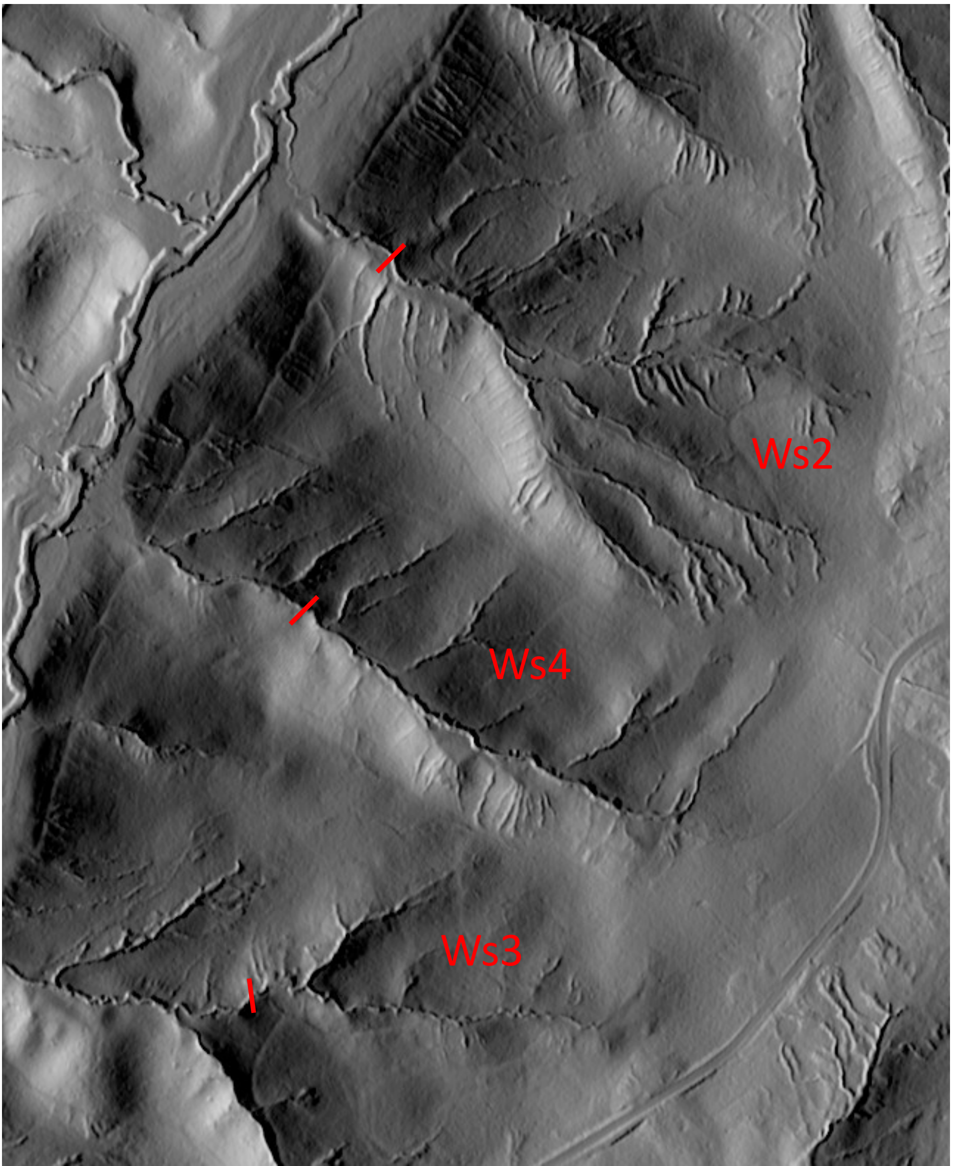


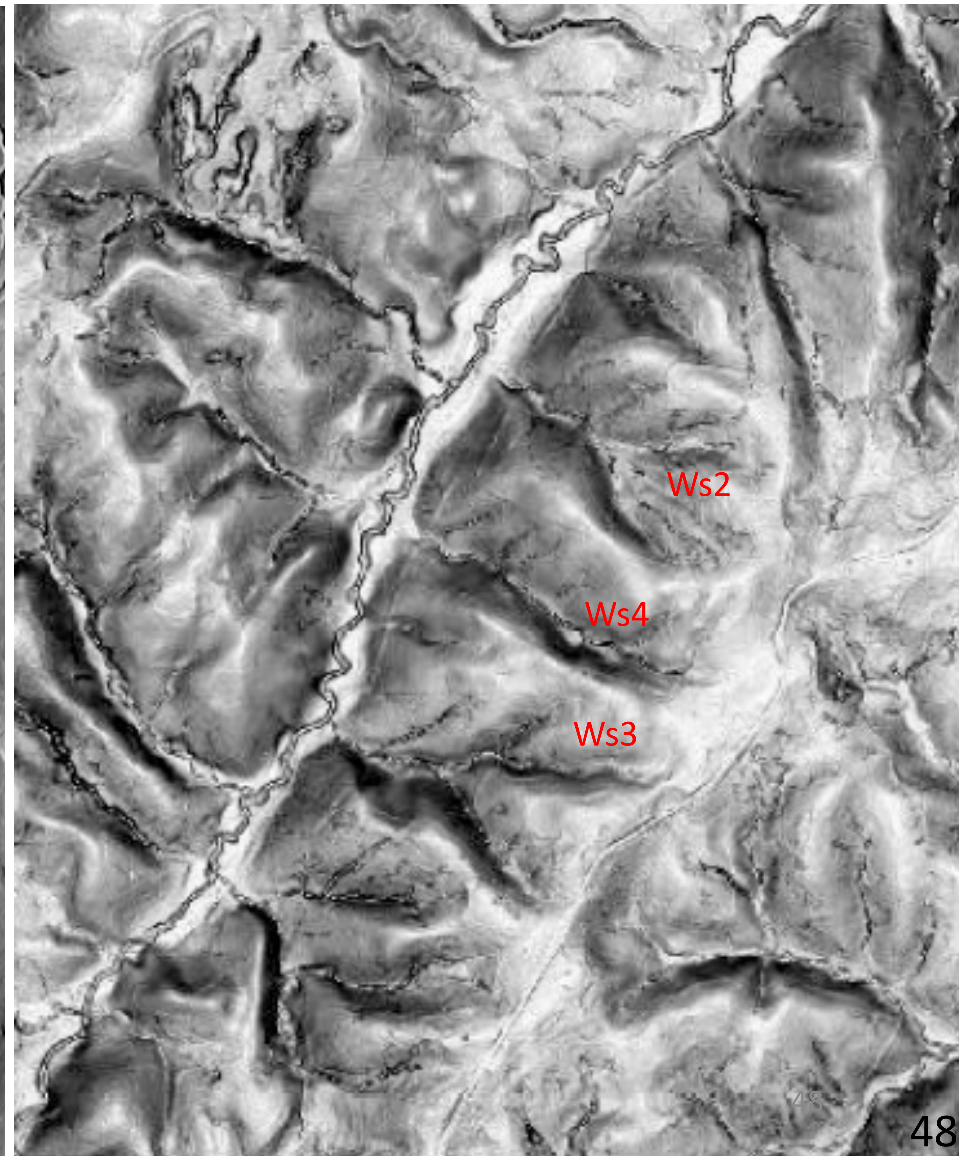

# Historic (Holocene) sedimentation in the Southern Piedmont

## Hupp, 1945 from Spartanburg Co.

Fig. [illegible]—Willow tree partly buried by sedimentation on Ferguson Creek flood plain, Spartanburg County, S. C. The tree had been partly girdled, and the section from which bark was stripped had then been partly covered by the new deposits. This is in an area where deposition was unusually rapid at the time, because of a local "plug" of sand in the small stream channel shown in figure 1. (Photo by Rittenhouse.)

Fig. [illegible]—A small Piedmont stream channel badly choked with sand. Ferguson Creek, Spartanburg County, S. C. (Photo by Rittenhouse.)

## Contemporary floodplain of CCZO

Holcombe's Branch Floodplain Legacy Sediment –

Elevations of legacy sediments

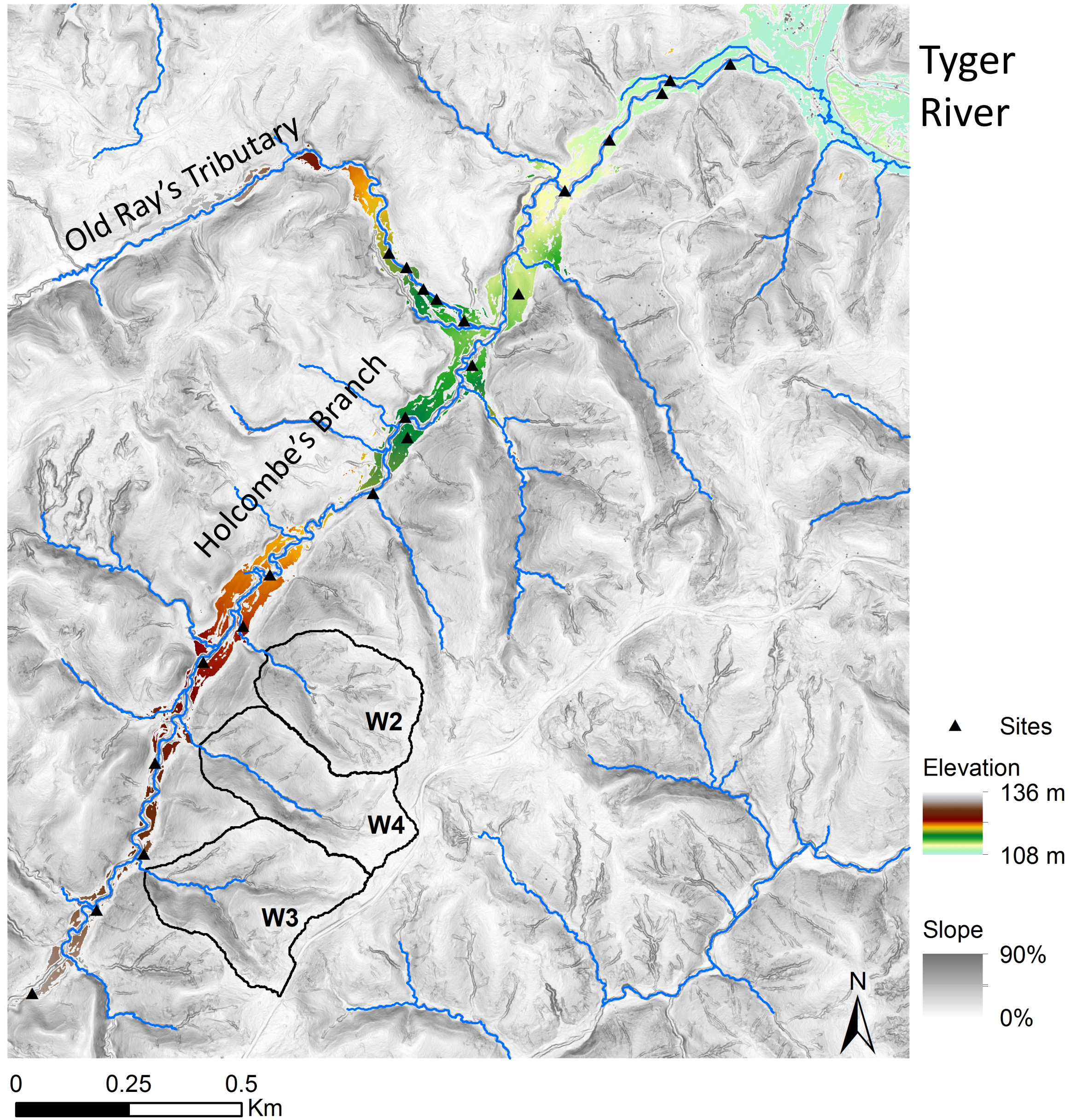

Bulk soil organic radiocarbon ($\Delta^{14}C$‰) of four alluvial soil profiles along 400m of Old Ray's Tributary

*Data courtesy of Alex Cherkinsky & Anna Wade*

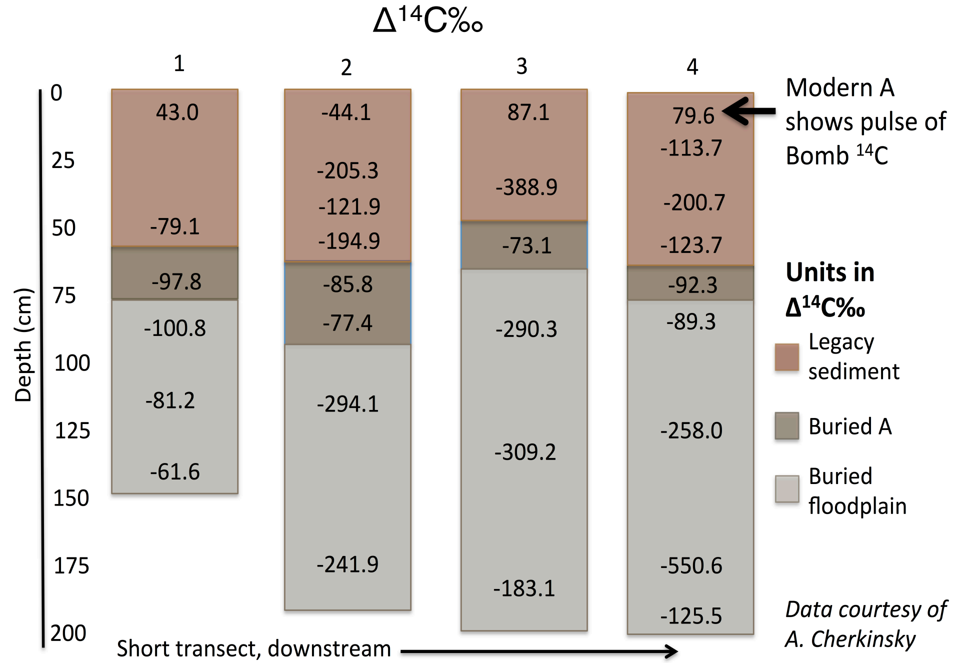


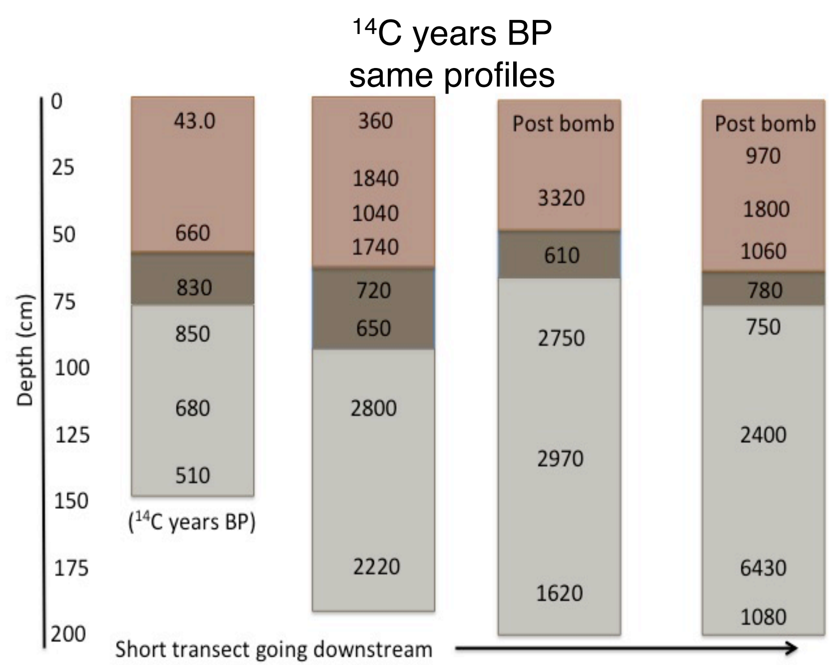

Review

New Phytologist

*Tansley review*

# 'One physical system': Tansley's ecosystem as Earth's critical zone

Author for correspondence:
*Daniel deB. Richter*
*Tel: +01 919 475 7939*
*Email: drichter@duke.edu*

Received: 29 October 2014
Accepted: 8 January 2015

**Daniel deB. Richter[1] and Sharon A. Billings[2]**

[1]Nicholas School of the Environment, Duke University, Durham, NC 27708, USA; [2]Department of Ecology and Evolutionary Biology and Kansas Biological Survey, University of Kansas, Lawrence, KS 66047, USA

## Contents



*New Phytologist* (2015) **206:** 900–912
**doi**: 10.1111/nph.13338

**Keywords:** biogeochemistry, biogeosciences, ecohydrology, ecosystem ecology, ecosystem metabolism, soil respiration, weathering profile.

## Summary

Integrative concepts of the biosphere, ecosystem, biogeocenosis and, recently, Earth's critical zone embrace scientific disciplines that link matter, energy and organisms in a systems-level understanding of our remarkable planet. Here, we assert the congruence of Tansley's (1935) venerable ecosystem concept of 'one physical system' with Earth science's critical zone. Ecosystems and critical zones are congruent across spatial–temporal scales from vegetation-clad weathering profiles and hillslopes, small catchments, landscapes, river basins, continents, to Earth's whole terrestrial surface. What may be less obvious is congruence in the vertical dimension. We use ecosystem metabolism to argue that full accounting of photosynthetically fixed carbon includes respiratory $CO_2$ and carbonic acid that propagate to the base of the critical zone itself. Although a small fraction of respiration, the downward diffusion of $CO_2$ helps determine rates of soil formation and, ultimately, ecosystem evolution and resilience. Because life in the upper portions of terrestrial ecosystems significantly affects biogeochemistry throughout weathering profiles, the lower boundaries of most terrestrial ecosystems have been demarcated at depths too shallow to permit a complete understanding of ecosystem structure and function. Opportunities abound to explore connections between upper and lower components of critical-zone ecosystems, between soils and streams in watersheds, and between plant-derived $CO_2$ and deep microbial communities and mineral weathering.

Global Change Biology

Global Change Biology (2015) **21**, 986–996, doi: 10.1111/gcb.12715

# Surficial gains and subsoil losses of soil carbon and nitrogen during secondary forest development

MEGAN L. MOBLEY[1,2], KATE LAJTHA[3], MARC G. KRAMER[4], ALLAN R. BACON[1,2,5], PAUL R. HEINE[2] and DANIEL DEB RICHTER[1,2]

[1]*University Program in Ecology, Duke University, Durham, NC 27708, USA,* [2]*Nicholas School of the Environment, Duke University, Durham, NC 27708, USA,* [3]*Department of Crop and Soil Science, Oregon State University, Corvallis, OR 97331, USA,* [4]*Soil and Water Science Department, University of Florida, Gainesville, FL 32601, USA,* [5]*School of Forest Resources and Conservation, University of Florida, Gainesville, FL 32601, USA*

## Abstract

Reforestation of formerly cultivated land is widely understood to accumulate above- and belowground detrital organic matter pools, including soil organic matter. However, during 40 years of study of reforestation in the subtropical southeastern USA, repeated observations of above- and belowground carbon documented that significant gains in soil organic matter (SOM) in surface soils (0–7.5 cm) were offset by significant SOM losses in subsoils (35–60 cm). Here, we extended the observation period in this long-term experiment by an additional decade, and used soil fractionation and stable isotopes and radioisotopes to explore changes in soil organic carbon and soil nitrogen that accompanied nearly 50 years of loblolly pine secondary forest development. We observed that accumulations of mineral soil C and N from 0 to 7.5 cm were almost entirely due to accumulations of light-fraction SOM. Meanwhile, losses of soil C and N from mineral soils at 35 to 60 cm were from SOM associated with silt and clay-sized particles. Isotopic signatures showed relatively large accumulations of forest-derived carbon in surface soils, and little to no accumulation of forest-derived carbon in subsoils. We argue that the land use change from old field to secondary forest drove biogeochemical and hydrological changes throughout the soil profile that enhanced microbial activity and SOM decomposition in subsoils. However, when the pine stands aged and began to transition to mixed pines and hardwoods, demands on soil organic matter for nutrients to support aboveground growth eased due to pine mortality, and subsoil organic matter levels stabilized. This study emphasizes the importance of long-term experiments and deep measurements when characterizing soil C and N responses to land use change and the remarkable paucity of such long-term soil data deeper than 30 cm.

*Keywords:* land use change, loblolly pine, long-term experiment, reforestation, secondary forest development, soil fractionation, soil nitrogen, soil organic carbon

REPORTS

GEOMORPHOLOGY

# Geophysical imaging reveals topographic stress control of bedrock weathering

J. St. Clair,[1*†] S. Moon,[2*†‡] W. S. Holbrook,[1] J. T. Perron,[2] C. S. Riebe,[1] S. J. Martel,[3] B. Carr,[1] C. Harman,[4] K. Singha,[5] D. deB. Richter[6]

Bedrock fracture systems facilitate weathering, allowing fresh mineral surfaces to interact with corrosive waters and biota from Earth's surface, while simultaneously promoting drainage of chemically equilibrated fluids. We show that topographic perturbations to regional stress fields explain bedrock fracture distributions, as revealed by seismic velocity and electrical resistivity surveys from three landscapes. The base of the fracture-rich zone mirrors surface topography where the ratio of horizontal compressive tectonic stresses to near-surface gravitational stresses is relatively large, and it parallels the surface topography where the ratio is relatively small. Three-dimensional stress calculations predict these results, suggesting that tectonic stresses interact with topography to influence bedrock disaggregation, groundwater flow, chemical weathering, and the depth of the "critical zone" in which many biogeochemical processes occur.

Weathered bedrock and soil are part of the life-sustaining layer at Earth's surface commonly referred to as the "critical zone." Its thickness depends on the competition between erosion, which removes weathered material from the land surface, and weathering, which breaks down rock mechanically and chemically and thus deepens the interface between weathered and fresh bedrock (1-3). Erosion at the surface can be studied both directly by observation (4) and indirectly using isotopic tracers (5). In contrast, weathering at depth is generally obscured by overlying rock and soil, making it more difficult to study. In this Report, we combine results from landscape-scale geophysical imaging and stress field modeling to evaluate hypotheses about the relationship of subsurface weathering to surface topography.

One hypothesis is that weathering at depth is regulated by the hydraulic conductivity and porosity of bedrock and the incision rate of river channels into bedrock, which together determine how rapidly groundwater flowing toward the river channels can drain bedrock pores of chemically equilibrated water (1). Another hypothesis, based on reactive transport modeling, predicts that the propagation of the weathered zone depends on the balance between mineral reaction kinetics and groundwater residence times (2, 6). These mechanisms are not mutually exclusive, and both emphasize the importance of fluid flow through bedrock. This implies that the development of fracture systems, which provide preferred fluid-flow paths in bedrock (7, 8), should help regulate the downward propagation of weathering.

Bedrock fractures may be inherited from past tectonic or thermal events, but the common observation that fracture abundance declines with depth (9) suggests that near-surface processes are capable of generating new fractures or reactivating existing ones. Examples of potential near-surface fracturing mechanisms include wedging due to growth of ice crystals (10), salt crystals (11), or roots (12); volume expansion due to weathering reactions of certain minerals (13); and stress perturbations associated with surface topography (14). Some of these mechanisms require specific conditions that only occur in certain geographic regions, rock types, or parts of the subsurface. For example, ice weathering requires repeated freeze-thaw cycles and is therefore limited to depths of a few meters, and volume expansion due to mineral weathering is most effective in rocks containing abundant biotite or hornblende. In contrast, surface topography always perturbs the bedrock stress field. Here we focus on this potentially widespread control on bedrock fractures.

Bedrock stress fields can be evaluated by considering the effects of local topography on gravitational stresses and regional tectonic stresses. Theoretical calculations have shown that the presence of topographic features such as ridges and valleys can cause vertical and lateral variations in the shallow subsurface stress field (15) and that these stress perturbations can be large enough to alter bedrock fracture patterns (14, 16). Some observational evidence suggests that topographic stresses influence near-surface fracture distributions (9, 17, 18) and groundwater flow (19-21), but it is unknown whether topographic stresses systematically affect the spatial distribution of bedrock weathering. In this study, we used geophysical surveys of seismic velocity and electrical resistivity to image the thickness of the weathered zone in three landscapes with similar topography but different tectonic stress conditions, and we tested whether the geometry of the weathered zone in each landscape matches the modeled topographic stress field.

A calculation of the stresses beneath an idealized topographic profile in the presence of regional tectonic stress illustrates how topographic stress might influence the geometry of the weathered zone (Fig. 1). We calculated the total stress field as the sum of the ambient stress due to gravity and tectonics and the stress perturbation due to topography (22). From the stress field, we calculated two scalar quantities that act as proxies for two mechanisms that could influence the abundance of fractures. As a proxy for shear fracturing or shear sliding on existing fractures, we calculated the failure potential (Φ) (23), defined as $(\sigma_{mc} - \sigma_{lc})/(\sigma_{mc} + \sigma_{lc})$, where $\sigma$ indicates a stress, and the subscripts denote the most compressive (mc) and least compressive (lc) principal stresses, with compression being positive. As a proxy for opening-mode displacement on fractures, we used the magnitude of $\sigma_{lc}$. Because we do not have prior knowledge of the orientations or abundances of existing fractures in a given landscape, we used both quantities to represent the propensity for generating open fractures. A larger Φ indicates that new shear fractures are more likely to form and that existing fractures oriented obliquely to the $\sigma_{mc}$ and $\sigma_{lc}$ directions are more likely to dilate as a result of sliding on the rough fracture surfaces (24). A smaller $\sigma_{lc}$ indicates that fractures oriented nearly perpendicular to the $\sigma_{lc}$ direction will be more likely to open (20, 25). Given that open fractures permit water to flow more quickly through bedrock and enhance the rate of chemical weathering, we expect that zones of larger Φ or smaller $\sigma_{lc}$ correspond to zones of more weathered bedrock.

In a scenario with a horizontal land surface and a stress field determined by both gravity and a low, uniform ambient horizontal compression, Φ declines and $\sigma_{lc}$ increases with depth beneath the land surface (Fig. 1, A and D). If topography is added and the ambient horizontal compression remains low, contours of Φ and $\sigma_{lc}$ generally parallel the surface (Fig. 1, B and E). This surface-parallel pattern occurs because $\sigma_{lc}$ is determined primarily by the overburden in this scenario, and therefore it increases with

[1]Department of Geology and Geophysics and Wyoming Center for Environmental Hydrology and Geophysics, University of Wyoming, Laramie, WY 82071, USA. [2]Department of Earth, Atmospheric and Planetary Sciences, Massachusetts Institute of Technology, Cambridge, MA 02139, USA. [3]Department of Geology and Geophysics, University of Hawaii, Honolulu, HI 96822, USA. [4]Department of Geography and Environmental Engineering, The Johns Hopkins University, Baltimore, MD 21218, USA. [5]Hydrologic Science and Engineering Program, Colorado School of Mines, Golden, CO 80401, USA. [6]Nicholas School of the Environment, Duke University, Durham, NC 27708, USA.
*Corresponding author. Email: jstclair@uwyo.edu (J.S.C.); sgmoon@mit.edu (S.M.) †These authors contributed equally to this work. ‡Present address: Department of Earth, Planetary, and Space Science, University of California–Los Angeles, Los Angeles, CA 90095, USA.





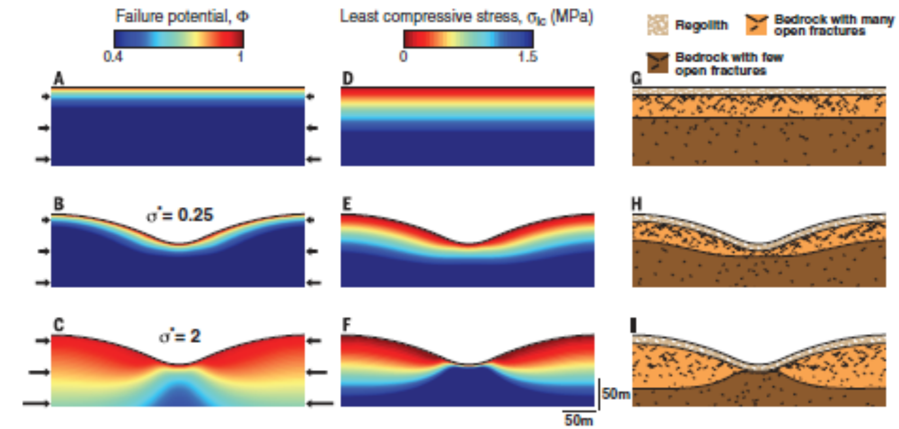


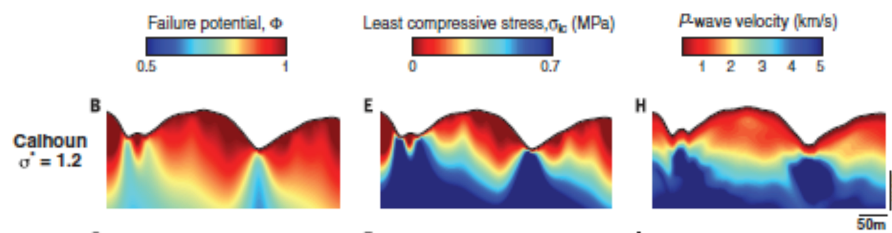


53

AGU PUBLICATIONS

Global Biogeochemical Cycles

RESEARCH ARTICLE

10.1002/2015GB005302

# Topographic variability and the influence of soil erosion on the carbon cycle

**Yannis G. Dialynas[1], Satish Bastola[1], Rafael L. Bras[2], Sharon A. Billings[3], Daniel Markewitz[4], and Daniel deB. Richter[5]**

[1]School of Civil and Environmental Engineering, Georgia Institute of Technology, Atlanta, Georgia, USA, [2]School of Civil and Environmental Engineering and School of Earth and Atmospheric Sciences, Georgia Institute of Technology, Atlanta, Georgia, USA, [3]Department of Ecology and Evolutionary Biology and Kansas Biological Survey, University of Kansas, Lawrence, Kansas, USA, [4]Warnell School of Forest Resources, University of Georgia, Athens, Georgia, USA, [5]Nicholas School of the Environment and Earth Sciences, Duke University, Durham, North Carolina, USA

**Key Points:**
- Topographic heterogeneity drives the spatiotemporal variation in erosion and fate of soil organic C
- Episodic representation of C erosion and burial improves prediction of C fluxes
- Small-scale complexity of C erosion leads to strong topographic variability of dynamic C replacement

**Supporting Information:**
- Supporting Information S1

**Correspondence to:**
Y. G. Dialynas,
ydialynas@gatech.edu

**Citation:**
Dialynas, Y. G., S. Bastola, R. L. Bras, S. A. Billings, D. Markewitz, and D. d B. Richter (2016), Topographic variability and the influence of soil erosion on the carbon cycle, *Global Biogeochem. Cycles*, *30*, doi:10.1002/2015GB005302.

Received 2 OCT 2015
Accepted 20 APR 2016
Accepted article online 22 APR 2016

**Abstract** Soil erosion, particularly that caused by agriculture, is closely linked to the global carbon (C) cycle. There is a wide range of contrasting global estimates of how erosion alters soil-atmosphere C exchange. This can be partly attributed to limited understanding of how geomorphology, topography, and management practices affect erosion and oxidation of soil organic C (SOC). This work presents a physically based approach that stresses the heterogeneity at fine spatial scales of SOC erosion, SOC burial, and associated soil-atmosphere C fluxes. The Holcombe's Branch watershed, part of the Calhoun Critical Zone Observatory in South Carolina, USA, is the case study used. The site has experienced some of the most serious agricultural soil erosion in North America. We use SOC content measurements from contrasting soil profiles and estimates of SOC oxidation rates at multiple soil depths. The methodology was implemented in the tRIBS-ECO (Triangulated Irregular Network-based Real-time Integrated Basin Simulator-Erosion and Carbon Oxidation), a spatially and depth-explicit model of SOC dynamics built within an existing coupled physically based hydro-geomorphic model. According to observations from multiple soil profiles, about 32% of the original SOC content has been eroded in the study area. The results indicate that C erosion and its replacement exhibit significant topographic variation at relatively small scales (tens of meters). The episodic representation of SOC erosion reproduces the history of SOC erosion better than models that use an assumption of constant erosion in space and time. The net atmospheric C exchange at the study site is estimated to range from a maximum source of 14.5 g $m^{-2}$ $yr^{-1}$ to a maximum sink of −18.2 g $m^{-2}$ $yr^{-1}$. The small-scale complexity of C erosion and burial driven by topography exerts a strong control on the landscape's capacity to serve as a C source or a sink.

Ecological Modelling 360 (2017) 108–119

ELSEVIER

Contents lists available at ScienceDirect

Ecological Modelling

journal homepage: www.elsevier.com/locate/ecolmodel

# Boom and bust carbon-nitrogen dynamics during reforestation

CrossMark

Anthony J. Parolari[a,b,*,1], Megan L. Mobley[c,d], Allan R. Bacon[e], Gabriel G. Katul[d], Daniel deB. Richter[d], Amilcare Porporato[b]

[a] Department of Civil, Construction, and Environmental Engineering, Marquette University, Milwaukee, WI, USA
[b] Department of Civil and Environmental Engineering, Duke University, Durham, North Carolina, USA
[c] Department of Crop and Soil Science, Oregon State University, Corvallis, OR, USA
[d] Nicholas School of the Environment, Duke University, Durham, North Carolina, USA
[e] School of Forest Resources and Conservation, University of Florida, Gainesville, Florida, USA

ARTICLE INFO

*Article history:*
Received 6 March 2017
Received in revised form 22 June 2017
Accepted 23 June 2017
Available online 15 July 2017

*Keywords:*
Reforestation
Nutrient cycling
Soil nitrogen
Plant-soil feedbacks
Dynamical systems
Land use legacy

ABSTRACT

Legacies of historical land use strongly shape contemporary ecosystem dynamics. In old-field secondary forests, tree growth embodies a legacy of soil changes affected by previous cultivation. Three patterns of biomass accumulation during reforestation have been hypothesized previously, including monotonic to steady state, non-monotonic with a single peak then decay to steady state, and multiple oscillations around the steady state. In this paper, the conditions leading to the emergence of these patterns is analyzed. Using observations and models, we demonstrate that divergent reforestation patterns can be explained by contrasting time-scales in ecosystem carbon-nitrogen cycles that are influenced by land use legacies. Model analyses characterize non-monotonic plant-soil trajectories as either single peaks or multiple oscillations during an initial transient phase controlled by soil carbon-nitrogen conditions at the time of planting. Oscillations in plant and soil pools appear in modeled systems with rapid tree growth and low initial soil nitrogen, which stimulate nitrogen competition between trees and decomposers and lead the forest into a state of acute nitrogen deficiency. High initial soil nitrogen dampens oscillations, but enhances the magnitude of the tree biomass peak. These model results are supported by data derived from the long-running Calhoun Long-Term Soil-Ecosystem Experiment from 1957 to 2007. Observed carbon and nitrogen pools reveal distinct tree growth and decay phases, coincident with soil nitrogen depletion and partial re-accumulation. Further, contemporary tree biomass loss decreases with the legacy soil C:N ratio. These results support the idea that non-monotonic reforestation trajectories may result from initial transients in the plant-soil system affected by initial conditions derived from soil changes associated with land-use history.

land

MDPI

*Article*

# Historical Land Use Dynamics in the Highly Degraded Landscape of the Calhoun Critical Zone Observatory

**Michael R. Coughlan *, Donald R. Nelson, Michael Lonneman and Ashley E. Block †**

Department of Anthropology, University of Georgia, Athens, GA 30602, USA; dnelson@uga.edu (D.R.N.); mclonn01@uga.edu (M.L.); ashley.block25@uga.edu (A.E.B.)
* Correspondence: coughlan@uga.edu; Tel.: +1-706-542-6160
† In memoriam.

Academic Editors: Fabian Löw, Alexander Prishchepov and Florian Schierhorn
Received: 26 January 2017; Accepted: 27 April 2017; Published: 2 May 2017

**Abstract:** Processes of land degradation and regeneration display fine scale heterogeneity often intimately linked with land use. Yet, examinations of the relationships between land use and land degradation often lack the resolution necessary to understand how local institutions differentially modulate feedback between individual farmers and the spatially heterogeneous effects of land use on soils. In this paper, we examine an historical example of a transition from agriculture to forest dominated land use (c. 1933–1941) in a highly degraded landscape on the Piedmont of South Carolina. Our landscape-scale approach examines land use and tenure at the level that individuals enact management decisions. We used logistic regression techniques to examine associations between land use, land tenure, topography, and market cost-distance. Our findings suggest that farmer responses to changing market and policy conditions were influenced by topographic characteristics associated with productivity and long-term viability of agricultural land use. Further, although local environmental feedbacks help to explain spatial patterning of land use, property regime and land tenure arrangements also significantly constrained the ability of farmers to adapt to changing socioeconomic and environmental conditions.

# Coupling meteoric $^{10}Be$ with pedogenic losses of $^{9}Be$ to improve soil residence time estimates on an ancient North American interfluve

Allan R. Bacon[1], Daniel deB. Richter[1], Paul R. Bierman[2], and Dylan H. Rood[3,4]
[1]University Program in Ecology, and Nicholas School of the Environment, Duke University, Box 90328, Durham, North Carolina 27708, USA
[2]Department of Geology and School of Natural Resources, University of Vermont, 180 Colchester Avenue, Burlington, Vermont 05405, USA
[3]Scottish Universities Environmental Research Centre (SUERC), East Kilbride G75 0QF, UK
[4]Earth Research Institute, University of California–Santa Barbara, 6832 Ellison Hall, Santa Barbara, California 93106, USA

**ABSTRACT**

**We couple meteoric $^{10}Be$ measurements with mass balance analysis of $^{9}Be$ to estimate the soil residence time (SRT) of a biogeomorphically stable Ultisol in the Southern Piedmont physiographic region of the southeastern United States. We estimate SRT after correcting the meteoric $^{10}Be$ inventory to account for observed $^{9}Be$ losses, which indicate that more than half of the $^{9}Be$ weathered from primary minerals has been leached from the upper 18.3 m of the Ultisol. Our estimates of minimum SRT range between 1.3–1.4 Ma and between 2.6–3.1 Ma under high and low (2.0 and $1.3 \times 10^{6}$ atoms $cm^{-2}$ $yr^{-1}$, respectively), estimates of $^{10}Be$ delivery. Denudation rates of the physiographic region corroborate our estimates. We redefine pedogenic time constraints in the Southern Piedmont, and demonstrate that the assumption of complete meteoric $^{10}Be$ retention in acidic soil systems cannot always be made; the latter has far-reaching consequences for soil, sediment, river, and ocean research using meteoric $^{10}Be$.**

We aim to estimate SRT of a highly weathered Southern Piedmont Ultisol, and hypothesize that the acidity of the soil system has facilitated meteoric $^{10}Be$ leaching. Rather than assuming complete retention, we propose that pedogenic losses of $^{9}Be$ (the predominant beryllium isotope in soils) can approximate meteoric $^{10}Be$ losses, and we estimate SRT by coupling measurements of meteoric $^{10}Be$ with an analysis of pedogenic $^{9}Be$ loss.

**METHODS**

GEOLOGY, September 2012; v. 40; no. 9; p. 847–850; Data Repository item 2012226 | doi:10.1130/G33449.1 | Published online 29 June 2012


# Chapter 18
# Evolution of Soil, Ecosystem, and Critical Zone Research at the USDA FS Calhoun Experimental Forest

**Daniel deB. Richter, Allan R. Bacon, Sharon A. Billings, Dan Binkley, Marilyn Buford, Mac A. Callaham, Amy E. Curry, Ryan L. Fimmen, A. Stuart Grandy, Paul R. Heine, Michael Hofmockel, Jason A. Jackson, Elizabeth LeMaster, Jianwei Li, Daniel Markewitz, Megan L. Mobley, Mary W. Morrison, Michael S. Strickland, Thomas Waldrop and Carol G. Wells**

*The past is never dead. It's not even past.*
(Faulkner, Requiem for a Nun, 1951)

**Abstract** The US Department of Agriculture (USDA) Forest Service Calhoun Experimental Forest was organized in 1947 on the southern Piedmont to engage in research that today is called restoration ecology, to improve soils, forests, and watersheds in a region that had been severely degraded by nearly 150 years farming. Today, this 2,050-ha research forest is managed by the Sumter National Forest and Southern Research Station. In the early 1960s, the Calhoun Experimental Forest was closed as a base of scientific operations making way for a new laboratory in Research Triangle Park, NC. Many papers were written during the Calhoun's 15 years of existence, papers that document how land-use history creates a complex of environmental forcings that are hard to unwind. One Calhoun field experiment remains active, however, and over nearly six decades has become a model for the study of soil and ecosystem change on timescales of decades. The experiment contributes greatly to our understanding of the effects of acid atmospheric deposition on soils, forests, and waters and of decadel changes in carbon and nutrient cycling in soils and forests. Perhaps the long-term experiment's major contribution is its clear demonstration that soils are highly dynamic systems on timescales of decades and that this dynamism involves both surface and deep subsoils. The ongoing experiment's success is attributed to relatively simple experimental design, ample plot replication, rigorous (but not too arduous) protocol for resampling and archiving, and to its ability to address changing scientific and management priorities that are important to society and the environment. In the last decade, the experiment has become a platform for research and education that explore basic and applied science. As this manuscript goes to press, the Calhoun Experimental Forest has been designated to become one of the National Science Foundation's national Critical Zone (CZ) Observatories, a development that will allow researchers to, return to the questions that originated the Calhoun Experimental Forest in the first place: how and why severely disturbed landscapes evolve through time.